Comparative -omics analyses to understand wood decay strategies and evolution of pathogenicity in *Armillaria* spp.

Ph.D. Dissertation

Neha Sahu

Supervisor: Dr. László G. Nagy

Synthetic and Systems Biology Unit

Institute of Biochemistry

Biological Research Centre, Szeged

Eötvös Loránd Research Network

Doctoral School of Biology, Faculty of Science and Informatics

University of Szeged

Szeged

2023

Table of Contents

List of abbreviations

AA - Auxiliary activity
ABC - ATP binding cassette
AI - Alien-index
ARCE - *Armillaria cepistipes*
AROS - *Armillaria ostoyae*
ASCO - Ascomycota
BR - Brown-rot
BUSCO - Benchmarking universal single copy orthologs
CAP - Cysteine-rich secretory proteins, antigen 5, and pathogenesis-related 1 proteins
CAZymes - Carbohydrate active enzymes
CBM - Carbohydrate-binding module
CDA - Chitin deacetylase
CE - Carbohydrate esterase
CPP - Cerato-platanins
DAP - Differentially abundant protein
DEG - Differentially expressed gene
ECM - Ectomycorrhizal
EXPN - Expansins
FC - Fold change
FCW - Fungal cell wall
FDR - False discovery rate
GH - Glycoside hydrolase
GO - Gene ontology
GST - Glutathione s-transferase
GT - Glycosyl transferase
HGT - Horizontal gene transfer
HT - Horizontally transferred
IPR - InterPro
ITS - Internal transcribed spacer
JGI - Joint Genome Institute
LDE - Lignin decaying enzyme
LD - Litter decomposer
LPMO - Lytic polysaccharide monooxygenase
LysM - Lysin motif
M - invasive mycelium
MDS - Multi-dimensional scaling
MEA - Malt extract agar

MFS - Major facilitator superfamily
ML - Maximum Likelihood
MRCA - Most recent common ancestor
MvsNIM - Invasive mycelium *vs* Non-invasive mycelium
NIM - non-invasive mycelium
NIR - non-invasive rhizomorphs
PATH - Pathogens
PCA - Principal component analysis
PCWDE - Plant cell wall degrading enzyme
Physac – Physalacriaceae
PL - Polysaccharide lyase
POD - Class II peroxidases
R - Invasive rhizomorph
ROS - Reactive oxygen species
RvsM - Rhizomorphs *vs* invasive mycelium ()
RvsNIR - Invasive rhizomorphs *vs* Non-invasive rhizomorphs
SCOG - Single copy orthogroup
SH-like - Shimodaira-Hasegawa-like
SOD - Superoxide dismutase
SR - Soft-rot
SSP - Small secreted protein
TMM - Trimmed mean of M-values
UR - Uncertain ecology
WR - White-rot

Chapter 1. Introduction

1.1. Fungi in forest ecosystems

1.1.1. Importance of fungi in forests

Fungi includes some of the most fascinating yet understudied and biotechnologically valuable groups of organisms (Gadd, 2013; Hyde et al., 2019; Volk, 2013). Fossil records of the earliest plants have shown their close association with fungi, and they still remain essential today as the most important decomposers in ecosystems and recycling nutrients as well as carbon back into the soil (Dance, 2017; Floudas, 2021). In addition, fungi also play a significant role in ecosystems, as they are highly connected to the root systems of plants and trees, transporting nutrients, water, and even chemical signals for communication between different organisms (Bahram and Netherway, 2022). Reportedly, about 90% of plant species depend on a mutually beneficial mycorrhizal relationship with fungi for their survival (Bonfante and Genre, 2010).

Interestingly, fungi share several features with both plants and animals, yet are so unique that they form their own kingdom. Fungi include both simple and advanced complex multicellular structures for which they followed unique evolutionary routes, from other multicellular lineages such as plants, animals, metazoans, and red and brown algae (Nagy et al, 2018). They also have cell walls, that, unlike plants, are made of chitin (He and Wu, 2016), reproduce both sexually and asexually, and produce spores (Virágh et al., 2022). Plants and animals comprise specialized cells that form different parts of the organism, but almost all fungal structures, regardless of their morphological complexity, are composed of the same filamentous hyphae that form the vegetative mycelium (Money, 2002; Nagy et al., 2018). The same hyphal

aggregates perform several biological and ecological functions, such as acting as a transport network for nutrients and water. A network of tubular and filamentous hyphae forms the mycelium, which spreads underground to acquire and absorb nutrients from various substrates (Bahram and Netherway, 2022).

Fungi, like animals, are heterotrophs, meaning they utilize nutrients from their surroundings by secreting various enzymes that break down complex organic matter into simpler molecules, making them very attractive enzyme sources for bio-based industries (McKelvey and Murphy, 2017; Treseder and Lennon, 2015). Based on how they interact and acquire nutrients from their surroundings, fungi in a forest are broadly divided into three categories - mutualists, saprotrophs, and pathogens (Peay et al., 2016).

1.1.2. Mutualists

A large majority of plants are associated with a diverse group of fungal species known as mycorrhizal fungi or mycorrhiza (Bonfante and Genre, 2010), which form associations with plant roots to increase nutrient uptake by their mycelium, absorbing nutrients from the soil and transferring them to the plant. Mycorrhizal fungi in soil form hyphal networks that can provide moisture and nutrients to plants and trees, in exchange for carbohydrates (Bonfante and Genre, 2010; Peter et al., 2016; Shah et al., 2016). Based on whether the fungus develops within the cells of the roots or colonizes the intercellular spaces, mycorrhizal fungi can be classified as endomycorrhizae and ectomycorrhizae respectively. Endomycorrhizae have been described in numerous crop plants and are further subdivided into orchid, ericoid, monotropoid, arbutoid and arbuscular mycorrhizae. Arbuscular mycorrhizal fungi such as *Acaulospora, Gigaspora, Glomus,* and *Sclerocystis* species are by far the most commonly found endomycorrhiza. Ectomycorrhizal (ECM) fungi such as *Suillus*, *Boletus*, *Tricholoma*, and *Amanita* species form associations between woody plants such as birch, beech, oak, and pine and individual trees can form associations with

multiple ECM fungi at one time (Rudawska et al., 2011). Several insights into mycorrhizal fungi have been gained through comparative genomic analyses, which highlighted that ECM fungi have evolved from white- and brown-rot (WR and BR, respectively), as well as litter-decomposing ancestors. Phylogenomic studies have also revealed that the evolution of ECM fungi is marked by extensive gene losses including the loss of enzymes that degrade plant cell walls, such as lignin-degrading class II peroxidases, cellulases, and sucrose invertases, presumably as a result of the adaptation of free-living to plant-associated symbioses, and an abundance of lineage-specific genes that degrade soil organic matter (Kohler et al., 2015; Marañón-Jiménez et al., 2021; Miyauchi et al., 2020; Shah et al., 2016; Strullu- Derrien et al., 2018). Moreover, high-throughput sequencing and imaging methods, along with recent advances in molecular biology and genetics have also enabled the detailed study of the biological mechanisms of symbiosis in mycorrhizae (Bonfante and Genre, 2010; Köhl et al., 2016; Stoian et al., 2019), further enabling the use of this new information in agriculture.

1.1.3. Saprotrophs

Saprotrophic fungi are the predominant decomposers and play a critical role in nutrient cycling in forest ecosystems. These fungi are crucial for maintaining the stability of ecosystems by retaining nutrients in late-succession soils and are considered key players in global carbon cycling. Saprotrophs include fungi that breakdown wood, soil organic matter, forest litter, and other complex plant components (carbohydrates, proteins, and extractives) into simpler sugars, thereby releasing carbon and inorganic nutrients into the environment (Baldrian and Valášková, 2008; Lebreton et al., 2021). These fungi have evolved various strategies to degrade the lignocellulosic plant biomass, such as by producing a wide arsenal of oxidative and plant cell wall-degrading enzymes (PCWDEs) (Eastwood et al., 2011; Floudas et al., 2015; Ruiz-Dueñas et al., 2021; Zhao et al., 2013) or through non-

enzymatic oxidative decay mechanisms (Floudas, 2021; Floudas et al., 2020; Riley et al., 2014).

Structurally, the linear and branched polysaccharide components of lignocellulose (cellulose and hemicellulose) are protected by a matrix of lignin, a recalcitrant compound composed of heterogeneous aromatic subunits. Due to its complexity, the presence of lignin in the plant structure confers rigidity, protecting the structural polysaccharides from microbial degradation (Ayuso-Fernández et al., 2019; Floudas, 2021). Therefore, lignin is the major obstacle to cellulosic biofuels/bioethanol production in the bio based industry (Canam et al., 2013; Yuan et al., 2021). Within the Dikarya, lignin degradation mostly occurs through the action of mushroom-forming Agaricomycetes, which based on their plant cell wall degrading gene repertoires and physical appearance of rot patterns, have traditionally been classified as either WR, which degrade all components of the plant cell wall including recalcitrant lignin, or BR, which perform a rather non-enzymatic decomposition of plant polysaccharides, leaving the lignin unaltered or only slightly modified (Ayuso-Fernández et al., 2019; Floudas et al., 2015; Ruiz-Dueñas et al., 2021). Additionally, the Ascomycota-specific decay type known as soft rot (SR), utilizes the plant polysaccharides from the lignocellulose matrix by forming cavities or erosions in the woody substrate. Understanding the evolution of these lignocellulose degradation mechanisms in wood decayers and litter decomposers (LD) was perhaps one of the most ecologically significant advancements in fungal biology (Floudas et al., 2015; Nagy et al., 2017).

Since then, increasing comprehensive genomics data on saprotrophs across the fungal phylogeny has further improved understanding of the evolution of PCWDE families and decay apparatus in fungi (Almási et al., 2019; Choi et al., 2017; Floudas et al., 2015, 2012; Hao et al., 2019; Krizsán et al., 2019; Nagy et al., 2016; Riley et al., 2014; Sipos et al., 2017; Zhao et al., 2013). Genome analyses with early-diverging Agaricomycetes revealed expanded gene repertoires carbohydrate active enzymes (CAZymes) responsible for the breakdown of crystalline cellulose (e.g. GH6, GH7, LPMOs), hemicellulases (GH43, GH74) and, lignin (AA2 and other dye decolorizing

peroxidases) (Lebreton et al., 2021; Nagy et al., 2016). Furthermore, the cellulose-related carbohydrate binding module 1 (CBM1), which facilitates the ability of enzymes to bind to crystalline cellulose, was found in white-rot species as opposed to brown-rot fungi, which appear to have few or no gene copies of CBM1 (Floudas et al., 2015). These studies imply that both genes gain and loss occurred along with the transitions from a WR to a BR lifestyle (Eastwood et al., 2011; Floudas et al., 2015; Lebreton et al., 2021; Nagy et al., 2016). Recent comparative genomics studies have highlighted that the existing WR and BR dichotomy doesn't precisely describe the diversity of wood decay mechanisms in fungi, and further research is needed to understand the diversity and mechanisms of wood decay (Almási et al., 2019; Floudas, 2021; Nagy et al., 2016; Riley et al., 2014). For instance, it has been shown that some species do not fall within the broad definition of either WR or BR, more recently addressed through the concept of gray-rot (Schilling et al., 2020) which refers to instances where genomic features do not correspond to the WR-BR dichotomy or lack gene-to-function links. Such as WR fungi showing a selective lignin degradation and others exhibiting a simultaneous breakdown of all components of wood including lignin, or lacking class II peroxidases and yet being able to breakdown lignin components. Such species can be found throughout the fungal phylogeny, although they appear to be more prevalent among the early-diverging Agaricales, such as the Schizophyllaceae, Fistulinaceae, and Physalacriaceae. Such fungi with unusual genomic and decay features prompt further reconsideration of this conventional dichotomy and might allow us to understand the evolution and diversity of wood decay strategies in fungi (Almási et al., 2019; Floudas et al., 2015; Nagy et al., 2016; Riley et al., 2014).

1.1.4. Plant pathogens

Plant pathogenic fungi are responsible for significant losses in agricultural yields and forest productivity worldwide. These fungi exhibit tremendous genomic and reproductive flexibility, and their wide distribution across the fungal phylogeny implies multiple transitions from non-pathogenic to pathogenic lifestyles and the other way

around (Möller and Stukentribrock, 2017). Moreover, plant pathogenic fungi have evolved several traits that allows them to infect and colonize all plant tissues (Lacaze and Joly, 2020; Möller and Stukenbrock, 2017). Based on how they interact with the host, plant pathogens can be broadly classified into biotrophs, necrotrophs and hemibiotrophs. Biotrophs (e.g. *Puccinia graminis, Ustilago maydis, Blumeria graminis, Magnaporthe oryzae*) (Duplessis et al., 2011; Koeck et al., 2011; Lanver et al., 2018; Liu et al., 2013; Zhang et al., 2017) form close relationship with host plants by suppressing the host immune system and obtaining nutrients from living plant cells. Conversely, necrotrophs (e.g. *Sclerotinia sclerotiorum, Rhizoctonia solani, Botrytis cinerea, Armillaria ostoaye)* (Chen et al., 2022; Foley et al., 2016; Liang and Rollins, 2018; Sipos et al., 2018) kill the host by secreting phytotoxic metabolites (Allan et al., 2019; Li et al., 2020; Stergiopoulos et al., 2013; Xu et al., 2021) and effector proteins (Liu et al., 2013; Shao et al., 2021; Tanaka and Kahmann, 2021; Toruño et al., 2016) and use dead plant tissue as a source of nutrition. Plant pathogenic fungi which first exhibit a biotrophic phase and, as the infection progresses switch to necrotrophy are known as hemibiotrophic fungi (e.g. *Colletotrichum*, *Moniliopthora* and *Phytopthora* species) (Bautista et al., 2021; McDowell, 2013; Meinhardt et al., 2014).

Over the years, the extensive literature on plant pathogenic fungi has emerged covering a wide range of topics, including their taxonomy, genetics, molecular biology, and interaction with host plants. This includes numerous studies on individual species or genera as well as comprehensive overviews of the entire field. This extensive research has laid the foundation for today's understanding of plant pathogenic fungi, which, together with new genomes and time-resolved omics data, improved our understanding of the insights into the evolution of genomic adaptations, gene expression, metabolism, mechanisms associated with lifestyle transitions, stages of fungal development during host interactions, and much more, in a level of detail not previously possible (Bautista et al., 2021; Collins et al., 2013; Duplessis et al., 2011; McDowell, 2013; Meinhardt et al., 2014; Möller and Stukenbrock, 2017; Olson et al., 2012; Ross-Davis et al., 2013; Teixeira et al., 2014; Zhang et al., 2017). These studies have demonstrated that plant pathogens invade their host by evading host defense

mechanisms, which include both physiochemical barriers, and secretion of specific proteins that target compounds produced by the pathogen (Dodds et al., 2009; Foley et al., 2016; Liang and Rollins, 2018; Möller and Stukenbrock, 2017; Shao et al., 2021; Tanaka and Kahmann, 2021; Zhang et al., 2017). Secreted proteins include the so-called effectors, that act either in the apoplastic space and symplastic space or inside the host cells to avoid recognition by the host immune system and suppress host defenses. Effector proteins are considered important in the virulence of the fungus or its ability to cause disease. Certain effectors are translocated to specific cellular compartments (such as chloroplasts or nuclei) where they disrupt cellular processes and transcription in host cells or manipulate host defenses by interfering with plant metabolism and facilitating pathogen invasion (Dodds et al., 2009, 2009; Houterman et al., 2008).

Plant cells can also trigger a surge of reactive oxygen species (ROS) in the apoplast when they first detect a pathogen (Foley et al., 2016; Newman and Derbyshire, 2020; Vylkova, 2017). The accumulation of ROS not only serves as a signaling molecule for plant's immune response but can also be directly harmful to pathogens. High concentrations of ROS in the host can lead to cell death, which prevents the spread of biotrophs but can promote the spread of necrotrophs, which feed off dead tissue. As a result, necrotrophs have evolved a variety of ways to exploit the host and increase ROS levels for their own benefit (Foley et al., 2016; Zhang et al., 2020). Even biotrophic fungi have evolved ROS scavenging mechanisms through the induction of genes related to stress response (Zhang et al., 2020).

In order to assist infection, pathogenic fungi use acidification or alkalization signaling pathways to alter host tissue pH (Newman and Derbyshire, 2020; Vylkova, 2017). Acidification of host tissues by fungal pathogens can damage the host tissue and reduce the plant's immune response, hence allowing early colonization. Reports have suggested that necrotrophs such as *Sclerotinia* and *Botrytis* produce oxalic acids to acidify the host tissues (Vylkova, 2017). Modulation of host pH not only enables the pathogen to adapt to the environmental pH but also may potentially increase fungal

virulence by either inducing expression of plant PCWDEs that facilitate softening or loosening of the host tissue, or by producing phytotoxic chemicals (Rodriguez-Moreno et al., 2018; Vylkova, 2017). For instance, the alkalinization of host pH by *Colletotrichum gloeosporiodes* enhances the expression of pectate lyases and appressorium formation during host penetration (Miyara et al., 2010, 2008). Alkalinization might be also advantageous for biotrophs as high pH can promote the expression of genes involved in nutrient absorption, expression of virulence traits, and secretion of lytic enzymes (Newman and Derbyshire, 2020; Rodriguez-Moreno et al., 2018; Vylkova, 2017).

In addition, to eliminate fungal pathogens and prevent the spread of infection, plants produce antimicrobial secondary metabolites such as flavonoids, phenols, terpenes, alkaloids, phytoalexins and phytoanticipins among others (Graham-Taylor et al., 2020). Necrotrophs with broad host ranges are able to detoxify these host-derived antifungal secondary metabolites with the help of detoxification enzymes and transporters such as ATP-binding cassette (ABC) transporters or major facilitator superfamily (MFS) transporters that can pump the toxic compounds out of the fungal cell (Newman and Derbyshire, 2020; Rodriguez-Moreno et al., 2018; Vylkova, 2017).

Overall, plant pathogens have evolved an extremely effective molecular toolkit to establish pathogenesis, the fate of which is ultimately governed by the ability of pathogen to compromise host defenses as well as the ability of the plant to defend the pathogen (Newman and Derbyshire, 2020; Rodriguez-Moreno et al., 2018; Vylkova, 2017). Our knowledge of the molecular mechanisms and evolutionary traits of plant pathogens, however, are far less known for Basidiomycota (other than rust and smut fungi) than for Ascomycota. A better understanding of the evolutionary underpinnings and functional perspective of broad range of plant pathogens across the fungal phylogeny requires further research.

1.2. Globally widespread *Armillaria* root-rot disease

1.2.1. *Armillaria* spp.

One of the most devastating necrotrophs of forests is *Armillaria* spp. (Fungi, Basidiomycota, Agaricales, Physalacriaceae), causing root-rot disease, which has been linked to severe losses in the economy, health, and long-term productivity of forest ecosystems (Baumgartner et al., 2011; Chen et al., 2019; Filip et al., 2009; Wong et al., 2020). The genus *Armillaria* comprises about 70 known species (Sipos et al., 2018). Based on the environmental conditions and host availability, *Armillaria* species can occur spanning across different geographical regions displaying their most prominent ecological lifestyle as facultative necrotrophs. Whilst being a pathogen, they are also beneficial in forest ecosystems as saprotrophs thus making them suitable for studying mechanisms of pathogenicity and wood-decay systems in fungi (Baumgartner et al., 2011; Chen et al., 2019; Prospero et al., 2004; Sipos et al., 2017). As a pathogen, they are reported to attack a broad range of plant hosts ranging from oak, and pine, as well as agronomic crops across both the Northern and Southern hemispheres and in a range of climates (Baumgartner et al., 2011). During the saprotrophic phase, they decay the woody plant biomass by producing a wide arsenal of PCWDEs, thereby playing an important role in carbon cycling and nutrient exchange (Hood et al., 1991; Sipos et al., 2017). Recently, all *Armillaria* species are perceived to have pathogenic abilities during their life cycle - even the saprotrophic ones (Alveshere et al., 2021).

Armillaria species have evolved a range of unique features, which conceivably emerged in the most recent common ancestor (MRCA). These include a very low mutation rate, extreme longevity, and size of colonies (>2,500 years, >900 hectares (Anderson et al., 2018; Anderson and Catona, 2014; Baumgartner et al., 2011; Sipos et al., 2018; Smith et al., 1992)), diploidy (Ullrich and Anderson, 1978), bioluminescence (Mihail and Bruhn, 2007), specialized underground structures known

as rhizomorphs (Porter et al., 2022; Sipos et al., 2017), potentially fix atmospheric N_2 (Koch et al., 2021), and, economically most importantly, the ability to infect and kill live trees (Baumgartner et al., 2011; Devkota and Hammerschmidt, 2020; Heinzelmann et al., 2019; Wong et al., 2020). Once *Armillaria* species infect the root system, they colonize and kill the cambium, ultimately causing plant death (Baumgartner et al., 2011; Ford et al., 2017). While the cause and spread of *Armillaria* root disease are well documented, we are still unclear about the molecular aspects of the infection process (Bendel et al., 2006; Devkota and Hammerschmidt, 2020; Ford et al., 2017; Heinzelmann et al., 2019, 2017; Prospero et al., 2003). Recent genome studies have identified that *Armillaria* genomes have an expanded repertoire of protein-coding genes that are enriched in PCWDEs, chitin-binding proteins, secondary metabolites, and putative pathogenicity genes (Baumgartner et al., 2011; Caballero et al., 2022; C. Collins et al., 2017; Collins et al., 2013; Heinzelmann et al., 2020; Kedves et al., 2021; Koch et al., 2021; Kolesnikova et al., 2019; Sipos et al., 2017; Wingfield et al., 2016).

1.2.2. Taxonomy

Typically, the basidiocarps/fruiting bodies of *Armillaria* species are characterized by the presence of annulated stipes (consisting of ring-like structure on the stipe) (Figure 1A-E), as well as exannulated (ringless) stipes found in the sister genus *Desarmillaria* (Figure 1F, G). Current advances with whole genome sequencing and phylogenetic analysis provided more sophisticated insights into the morphology and geographical distribution of *Armillaria* species into distinct Northern and Southern Hemispheres (Figure 1), which earlier were largely based on the appearance of the basidiocarps or mating compatibility. Previous time-calibrated phylogenetic analysis and morphological data (Koch et al., 2017), reported a three-genus composition of the armillarioid clade (lineage comprising the mushroom-forming genus *Armillaria* and *Desarmillaria*, along with *Guyanagaster*). The earliest diverging lineage and sister clade to mushroom-forming armillarioid species was the rhizomorph-producing gasteroid genus *Guyanagaster*. The next lineage consisted of the exannulate,

mushroom-forming subgenus *Desarmillaria* which includes *Armillaria tabescens* and *Armillaria ectypa*. Neither of these species forms ring-like structures on stipes, unlike typical armillaroid species. Furthermore, based on its ecology, *A. ectypa* is an unusual species growing on mosses (Kim et al., 2022; Koch et al., 2017). *A. tabescens* however does not have unusual substrate preferences and is pathogenic to *Eucalyptus* and *Quercus* species, which is more characteristic of *Armillaria*. The *Desarmillaria* subgenus was followed by the final lineage of annulated species described as the genus *Armillaria sensu stricto* (Koch et al., 2017).

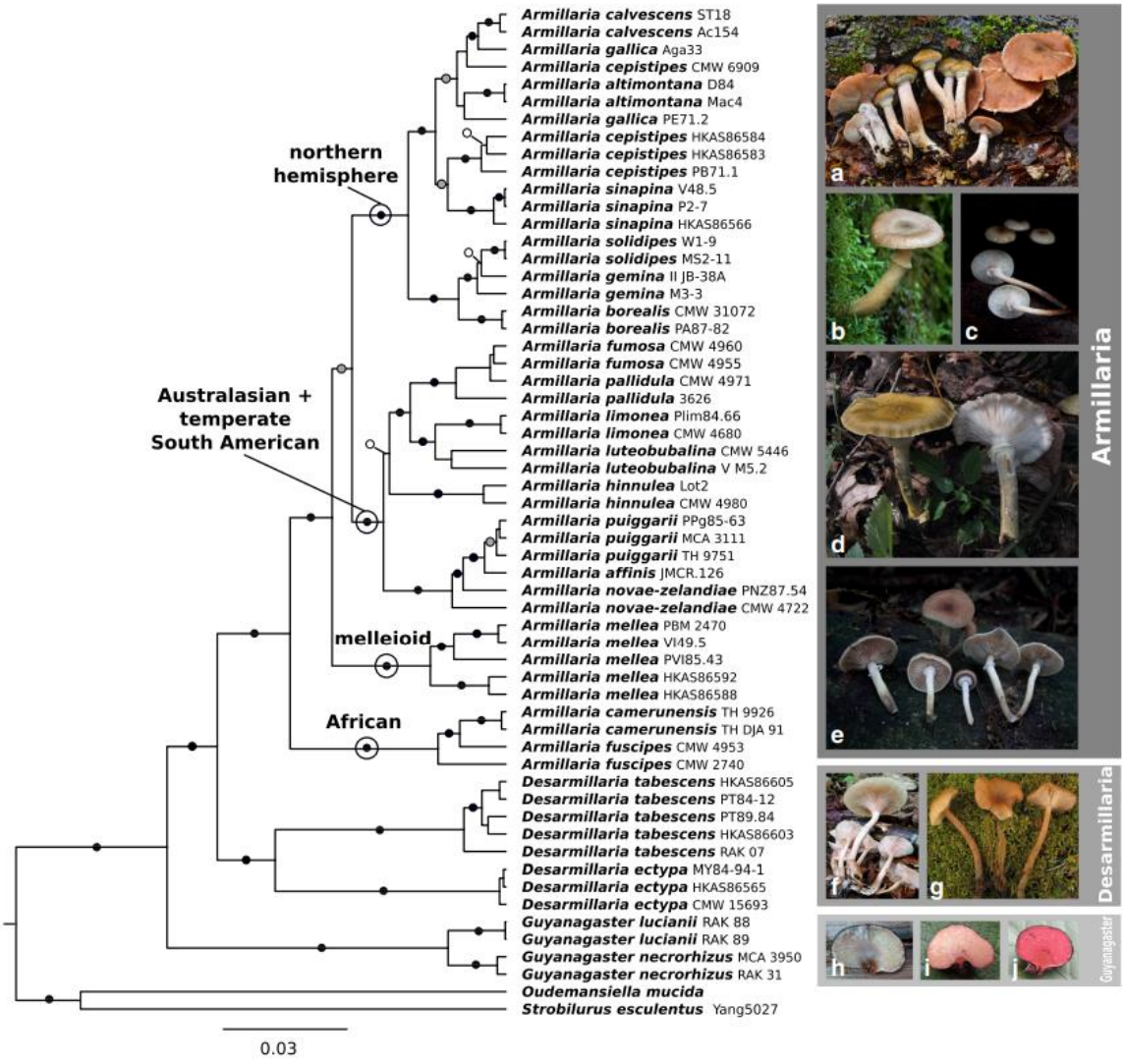

Figure 1: Armillaria phylogeny. Armillaria phylogeny (left) and pictures (right) represent the three lineages: Guyanagaster, Desarmillaria and Armillaria sensu stricto. (Koch et al., 2017).

1.2.3. Life cycle and dispersal strategies

Similar to a majority of fungi, mating in *Armillaria* species is regulated by a bifactorial, tetrapolar heterothallic mating system (Ullrich and Anderson, 1978) in which mating can be successful only with two compatible colonies. Species from this genus also have an unifactorial, bipolar homothallic mating system, meaning sexual reproduction can occur in a single thallus (Heinzelmann et al., 2019; Kim et al., 2022; Koch et al., 2017). Generally, *Armillaria* basidiospores germinate on woody substrates generating a haploid (n) mycelium, which fuses with a compatible basidiospore and forms a transient heterothallic dikaryotic mycelium (n+n). Subsequently, the heterokaryotic mycelium diplodizes and forms a diploid mycelium, which is the long-lived primary vegetative state in *Armillaria*. The diploid mycelium is responsible for colonizing the woody substrates (Heinzelmann et al., 2019; Kim et al., 2022; Koch et al., 2017) (Figure 2).

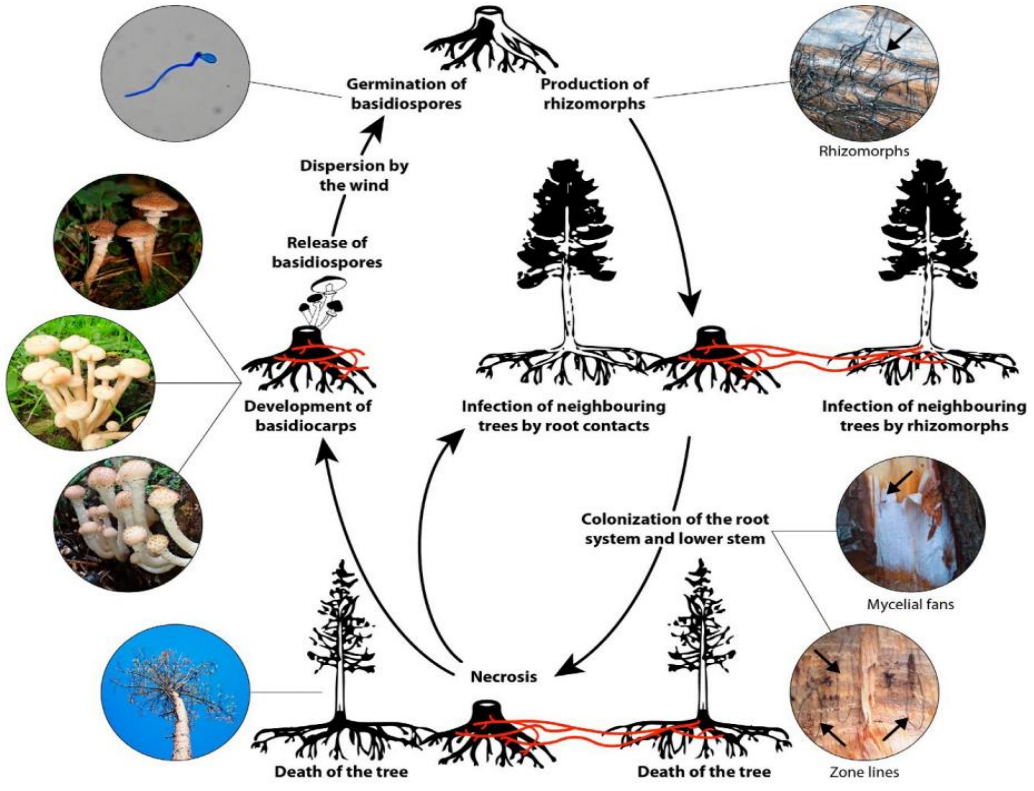

Figure 2: Armillaria lifecycle (Kim et al., 2022).

Armillaria species are unique from other Basidiomycetes and plant pathogenic fungi, due to their two-scale dispersal strategy. The first and more common phenomenon across other fungi is dispersal via sexual basidiospores (Baumgartner et al., 2011; Heinzelmann et al., 2019; Kim et al., 2022; Sipos et al., 2018, 2017) (Figure 2). After mating, a network of tubular and filamentous vegetative hyphae forms the diploid mycelium, which spreads underground to acquire and absorb nutrients from various substrates (Bahram and Netherway, 2022; Kim et al., 2022). Further, the mycelium spreads to new areas by branching and aggregating as even more densely packed strands of hyphae to form complex multicellular shoe-string-like structures called rhizomorphs (Anderson and Ullrich, 1982; Townsend, 1954) (Figure 2). This is the second and a rather unique dispersal strategy employed by *Armillaria* species, which involves local spread and direct root contact with the hosts using rhizomorphs. These underground intricate networks of rhizomorphs can eventually reach tremendous distances, leading to the formation of very large clonal individuals. A well-known example of this phenomenon is the largest organism on Earth - the humongous fungus of the Malheur National Forest in Oregon's Blue Mountains - *Armillaria ostoyae,* which according to reports covers an area of 2.5 square miles and could be as old as 9,600 years (Schmitt and Tatum, 2008). In fact, several reports suggest that many existing *Armillaria* species are both large and old, spanning under acres of the forest floor, with highly stable genomes and extremely low mutation rates - approximately three orders of magnitude below the expected rates (Aanen, 2014; Anderson et al., 2018; Anderson and Catona, 2014). Rhizomorphs are generally believed to serve as migratory organs for exploring substrates over distances, however, the studies also indicate that rhizomorphs produced by saprotrophic basidiomycetes can also take up inorganic nutrients and water from the soil (Anderson and Ullrich, 1982; Cairney, 1991; Cairney et al., 1988; Clipson et al., 1987; Granlund et al., 1985; Wells and Boddy, 1990). Experiments with *Armillaria mellea* (Anderson and Ullrich, 1982; Granlund et al., 1985; Jennings, 1987) and *Serpula lacrymans* (Brownlee and Jennings, 1982a, 1982b; Watkinson, 1971) showed translocation of various nutrients, water, and carbon within the rhizomorphs. *Armillaria* rhizomorphs can even persist underground in

nutrient deficit or stressed environment, thereby making them ubiquitous and persistent in forest ecosystems. Once the growth-favoring conditions are met, the fungus establishes infection in new hosts creating a patch of dead trees, especially noticeable in forests, vineyards, and orchards as a disease hub (Heinzelmann et al., 2019; Kim et al., 2022) (Figure 3).

Figure 3: Symptoms and indicators of Armillaria root disease (Baumgartner et al., 2011).

1.2.4. Geographical distribution and host range

Armillaria species have a worldwide distribution in a variety of woody ecosystems, including temperate forests, tree plantations, ornamental plants, vineyards, as well as gardens. The geographical distribution of *Armillaria* species spans across each continent (Heinzelmann et al., 2019), which can also be seen as distinct clades in the *Armillaria* phylogeny (Figure 1). This tallies to approximately 60-70 officially described and recognized species (Koch and Herr, 2021; Sipos et al., 2018) (Figure 4), of which approximately 40 are well-characterized (Heinzelmann et al., 2019).

Figure 4: Geographic distribution of Armillaria and Desarmillaria species (Kim et al., 2022).

In spite of their worldwide distribution, based on geographical niches, *Armillaria* species can have different host preferences (Guillaumin et al., 1993). The most aggressive pathogenic *Armillaria* species leading to tree mortality and prominent agronomic losses in the Northern Hemisphere include three species - *A. ostoyae* (preferred host - gymnosperms), *A. mellea* (preferred host - angiosperms) and *A. tabescens* (preferred host - angiosperms) (Koch et al., 2017; Sipos et al., 2018).

Armillaria ostoyae is known for causing colossal losses in coniferous forests as well as timber plantations across Central, Northern, and Eastern Europe, Northern and Southwestern America, Southern Canada as well as Eastern Asia (Kim et al., 2022; Koch et al., 2017). *Armillaria mellea* is the primary pathogen (can cause root-rot disease, regardless of the host immune system) causing tremendous damage to broad-leaved trees, orchard and forest plantations, and vineyards in southern Europe, eastern, central, southeastern, and southwestern regions of America, southern Mexico, and eastern Asia. *A. tabescens* was also reported to be pathogenic species, affecting eucalyptus and teak plantations in southern Europe, southeastern, eastern, and central USA, southern Mexico, and China. In central Mexico, *A. mexicana* and *A. mellea* have been identified as primary necrotrophs of peach orchards. Other species that degrade wood across the Northern Hemisphere include *Armillaria. altimontana*, *A. borealis*, *A. calvescens*, *A. cepistipes, A. gallica, A. gemina, and A. nabsnona* are more often known as opportunistic necrotrophs or even saprotrophs (Kim et al., 2022). *A. ectypa* on the other hand, has a unique and rare lifestyle confined to sphagnum mosses and marshes, with a discontinuous distribution across Europe (Koch et al., 2017).

The recently described *A. fuscipes* and *A. camerunensis* (Koch et al., 2017) together with *A. gallica* and *A. mellea* comprise the African Armillaria lineage (Kim et al., 2022). The indigenous African *Armillaria* lineage is widely distributed across the African continent, primarily as an opportunistic pathogen of native forests. However, a major pathogen of tea plantations is accounted by African-*mellea* lineage, which is found confined to the western and eastern regions of Africa and is characterized by a homothallic life cycle (Kim et al., 2022).

Among the Southern Hemisphere, the distribution of *Armillaria* species in New Zealand includes *A. novae zelandiae*, *A. limonea, A. hinnulea* and *A. aotearoa*. *A. novae zelandiae* is one of the most ubiquitous species found in New Zealand along with Australia, Fiji and New Guinea (Kim et al., 2022; Koch et al., 2017). The major causative agents of root-rot diseases in broad-leaved as well as confierous trees

include *A. novae zealandiae* and *A. limonea*, with a reported increase in pine tree mortality and losses in kiwi plantations. *Armillaria* species confined to New Zealand cause more disease impact on pioneer plantations, which slowly reduces over time with the growth of successors (Kim et al., 2022). On the other hand, *Armillaria* species confined to Australia are predominantly saprotrophs or weak pathogens including *A. fumosa* and *A. pallidula*, except *A. luteobubalina*, which is a dominant pathogen causing root-rot disease in Eucalypt and pine forests as well as other fruit-bearing trees. Further, *Armillaria* identified from South America include several species (Figure 4), however, their taxonomy and systematics still remain unexplored (Heinzelmann et al., 2019). In this region, *Armillaria* species are reported to attack beech trees, as well as several grapevines, eucalyptus and pine plantations.

1.2.5. Lifestyle as a pathogen and saprobe

Armillaria species are necrotrophs of woody plants, ranging from angiosperms (e.g. *A. mellea* with more than 600 host species (Raabe, 1962)) to gymnosperms (e.g. *A. ostoyae* with spruce/pine/fir trees as preferred hosts (Woods, 1994)). The vast majority of *Armillaria* species (e.g. *A.borealis, A.calvescens, A. fuscipes, A. gemina, A. limonea, A. luteobubalina, A. mellea, A. ostoyae* and *A. tabescens*) are reported to be necrotrophs that primarily kill the host, and their impact on forests tremendously affects agronomic and timber plantations as well as direct mortality of host trees (Baumgartner et al., 2011; Heinzelmann et al., 2019; Koch et al., 2017). With broad host range and varying virulence abilities, ecologically, *Armillaria* species as necrotrophs, infect the host by colonizing the root cambium (pathogenic phase) followed by killing the host and feeding on the dead plant biomass (saprobic phase) (Baumgartner et al., 2011; Rishbeth, 1968). The pathogenic phase starts with first attacking the pre-weakened or stressed trees by colonizing their root systems and cambium followed by subsequent cambium killing (Heinzelmann et al., 2019; Koch et al., 2017). After the pathogenic phase, the fungus enters its saprobic phase for utilizing nutrients from the woody substrate (Baumgartner et al., 2011; Prospero et al., 2004).

As a saprobe, *Armillaria* species are reported as white-rot fungi, making them crucial in natural ecosystems, where they play an important role in lignin degradation and carbon cycling. White rot fungi remove lignin from wood using high-redox potential oxidoreductases (e.g., class-II peroxidases (Ayuso-Fernández et al., 2019; Floudas et al., 2012)) and degrade complex polysaccharide polymers using diverse glycosyl hydrolase (GH), auxiliary activity (AA), carbohydrate esterase (CE). and polysaccharide lyase (PL) cocktails (Lundell et al., 2010; Rytioja et al., 2014).

1.2.6. Other unique lifestyles and interactions

Apart from the known necrotrophic and wood-decaying nutritional modes, some *Armillaria* species exhibit unique host ranges and interactions. For instance, *A. ectypa* is reported to possess quite different ecological preferences from all other *Armillaria* species, as it is generally associated with non-woody marshes and bryophytes. Not much is known about its pathogenic abilities, though it is reported to be saprotrophic on decaying moss (Kim et al., 2022; Koch et al., 2017). Few *Armillaria* species have also been reported to form a rare type of mycorrhizal associations with achlorophyllous and mycoheterotrophic orchids (e.g. *Geleola*, *Gastrodia* and *Cyrtosia*), where the plant acts as a parasite, whereas *Armillaria* serves as the host (Baumgartner et al., 2011; Guo et al., 2016; Kim et al., 2022). *Armillaria* species can also engage in symbiosis with other fungi (e.g. *Entoloma abortivum*, *Wynnea*), where they act either as host or parasite depending on the species they are interacting.

Co-occurrence of *Armillaria* and insects has also been reported in the Northern Hemisphere, although the nature of these interactions is often difficult to interpret (Kedves et al., 2021). Because defoliating pests such as the gypsy moth (*Lymantria dispar*), maple webworm (*Tetralopha asperatella*), eastern and western spruce budworm (*Choristoneura fumiferana* and *Choristoneura occidentalis*), saddled prominent caterpillar (*Heterocampa guttavitta*) also attack stressed and weakened trees, these insects are thought to make their hosts susceptible to *Armillaria* infection

(Kedves et al., 2021; Kim et al., 2022). On the other hand, *Armillaria* infection can trigger the production of aromatic and volatile compounds in conifers that are known to attract bark beetles. Infestations by *Hylobius* spp. are speculated to promote *Armillaria* infection by causing lesions that act as ports of entry for the pathogen. In several other instances, *Armillaria* and insects can co-occur without direct interaction, while details of interactions between *Armillaria* and insects are yet unknown (Kedves et al., 2021; Kim et al., 2022).

1.3. Advances in *Armillaria* research

1.3.1. Control of *Armillaria* root-rot disease

Most research on *Armillaria* root rot control focuses on preventing infestation of agricultural crops and trees for other commercial uses. Soil fumigation is one of the primary methods used on high-value crops on sites previously infested by *Armillaria* species (Baumgartner et al., 2011; Kedves et al., 2021). Chemical fumigants such as methyl bromide and carbon disulfide are sprayed on the soil to eradicate mycelium, which in the case of *Armillaria* root rot is found in partially decomposed tree roots. However, the success of this method varies based on the soil characteristics and the extent of the diseased roots (Robinson and Smith, 2001). Considering the possible restriction of the use of hazardous chemicals that may have adverse effects on the surrounding microbiome, the overall environment, and human health, alternative control strategies are needed (Baumgartner et al., 2011; Heinzelmann et al., 2019).

Since *Armillaria* species can colonize new stumps, roots, and woody debris, silvicultural methods like clear-cutting, selective-cutting, replanting, and thinning may also not be successfully eliminating *Armillaria* infections in forest ecosystems (Chen et al., 2019; Kedves et al., 2021). Although *Armillaria* root rot can be controlled by inoculum removal techniques such as a stump or root removal (Robinson and Smith,

2001), these, however, can cause reoccurrences as the underground rhizomorphs can still persist in soils until the onset of favorable conditions or substrate. Additionally, these treatments are costly and time-consuming and do not offer long-term control. *Armillaria* root disease can be slowed by using chemical fungicides that can inhibit the development of the fungus. However, their use can be expensive and labor-intensive, and it can also have a detrimental effect on the environment and pose safety concerns (Baumgartner et al., 2011; Chen et al., 2019; Kedves et al., 2021).

Biocontrol methods, which use naturally occurring antagonistic microorganisms to control the spread of Armillaria, are being considered as alternatives to chemical and silvicultural methods (Baumgartner et al., 2011; Chen et al., 2019; Kedves et al., 2021). Studies have shown that *Trichoderma* species can effectively inhibit the growth of a number of *Armillaria* species (Chen et al., 2019; Rees et al., 2021), but producing sufficient concentrations of these microorganisms in forest soils can be challenging. Inoculating wood with wood-decaying saprotrophs, such as *Ganoderma lucidum, Schizophyllum commune* and *Xylaria hypoxylon* have also been shown to suppress the growth of *Armillaria* mycelium (Cox and Scherm, 2006). However, using biological control agents to control *Armillaria* root disease can be difficult and site-specific, and requires further research to determine their effectiveness. In addition to biocontrol, post-infection treatments that reduce yield losses have been used for high-value crops such as grapevines, walnuts, and peaches. These treatments include root collar excavation and the application of commercial inoculants containing antagonistic microorganisms. These methods have demonstrated an increase in yield and enhanced vascular tissue performance (Baumgartner, 2004; Baumgartner et al., 2011).

The study of the *Armillaria* infection process is limited by gaps in knowledge, particularly regarding the patterns of root infection by rhizomorphs and hyphae. Gene expression studies have been used to understand the molecular basis of the interaction between grapevines and *Armillaria* to identify genes involved during the infection process, revealing that grape expresses an antifungal protein that inhibits

colony expansion in response to infection by *A. mellea*, and that *Armillaria* induces the expression of several genes in the ethylene and jasmonic acid signaling pathways, which are involved in host defense responses (Perazzolli et al., 2010). However, most studies on gene expression studies in *Armillaria* are focused on the plant cell wall decay response (C. Collins et al., 2017; Collins et al., 2013; Devkota and Hammerschmidt, 2020; Ford et al., 2017; Heinzelmann et al., 2017; Ross-Davis et al., 2013), and the molecular mechanisms involved in host-pathogen interaction are not well understood. Using genomic approaches to study differential gene expression changes in resistant and susceptible hosts could lead to the discovery of molecular markers of resistance, which could be used in classical breeding approaches to rapidly identify resistant progenies. The development of genetic manipulation tools in *Armillaria* and the molecular characterization of the host response will greatly advance our understanding of the infection process. Moreover, research on the molecular level details of the infection and how the course of infection differs between resistant and susceptible hosts will be crucial for identifying the specific mechanisms that cause resistance and developing effective strategies for controlling the disease (Collins et al., 2013; Heinzelmann et al., 2019; Kim et al., 2022).

1.3.2. Overview of recent *Armillaria* studies

Although the cause and distribution of *Armillaria* root disease are well researched, the genetic details of the infection process have not been fully explored, largely due to the lack of appropriate molecular tools for this non-model organism. However, over the past decade, increasing genomic and transcriptomic studies of several *Armillaria* species have provided insights into understanding various aspects of *Armillaria* biology (e.g., fruiting body development, rhizomorph development, and morphology, mechanisms of wood-decay, putative pathogenicity factors). The first genome sequence and proteomic analysis of *A. mellea* revealed the large genome size (58.35 Mb) and vast repertoire of carbohydrate-active enzymes, reminiscent of CAZy arsenals of both Basidiomycota and Ascomycota (Collins et al., 2013). More recent

comparative genomic studies in *Armillaria* species (*A. ostoyae, A. cepistipes, A. gallica,* and *A. solidipes*) also revealed unusually larger genomes (58-85 Mb) as compared to other white-rot fungi. These genome expansions were not accounted for by the proliferation of transposable elements as observed in other plant pathogenic fungi (Lorrain et al., 2021). Phylogenomic and comparative genomic approaches showed that *Armillaria* species underwent extensive genome duplications and diversification, resulting in expanded repertoires of protein-coding genes enriched in lineage-specific genes for rhizomorph morphology and development, various extracellular functions such as plant cell wall degradation especially pectin degradation, and putative pathogenicity genes (Sipos et al., 2017). However, these likely cover only a fraction of virulence genes in *Armillaria*, leaving much of the pathogenic arsenal unknown. In addition, the increasing availability of genomic and transcriptomic information will provide further insight into the ongoing processes involved in host-pathogen interactions and the genomic features of *Armillaria* species with different ecological strategies.

1.3.3. Non-conventional wood-decay

Armillaria spp. can break down the complex lignocellulosic plant biomass into simpler sugars, and thus are ecologically significant for releasing sequestered organic carbon to the soil. Previous comparative genomic studies on *Armillaria* highlighted PWCDE repertoires reminiscent of WR fungi (Collins et al., 2013; Ross-Davis et al., 2013; Sipos et al., 2018, 2017), with a characteristic enrichment of pectinolytic genes (Collins et al., 2013; Sipos et al., 2017). Accordingly, recent studies treated *Armillaria* spp. as WR based on the presence of lignin decaying enzymes (LDEs) encoding genes (C. Collins et al., 2017; Collins et al., 2013; Floudas et al., 2015), which are however underrepresented in their genomes unlike other WR fungi (Sipos et al., 2018, 2017). Additionally, previous studies have also shown that *Armillaria* species primarily decay the cellulose, hemicellulose, and pectin components of the plant cell wall, and leave lignin unattacked during early stages of decay (Campbell, 1932; Schwarze,

2007). Chemical and microscopic analyses of wood decay by *Armillaria* produced contradictory results. *A. mellea* was classified as Group II WR fungi which attack celluloses and pentosans at early stages and lignin remains unaffected (Campbell, 1932). Others reported a type-I SR decay where the fungal hyphae grow through the secondary cell wall layer, producing characteristic cavities in the tracheids, axial, and xylem ray parenchyma cells (Schwarze, 2007). Soft rot fungi by definition are now restricted to Ascomycota (Blanchette et al., 2004; Worrall et al., 1997); however, there are many Agaricomycetes that produce symptoms resembling soft rot or that do not fit the traditional white rot/brown rot dichotomy (Floudas et al., 2015; Nagy et al., 2016; Riley et al., 2014). Soft-rot was suggested in *Cylindrobasidium* spp., a close relative of *Armillaria*, that also has a lower number of LDEs than typical WR decayers (Floudas et al., 2015; Sipos et al., 2017). Fungi from multiple WR and BR clades have been used to study the wood-decay-associated gene expression (Gaskell et al., 2014; Oghenekaro et al., 2016; Olson et al., 2012; Teixeira et al., 2014; Vanden Wymelenberg et al., 2011). These studies highlighted substrate and species-specific responses, sequential activation of degradative enzymes, along with lifestyle-driven differences among species highlighting the ambiguity of extant decay-type classification. Altogether, genomic and transcriptomic studies on *Armillaria* have revealed their unusual gene repertoire (Sipos et al., 2018, 2017), making them suitable candidates to understand where *Armillaria* fits in the ever-growing array of decay types.

1.3.4. Origins of pathogenicity

The genus *Armillaria* evolved from a clade of non-pathogenic wood-decaying saprotrophs, representing an independent origin of necrotrophy for which, the molecular mechanisms are still not well explored *Armillaria* genomes encode genes associated with pathogenicity and modulation of the host immune systems (Sipos et al., 2017). These include expansins that contribute to the loosening of the complex plant cell wall matrix and cerato-platanins that also help loosen the plant cell wall and

trigger cell death in the host. Additionally, *Armillaria* genomes were reported to have an enrichment of carboxylesterase and salicylate hydroxylases, similar to what is observed in other plant pathogens like *Moniliopthora* species and *Marasmius fiardii* (Sipos et al., 2017). These enzymes may contribute to the detoxification and the development of tolerance to salicylic acid, which plays an essential role in plant defense. *Armillaria* genomes also show an overrepresentation of secondary metabolism-related genes that were found to be homologous to *Heterobasidion* (Olson et al., 2012), small secreted proteins (SSPs), and other pathogenicity-related genes such as those involved in stress response or competition against microbes (Collins et al., 2013; Fox and Howlett, 2008; Sipos et al., 2017).

In addition, plant pathogenic fungi secrete specialized effectors, which are also small proteins that can suppress host defense response by either preventing their host from recognizing them or manipulating host metabolism (Shao et al., 2021). Among the many are fungal lysin motif (LysM) effectors that prevent, mask, or sequester the release of chitin oligomers from the fungal cell wall (FCW). Compared to other Agaricales, LysM effector domains have been shown to be significantly overrepresented in *Armillaria* (Sipos et al. 2017). These domains may play a role in inhibiting chitin-triggered host immunity and protecting the FCW against hydrolysis by chitinases and other hydrolytic enzymes released by the host or surrounding microbes (Akcapinar et al., 2015; de Jonge et al., 2010; Liu et al., 2013). Specialized necrotrophic and hemibiotrophic effectors can also inhibit host peroxidases to protect the pathogen from ROS or directly influence the host metabolism by producing virulence factors that induce cell death (Jwa and Hwang, 2017; Toruño et al., 2016). However, the current knowledge on effector biology related to the modulation of host defence and host death are largely based on model organisms from the Ascomycota and other rusts or smut fungi (de Jonge et al., 2010; Jwa and Hwang, 2017; Liu and Zhang, 2022; Shao et al., 2021; Toruño et al., 2016). For instance, the gene-for-gene model (Flor, 1971) in plant-pathogen interactions, where an effector protein produced by the pathogen interacts with the host resistance gene, causing a hypersensitive response resulting in cell death (Friesen et al., 2007; Kanyuka et al., 2022; Shao et

al., 2021). This type of interaction model has been well-documented in pathogens from the Ascomycota and a few Basidiomycota (rusts and smut fungi) (Bourras et al., 2016; Dodds et al., 2006; Friesen et al., 2007; Houterman et al., 2008; Huang et al., 2014). Whether such models of host-pathogen interaction exist in *Armillaria* species or necrotrophs from other Basidiomycota remain still unexplored due to the lack of easy-to-deploy genetic manipulation tools for these species.

Overall, the concurrent overrepresentation of pathogenicity-related genes with other plant-pathogenic fungi from Basidiomycota, suggests convergent origins of pathogenicity in Agaricales (Sipos et al., 2017). However, more research is needed to fully understand the evolutionary origins and molecular mechanisms of pathogenicity in broad-range plant pathogens and their interactions with host plants.

Chapter 2. Objectives

The genus *Armillaria* includes mushroom-forming fungi that are among the largest and oldest terrestrial organism on Earth. These species efficiently degrade lignocellulosic plant biomass and are also known to cause root-rot disease in woody ecosystems worldwide. Depending on geographical regions, environmental conditions, and host health, each *Armillaria* species can persist as pathogens (necrotrophs) or saprotrophs. Among which the most important are necrotrophs, which first bypass the host immune system, colonizing and killing the living root systems and subsequently using the dead plant biomass as a nutrient source. Despite their huge impact on forest ecosystems, the biology of *Armillaria* species, especially the molecular level details of the interaction between *Armillaria* and host plants, as well as the strategies for wood-decay are not well explored. A major reason for this is the lack of genetic manipulation tools available for these non-model fungi.

In my doctoral research, we used a combination of gene-expression studies and phylogenomic comparisons to explore the evolutionary routes that contributed in making *Armillaria* species such devastating forest pathogens and efficient wood-decaying saprotrophs.

The objectives of this thesis were to answer the following questions:

- What are the wood decay strategies employed by pathogenic and saprobic *Armillaria?*
- Do gene repertoire variations drive the functional diversity in *Armillaria?*
- How distinct wood-decay traits and pathogenicity evolve in *Armillaria?*
- What are the molecular mechanisms underlying the infection process?

Chapter 3. Methods

3.1. Wood-decay omics in two *Armillaria* species

3.1.1. Experimental setup

Cultures of *Armillaria ostoyae* C18 and *Armillaria cepistipes* B2 (Guillaumin et al., 1993; Prospero et al., 2004) were inoculated onto malt extract agar (MEA) and incubated for one week at 25ºC in the dark. 4-5 cm long spruce roots, sterilized in an autoclave, were placed next to the one-week-old cultures of *A. ostoyae* and *A. cepistipes* and again kept at 25ºC in the dark for 2-3 weeks until colonized by the fungi. After colonization, roots were dissected to collect the mycelium under the outer bark layer and the rhizomorphs emerging from the colonized wood *Armillaria* cultures without the addition of sterilized spruce roots were used as non-invasive controls. Total RNA was extracted from the four tissue types in three biological replicates using the Quick RNA Miniprep kit (Zymo Research) according to the manufacturer's protocol. The concentration of the extracted RNA was measured using Qubit fluorometer (ThermoFisher) according to the manufacturer's instructions and samples were further processed for RNA-Seq and proteomics analysis.

3.1.2. Sample preparation and sequencing

RNA-Seq analyses *(performed by SeqOmics Biotechnology Ltd., Mórahalom, Hungary)* were done using the Ribo-Zero rRNA Removal Kit (Yeast; Illumina) to remove rRNA from total RNA. Samples were processed using the Illumina TruSeq V2 library preparation protocol. Libraries were sequenced on an Illumina NextSeq 500 instrument yielding 2×150 nt reads.

For protein extractions, *(performed by Dr. Rebecca Owens at Maynooth University, Ireland)* tissues were snap-frozen in liquid N_2 and bead beaten periodically (30 Hz, 2 min), with snap-freezing between cycles. Lysis buffer (6 M guanidine-HCl, 0.1 M Tris-HCl, 50 mM DTT pH 8.6) was added to crushed fungal tissue, and bead beating was repeated. Samples were further disrupted using sonication (MS72 probe, 3 × 10 seconds), with cooling on ice between sonication steps. Samples were purified by centrifugation, and the supernatant was filtered (3 kDa cut-off filters (Millipore) for concentration and buffer exchange in PBS. Protein samples were precipitated with TCA (final 15% w/v), and pellets were washed with ice-cold acetone. Protein pellets were resuspended in UT buffer (6 M urea, 2 M thiourea, 0.1 M Tris-HCl pH 8) and concentrations were normalized according to the Bradford protein assay. Samples were digested according to (Moloney et al., 2016), and ZipTips (Millipore) was used for sample cleanup. Peptide samples were analyzed with high mass accuracy using the Q-Exactive mass spectrometer coupled to a Dionex Ultimate 3000 nanoLC with an EasySpray PepMap C18 column (50 cm × 75 µm). Peptide mixtures were separated as described by Collins et al. (C. Collins et al., 2017) and the resulting data were analyzed using MaxQuant (v 1.5.3.30) (Cox et al., 2014) with the label-free quantitation algorithms and searching against the protein database (filtered models) in JGI MycoCosm (Grigoriev et al., 2014; Sipos et al., 2017).

3.1.3. Analysis of multi-omics data

Paired-end Illumina (HiSeq, NextSeq) reads were trimmed for quality using the CLC Genomics Workbench tool version 11.0 (CLC Bio/Qiagen) *(performed by Dr. Balázs Bálint at SeqOmics Biotechnology Ltd., Mórahalom, Hungary)*, removing ambiguous nucleotides and all low-quality read-end parts. The quality cutoff value (probability of error) was set to 0.05, corresponding to a Phred score of 13. Trimmed reads containing at least 40 bases were mapped into CLC using the RNA-Seq Analysis 2.16 package (Qiagen), requiring at least 80% sequence identity over at least 80% of the read lengths; strand specificity was omitted. Reads with fewer than 30

equally scoring mapping positions were mapped to all possible locations while reads with more than 30 potential mapping positions were considered uninformative repeat reads and removed from the analysis. "Total counts" RNA-Seq count data were imported from CLC in R version 3.0.2 (Qiagen).

For the calculation of differentially expressed transcripts, genes were filtered based on their expression levels, considering only those features detected by at least five mapped reads in at least 25% of the samples, for each of the species were included in the study. Subsequently, "calcNormFactors" from "edgeR" version 3.4.2 (Robinson et al., 2010) was used to perform scaling of the data based on the "trimmed mean of M-values" (TMM) method (Robinson and Oshlack, 2010). Log transformation was performed using the "voom" function of the "limma" package version 3.18.13 (Ritchie et al., 2015). Linear modeling, empirical Bayes moderation, and calculation of differentially expressed genes were performed using "limma". Genes that showed at least a two-fold change in gene expression with a false discovery rate FDR value below 0.05 were considered significant. Multidimensional scaling (function "plotMDS" in edgeR) was used to visually summarize gene expression profiles. In addition, unsupervised cluster analysis with calculation of Euclidean distance and full linkage clustering was performed for the normalized data using the "heatmap.2" function from the R package "gplots". To check the reliability of the expression data in the two species, we used the superSeq package (Bass et al., 2019) which uses a subsampling approach to simulate and predict the number of differentially expressed genes at lower read depths and random sampling points from the original dataset. These subsampled reads are then extrapolated to predict the relationship between statistical power and read depth.

Proteomics results were organized and statistical analyses were performed *(by Dr. Rebecca Owens at Maynooth University, Ireland)* using Perseus (v 1.5.4.0) (Tyanova et al., 2016). Qualitative and quantitative analyses were performed to determine the relative changes in protein abundance in each sample type. Quantitative analysis was done in Perseus (v 1.5.4.0) (Tyanova et al., 2016), a Student's t-test was performed

with a p-value of 0.05 and a $\log_2$ (fold change; FC) ≥ 1. Qualitative analysis revealed proteins that were detected in 2/3 of the replicates for a sample type and were undetectable in all replicates of the comparison group. For the qualitative results, a theoretical minimum fold change was determined based on a calculated minimum detectable protein intensity (mean + 2 standard deviations of the lowest detectable protein intensity for each replicate in the experiment) (Moloney et al., 2016). Based on this theoretical minimum fold change, some qualitative results were excluded due to intensity values approaching the minimum detectable levels. The qualitative and quantitative results were combined, and the total number of differentially abundant proteins (DAPs) was summarized.

3.1.4. Clustering and functional annotations

The predicted protein sequences from JGI MycoCosm (Grigoriev et al., 2014) were used to find the orthologs in *A. ostoyae* and *A. cepistipes* using OrthoFinder v2.3.1 (Emms and Kelly, 2015) (default parameters). Single-copy orthologs for the two species were further analyzed to compare expression patterns in the two species. Functional annotation was performed based on InterPro (IPR) domains using IPR Scan v5.24-63.0 (Jones et al., 2014).

Enriched gene ontology (GO) terms for different comparisons were predicted with the topGO package (Alexa and Rahenfuhrer, 2016) using the weight01 algorithm and Fisher testing. Terms with p-values less than 0.05 were considered significant and plotted with respect to their gene ratios, where the gene ratio is the number of a given GO term in a specific comparison type relative to the total number of that term in the gene list for that organism.

CAZyme copy numbers in *A. ostoyae* and *A. cepistipes* were taken from the JGI Mycocosm annotations based on the CAZy annotation pipeline (Lombard et al., 2014). CAZy families were separated based on their substrate-specific plant cell wall degradation abilities (Table S1) and analyzed copy numbers of differentially expressed

genes and DAPs for cellulases, hemicellulases, pectinases, expansins, and ligninases in the invasive mycelium *vs* non-invasive mycelium (MvsNIM) and invasive rhizomorphs *vs* non-invasive rhizomorphs (RvsNIR) comparisons.

Transporters were identified using DeepLoc (Almagro Armenteros et al., 2017) to select plasma membrane-localized proteins from the proteomes of both species. Plasma membrane-localized proteins with more than one transmembrane domain were used to obtain a list of nonredundant IPR domains that were manually checked for their functional role in transport.

3.2. Comparative phylogenomics

3.2.1. Sample preparation for sequencing

Armillaria strains obtained from different sources (Table 2) were inoculated onto MEA and incubated for 7-10 days at 25°C in the dark. The identity of each strain was confirmed by amplification and sequencing of the fungal internal transcribed spacer region (ITS1-5,8S-ITS2), and bacterial contamination was checked using universal 16S primers. Strains with confirmed identity were used to inoculate malt extract broth in 500 ml Erlenmeyer flasks and incubated at 25°C in the dark for 4-5 weeks until a substantial amount of fungal biomass had grown. The fungal biomass was stored at -80°C until DNA and RNA extraction. DNA extraction was performed using Blood & Cell Culture DNA Maxi Kit (Qiagen) and RNA extraction was performed using RNeasy Midi Kit (Qiagen) according to the manufacturer's instructions. Using the DNA, we re-confirmed strain identity by sequencing the ITS region and nucleic acid quantity was measured using Qubit fluorometer (ThermoFisher) according to the manufacturer's instructions. Genomic and transcriptomic library preparation, sequencing, assembly and annotations were performed in collaboration with JGI Mycocosm (Grigoriev et al., 2014; Kuo et al., 2014).

3.2.2. Taxon sampling and datasets

We used three datasets in this study. Dataset 1 comprises 66 species (64 Agaricales, 2 Boletales outgroups), which were used to analyze gene family evolution in *Armillaria* (Table S2). This was extended into a phylogenetically more diverse Dataset 2, which was used to perform gene copy number analysis of wood-decay gene repertoires and comprised 131 fungal species from both Basidiomycota and Ascomycota, including species with various lifestyles such as white-rotters, brown-rotters, litter-decomposers, ECM fungi, pathogens, and species with uncertain ecologies (Table S2). Dataset 3 was used to identify horizontally transferred genes and comprised 942 species, including fungi, bacteria as well as plants. All the species used in these datasets are published and publicly available sequences from JGI Mycocosm (*except three species that were used with Author's permission, see Table S2*). Proteomes of all the species used in this study were functionally annotated by using IPR Scan (v.5.46-81.0) (Jones et al., 2014). Secreted and small secreted (at least 300 amino acids) proteins were identified as described previously (Almási et al., 2019).

3.2.3. Gene family evolution in *Armillaria*

Reconstruction of genome-wide gene family evolution was performed using Dataset 1. Predicted protein sequences were clustered into orthogroups using OrthoFinder (v2.3.1) (Emms and Kelly, 2019, 2015) with default settings. For the species tree, multiple sequence alignment for 81 single copy orthogroups (SCOGs) were inferred using MAFFT (-auto) (Katoh and Standley, 2013), followed by removal of gapped regions from the alignments using TrimAl (Capella-Gutierrez et al., 2009) with a gap threshold of 0.9. Trimmed alignments were then concatenated into a supermatrix using an in-house R-script. The species tree was reconstructed in RAxML (v8.2.12) (Stamatakis, 2014) with the option of rapid bootstrap analysis and search for

the best-scoring maximum likelihood (ML) tree under the PROTGAMMAWAG model of protein evolution. The tree was rooted using FigTree.

We analyzed the genome-wide duplications and losses across gene families using the COMPARE method (Nagy et al., 2014) which uses reconciled gene trees to perform Dollo parsimony mapping and ortholog coding to tell apart duplications from speciation events. To obtain the reconciled gene trees for COMPARE, we first inferred multiple sequence alignments for the Orthofinder orthogroups with at least four proteins using MAFFT (-auto) (Katoh and Standley, 2013). Aligned clusters were trimmed to remove spurious regions using TrimAL (Capella-Gutierrez et al., 2009) with -strict parameter. Clusters for which TrimAL resulted in blank alignments (due to -strict parameter) were used in their non-trimmed form. In total, 16,936 trimmed and 819 non-trimmed clusters were used in RAxML (v8.2.12) (Stamatakis, 2014) for gene tree inference, followed by Shimodaira-Hasegawa (SH)-like branch support calculation also in RAxML under the PROTGAMMAWAG substitution model. The 17,755 gene trees with their SH-like support values, along with the species tree were used for rerooting, followed by gene tree species tree reconciliation in Notung (v2.9) run in batch mode with edge weight threshold set to 70. Reconciled gene trees were used to reconstruct the gene duplication/loss scenarios in orthogroups along the species tree using the COMPARE pipeline (available at https://github.com/laszlognagy/COMPARE). For each gene family, the number of gains, losses, net gains (sum of gains and losses), and ancestral copy numbers were obtained and their summary was mapped back onto the species tree. GO terms significantly enriched (p-values < 0.05) among the duplications at *Armillaria* most recent common ancestor (MRCA) were identified by topGO (Alexa and Rahenfuhrer, 2016) using the weight01 algorithm and Fisher testing.

3.2.4. Analyses of CAZymes in *Armillaria* spp.

Dataset 2 was used to analyze where Physalacriaceae (including *Armillaria*) fits in terms of their wood-decay repertoires. Annotation of CAZymes for the required species were downloaded from JGI Mycocosm (species whose CAZymes were not present in JGI Mycocosm were annotated using the CAZy annotation pipeline (Lombard et al., 2014). Annotated CAZymes were assigned to their putative roles in plant cell wall degradation or FCW-related functions. For this, a literature review was conducted for recent studies published in the last decade and focused on identifying plant biomass-degrading enzymes involved in the degradation of cellulose, hemicellulose, pectin, lignin and CAZymes with a speculated role in the degradation of lignin monomers. Proteins related to FCW-related CAZymes such as the ones acting on chitin, glucan, and mannans were identified. A total of 21 published studies (Table S1) were used to compile a diverse range of plant cell wall degrading enzymes, including cellulases, xylanases, pectin lyases, pectinases, polygalacturonase, laccases and peroxidases. These CAZymes and their preferred substrate(s) are provided in Table S1, of which, families with a putative role in plant cell wall degradation were retained for further copy number-based analyses. We subjected the proteomes of these 131 species to OrthoFinder (v2.3.1) (Emms and Kelly, 2019, 2015) with default settings, giving us a total of 41,205 orthogroups. For inferring the species tree, we generated SCOGs using a set of in-house R scripts which gave us 548 orthogroups in which the duplications were caused by gains at species levels (or terminal gains). From these, we omitted proteins showing less similarity based on amino acid distance against the other members of the cluster. In this step, we used at least 40% of all species for each cluster. Finally, the resulting 514 SCOGs were concatenated (minimum 60 lengths of amino acids, and at least 66 species) into one supermatrix and followed by species tree inference in IQ-Tree (Nguyen et al., 2015).

We generated phylogenetic principal component analysis (PCA) using the phyl.pca (Revell, 2009) function from Phytools (Revell, 2012) for Physalacriaceae along with WR and LD fungi. We compare *Armillaria* and other Physalacriaceae to only WR and LD fungi, because including BR and mycorrhizal species, which have huge differences in gene content, reduced the resolution of the plots. We provided the function with a

gene copy number matrix normalized according to proteome sizes for each substrate category and the above-described ML species tree (subsetted to WR, LD and Physalacriaceae species) as inputs. Independent contrasts were calculated under the Brownian motion model and the parameter mode="cov" (Revell, 2012). We also plotted their proteome-size normalized copy numbers into bar plots for visualization of copy numbers across the phylogeny

We further investigated the shared CAZymes between Physalacriaceae members and Ascomycota. For this, we first identified the CAZy orthogroups from the 131 species, by selecting orthogroups with at least 50% of the proteins annotated as CAZymes, and at least 5 proteins. This gave us 401 CAZy orthogroups which were used to perform Fisher's exact test-based enrichment for identifying co-enriched CAZy families in Physalacriaceae and Ascomycota with respect to WR and LD.

3.2.5. Analyses of horizontally transferred genes

In order to check if Physalacriaceae species are more similar to Ascomycota than expected by chance, which could either come from horizontal gene transfer or long-retained ancestral genes, we compiled the Dataset 3. This comprised a taxonomically diverse dataset with a total of 942 species, ranging from 110 fungi from Basidiomycota (including 20 Physalacriaceae), 741 from Ascomycota, 26 from Mucoromycota, 10 from Zoopagomycota, 13 from Chytridiomycota and 17 other early-diverging fungi as well as 15 bacterial and 10 plant species.

We identified candidate horizontally transferred (HT) genes using the Alien index (AI), for which we ran MMseqs (easy-search, e-value cutoff 0.001) (Steinegger and Söding, 2017) using all Physalacriaceae proteomes merged together as our query, against a database of proteomes of all the other species as our subject. Using an in-house R-script, we parsed the output to retain only the top hits (based on e-values) for each taxonomic group. AI scores were calculated as [$\log_{10}$(best hit to species within

the group lineage + $1x10^{-200}$) - $\log_{10}$(best hit to species outside the group lineage + $1x10^{-200}$)] (Alexander et al., 2016; Wisecaver et al., 2016).

Further, for phylogenetic validation of HGT events, we used a subset of 329 species from Dataset 3 based on AI of top HGT donors. In this case, we restricted our donor list to major HGT contributors only, *viz.* Ascomycota, followed by Mucoromycota and Zoopagomycota as outgroups. The proteomes of these 329 species were subjected to OrthoFinder (v2.5.4) (Emms and Kelly, 2019, 2015) clustering with default settings. From there, we fished out the orthogroups with at least one AI-based HT gene and also the orthogroups containing CAZymes. Further, we retained orthogroups having at least one Physalacriaceae and one Ascomycota/Mucoromycota/Zoopagomycotina species, resulting in a total of 675 orthogroups.

Proteins from these 675 orthogroups were aligned using MAFFT (-auto) (Katoh and Standley, 2013), and spurious regions in the alignments were trimmed by TrimAL (-strict) (Capella-Gutierrez et al., 2009). Trimmed alignments were used to infer gene trees using IQ-Tree (Nguyen et al., 2015) with ultrafast bootstrap (1000 replicates) under the WAG+G substitution model. Using an in-house R-script (developed by Zsolt Merényi), we identified potential HGT events by extracting clades from the gene trees based on support values (>70%) and taxon occupancy (receiver clade with >70% Physalacriacae species, donor clade with >70% Ascomycota, and finally sister clade with >70% Ascomycota to ensure the direction of gene transfer). Physalacriceae proteins from these putative HT clades, were used as a query against the UniRef100 database (Suzek et al., 2015) from the UniProt Reference Cluster using MMSeqs easy-search, e-value 0.001) (Steinegger and Söding, 2017). To remove the matches with low sequence similarity matches and low coverage, we retained hits with percent identity and bidirectional coverage of more than 45%. We parsed the filtered hits to retain only the top 100 hits (based on percent identity) for each query, and the taxonomic category contributing predominantly among the top 100 hits was assigned as the putative donor. Further, we classified the assigned donor into two categories:

Type A, where the top 100 hits were dominated and confidently associated with Ascomycota, and Type B, where the top 100 hits were dominated by non-Agaricomycetes species, however ambiguously distributed among different taxa.

3.2.6. Analysis of new expression data

In addition to our wood-decay omics in *A. ostoyae* and *A. cepistipes*, we analyzed RNA-Seq data from two new *in vitro* pathosystems (for *A. ostoyae, A. borealis* and *A. luteobubalina*), for which experiments were originally performed by our collaborators (*Prof. György Sipos and Dr. Jonathan Plett*). These included *in vitro* fresh stem invasion assays with highly and less-virulent isolates of both *A. ostoyae* and *A. borealis* and *in planta* time-series experiment of *A. luteobubalina* infecting *Eucalyptus grandis* seedlings from 24 hours to 2 weeks. For the stem invasion assay, the estimated counts matrix was used for differential expression analysis using Limma-Voom (Ritchie et al., 2015). Prior to running the differential expression analysis, counts were normalized using TMM using edgeR v3.38.1 (Robinson et al., 2010) and lowly expressed genes (cpm ≤ 10) were filtered. Differential gene expression analysis for the *in-planta* pathosystem data were carried out as explained in the previous section sub-chapter (3.1.3).

In both analyses, at least two-fold gene expression change between samples and FDR value <=0.05 were considered statistically significant. Multidimensional scaling ("plotMDS" function in edgeR) was applied to visualize gene expression profiles. Expression heatmaps were generated by hierarchically clustering based on the average linkage of FPKM values with heatmap.2 function from gplots package.

Chapter 4. Results

4.1. Mycelium is the key player in wood decay

4.1.1. Morphological observations from wood-decay setup

We introduced sterilized spruce roots into week-old cultures of *A. ostoyae* and *A. cepistipes* and incubated them at 25^{o}C in the dark for 3-4 weeks until the roots were fully colonized. Abundant mycelial growth was observed on and under the bark layer (Figure 5). Although previous studies suggested that colonization occurs through direct contact with and penetration of the rhizomorphs into the wood (Baumgartner et al., 2011; Leach, 1937; Pronos and Patton, 1978; Redfern, 1978; Sipos et al., 2018, 2017; Wong et al., 2020; Yafetto et al., 2009), we found no evidence of mechanical penetration of the rhizomorphs into the wood. Instead, the rhizomorphs switch to hyphal growth upon contact with the root and continue to spread as mycelium (Figure 5). Both species exited the root section as rhizomorphs that grew out of the piece of wood. These observations suggest that mycelium might be the primary colonizing structure of the wood, which is consistent with the higher surface-to-volume ratio of hyphae, which are more suitable for a nutrient acquisition than rhizomorphs. Rhizomorphs probably develop much later, possibly to transfer nutrients, as is often seen commonly under the bark of decayed logs (Baumgartner et al., 2011).

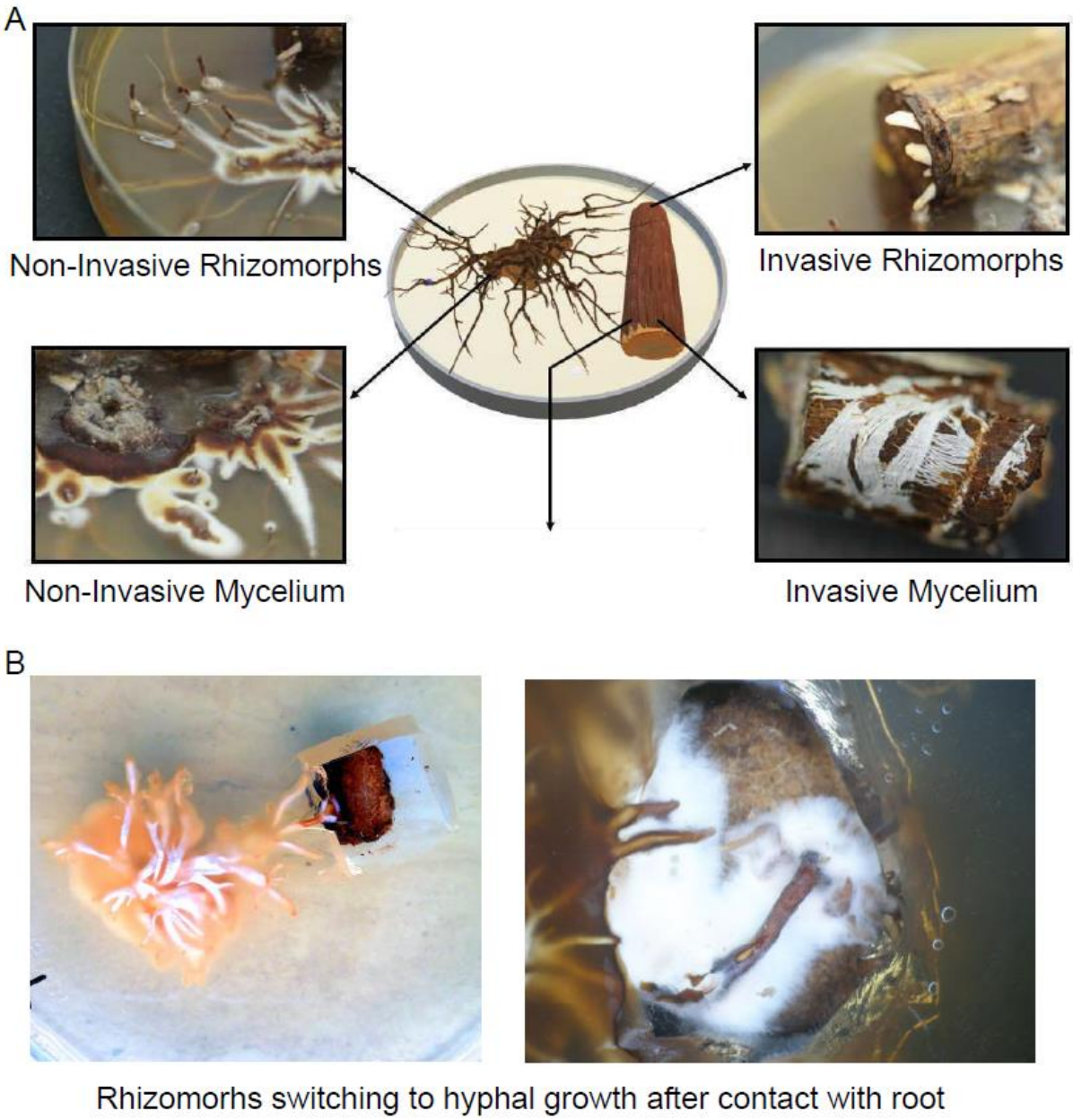

Figure 5: Overview of the experimental approach for root decay studies. A) Representation of tissue types sampled for transcriptomics and proteomics analysis viz. invasive mycelium (growing beneath the outer layer of the root), invasive rhizomorphs (emerging out of the roots), non-invasive mycelium, and non-invasive rhizomorphs (Armillaria growing in absence of root). B) Pictures showing rhizomorphs differentiating into hyphae in contact with the spruce root.

4.1.2. Overview of wood-decay -omics data

Four tissue types from both species in three biological replicates were analyzed using transcriptomics and proteomics (Figure 6). The mycelium and rhizomorphs collected from colonized roots are hereafter referred to as invasive mycelium (M) and invasive rhizomorph (R), while those grown in the absence of roots are referred to as non-invasive mycelium (NIM) and non-invasive rhizomorphs (NIR), respectively. This resulted in 12 samples for both *A. ostoyae* and *A. cepistipes*.

Ribosomal RNA-depleted libraries and sequenced them to a depth of 46.7-93.4 million paired-end reads on the Illumina NextSeq 500 platform were performed by SeqOmics Biotechnology Ltd., Mórahalom, Hungary. On average, 69% and approximately 38% of reads mapped to the transcripts in *A. ostoyae* and *A. cepistipes*, respectively. Concerning the low mapping percentages in *A. cepistipes* we find that they were either with genomic DNA contamination or a poor annotation of the reference species (~50% of unmapped reads mapped to intergenic regions rather than transcripts). Although such factors can dampen the signal of differential gene expression, we found that in our case this did not significantly compromise our differential gene expression analysis (see the clear separation of samples in the multi-dimensional scaling (MDS) and the high number of differentially expressed genes (DEGs), Figure 6 and Figure 7A, B). At the same time, there was a limited correlation between the fold-change values acquired for transcripts and proteins (Figure 8), which is not unusual among proteomic and transcriptomic datasets. Additionally, SuperSeq revealed that the analysis detected 86-92% of DEGs in *A. cepistipes* in the M and R when compared to their non-invasive counterparts, whereas, in *A. ostoyae*, we could variably detect 70-90% of DEGs in the same sample comparisons (Figure 9A). Label-free comparative proteomics provided a total of 37,879 and 36,087 peptides were identified from *A. ostoyae and A. cepistipes*, respectively, which were subsequently grouped into protein groups, with mean protein sequence coverage ranging from 30.1 to 34%.

MDS plots show strong clustering of biological replicates in both transcriptomic and proteomic data of both species. The MDS plots show a clear separation of the M and NIM samples, while the invasive R and the NIR show similarity (Figure 6), suggesting that the greater difference is between invasive and NIM. In *A. ostoyae*, RNA-Seq detected and quantified 17,198 transcripts, while label-free proteomic analysis detected 3,177 proteins. For *A. cepistipes*, we obtained data for 15,861 transcripts and 3,232 proteins (Figure 7A). The overlap between the two -omics datasets was substantial, with approximately 99.8% of the detected proteins also present in the RNA-Seq data (Figure 7A).

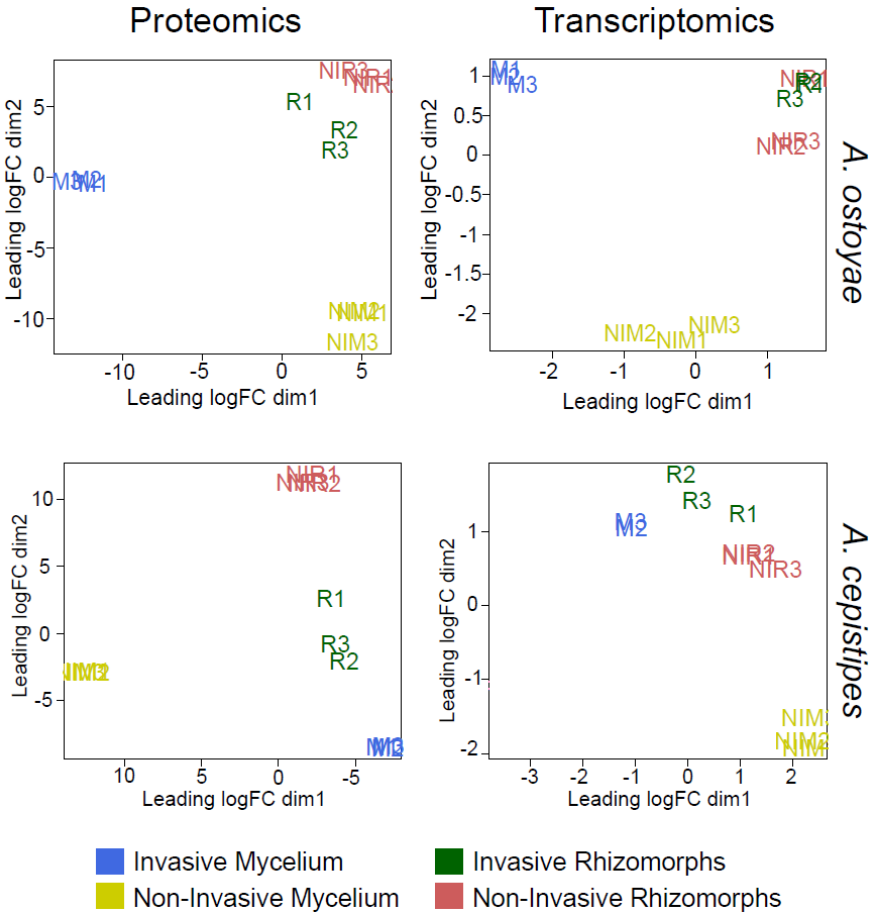

Figure 6: Multidimensional scaling of three biological replicates from each of the tissue types in A. ostoyae (top) and A. cepistipes (bottom) for proteomics (left) and transcriptomics (right). Replicates are colored according to sample types. (M: invasive mycelium, R: invasive rhiopmorphs, NIM: non-invasive mycelium and NIR: non-invasive rhizomorphs)

Analyses were performed to identify DEGs. In *A. ostoyae*, we found 987 and 35 up-regulated genes ($log_2FC > 1$, p-value < 0.05) in M*vs*NIM and R*vs*NIR, respectively (5.74% and 0.2% of the transcriptome). Considerably more, 2,108 and 327 genes were upregulated in M*vs*NIM and R*vs*NIR in *A. cepistipes* (13.29% and 2.06% of the transcriptome, respectively). The number of DAPs in the proteomic analysis was lower: we detected 279 and 108 proteins with increased abundance in M*vs*NIM and R*vs*NIR in *A. ostoyae* (8.78 and 3.40% of the detected proteome, respectively) and 439 and 282 proteins with increased abundance in M*vs*NIM and R*vs*NIR in *A. cepistipes* (13.58 and 8.73% of the detected proteome, respectively).

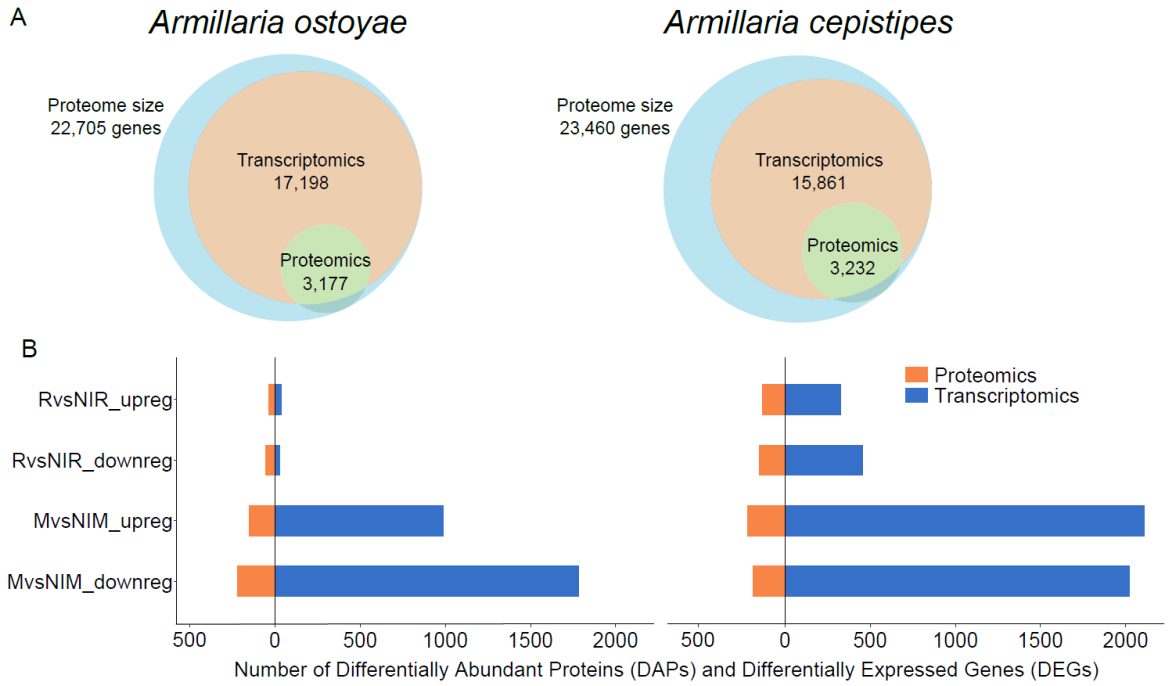

Figure 7: Overview of transcriptomics and proteomics analyses. A) Proportion and number of transcripts and proteins detected in the two -omics analysis. Blue circle represents the whole proteome, orange depicts the transcripts detected in the RNASeq, and green represents the proteins detected in the proteomics analyses. B) The number of differentially expressed genes (DEG, blue) and differentially abundant proteins (DAP, orange) detected in the two species. Sample comparisons analyzed for DAPs and DEGs are shown on the y-axis.(MvsNIM: invasive mycelium vs non-invasive mycelium and RvsNIR: invasive rhizomorphs vs non-invasive rhizomorphs)

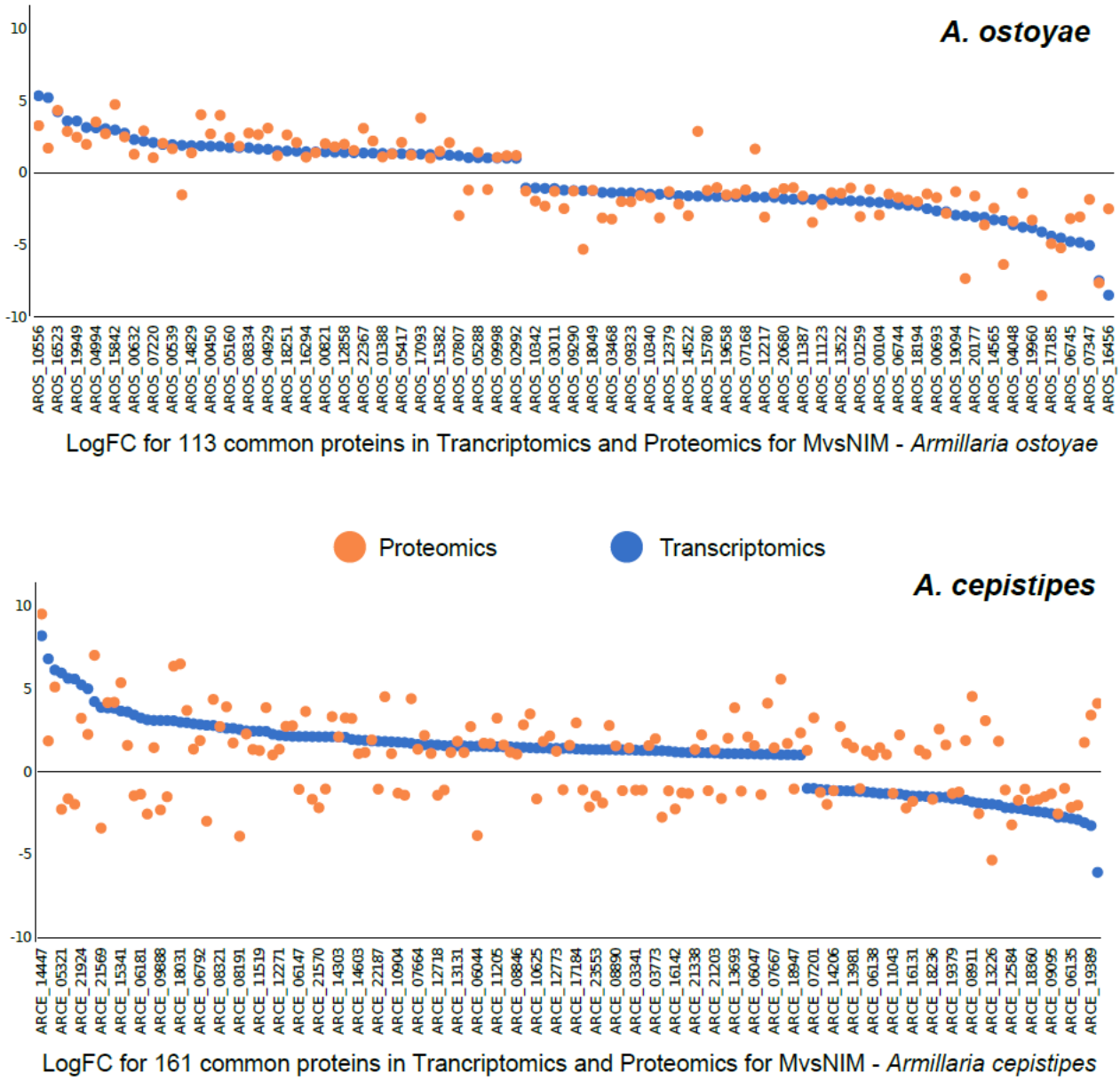

Figure 8: Log fold changes in MvsNIM of genes identified in both transcriptomics and proteomics data in A. ostoyae (top) and A. cepistipes (bottom). The logFC for transcripts (blue) are arranged from increasing to decreasing order, overlaid with logFC from proteomics (orange) showing a limited correlation between the two omics approaches. (MvsNIM: invasive mycelium vs non-invasive mycelium)

We found considerably more DEGs/DAPs in the mycelium than in the rhizomorphs in both species (Figure 7), suggesting that the mycelium is more active in colonizing wood tissues than the rhizomorphs. This is consistent with the morphological observations and an invasion of roots mainly by individual hyphae. A more surprising observation is that the saprotrophic *A. cepistipes* has a higher number of DEGs/DAPs than the pathogenic *A. ostoyae* (Figure 7). To confirm that this was not due to higher baseline expression of some genes in *A. ostoyae*, we compared the distribution of raw expression values of OrthoFinder clustering-based co-orthologs in the M and NIM samples of *A. cepistipes* (Figure 9). This showed that the baseline expression of genes in non-invasive mycelia of *A. ostoyae* was not higher than that in *A. cepistipes*, suggesting that the higher number of DEGs in *A. cepistipes* is indeed the result of the stronger response of this species to wood. We speculate that this is because saprotrophs, in order to gain a competitive advantage over other microbes, have to colonize/degrade wood more rapidly than necrotrophs such as *A. ostoyae*, which can both feed on living parts of the tree and upon killing the host, can be the first colonizers of the wood (Shi et al., 2019; Sipos et al., 2017).

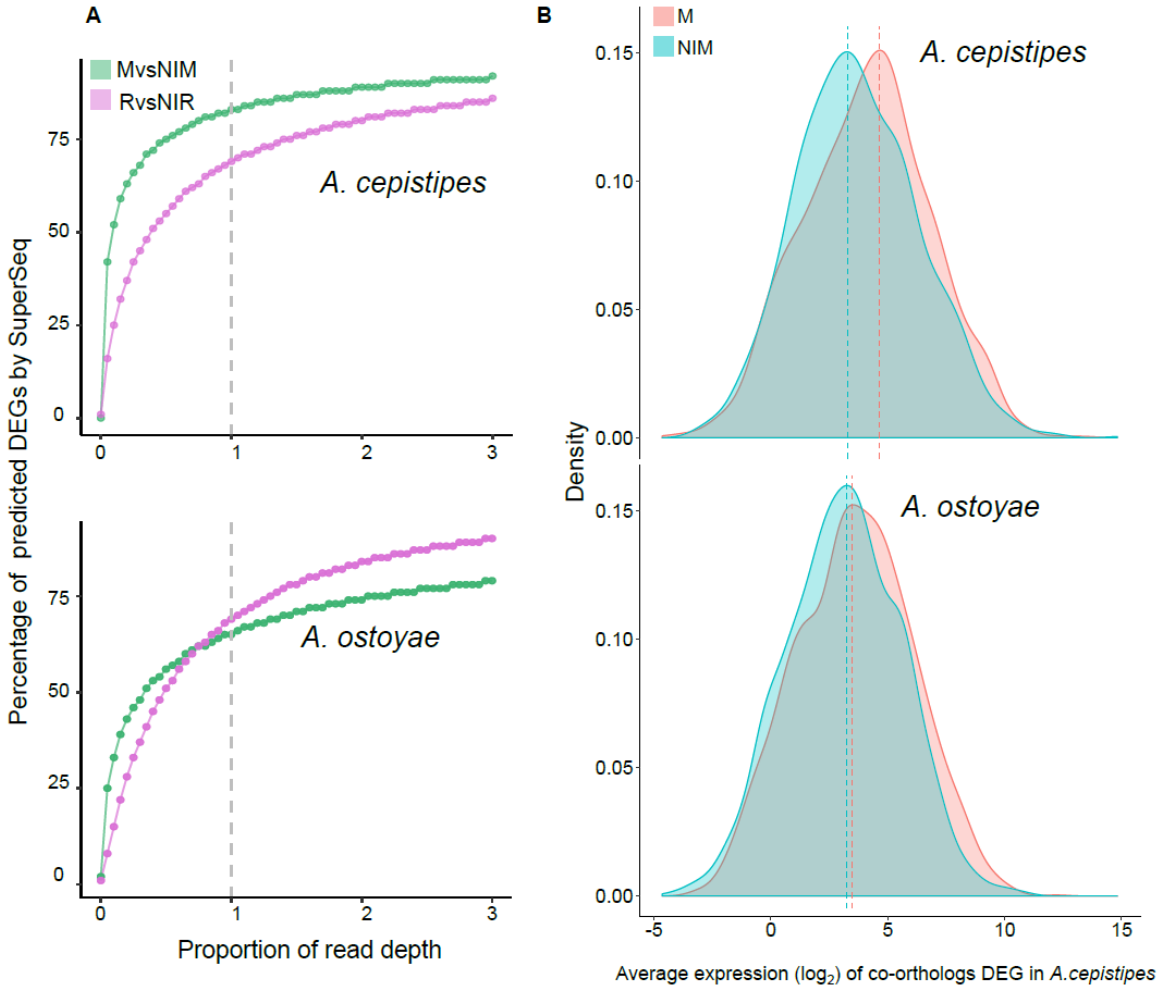

Figure 9: Validation of transcriptomics data and baseline gene expression. A) SuperSeq analyses of transcriptomics data in A. ostoyae and A. cepistipes. Percentage of differentially expressed genes (y-axis) obtained at current (dashed vertical line) and estimated proportion read depth (x-axis) for different sample comparisons. Colors represent different sample comparisons. B) Distribution of raw expression values (log_2 transformed) in both species for co-orthologs differentially expressed in MvsNIM of A. cepistipes. Baseline expression of genes in non-invasive mycelia (green) of A. ostoyae was not higher than that in A. cepistipes, indicating a stronger response of A. cepistipes invasive mycelia to wood. (MvsNIM: invasive mycelium vs non-invasive mycelium and RvsNIR: invasive rhizomorphs vs non-invasive rhizomorphs)

4.1.3. Enrichment analysis for Gene Ontology (GO)

In the transcriptomics data, we found 25 and 11 GO terms significantly enriched (*p < 0.05, Fisher's exact test*) among upregulated genes in MvsNIM and RvsNIR, respectively. In contrast, the proteomics data revealed 18 and 12 significantly enriched terms in MvsNIM and RvsNIR, respectively (Figure 10). We observed a similar pattern, with more enriched GO terms in *A. cepistipes* than in *A. ostoyae*. In transcriptomics, we found 57 and 29 GO terms significantly enriched among upregulated genes in MvsNIM and RvsNIR, respectively, followed by 35 and 19 terms in MvsNIM and RvsNIR for proteomics data. (Figure 11). Terms enriched in M vs NIM included pectinesterase activity (GO:0030599), polygalacturonase activity (GO:0004650), cellulase activity (GO:0008810), cellulose binding (GO:0030248), carbohydrate binding (GO:0030246), hydrolase activity (GO:0004553), and cell wall modification (GO:0042545), cell wall-related terms (GO:0005199, GO:0009277, GO:0005618), and carbohydrate metabolic processes (GO:0005975).

In both species, genes upregulated in M were enriched in terms related to oxidation-reduction process (GO:0055114), lipid metabolic process (GO:0006629), transmembrane transport (GO:0055085, GO:0034755, GO:0005381), iron ion (GO:0005506), and heme-binding (GO:0020037) processes, as well as for the terms fungal type cell wall (GO:0009277) and structural constituent of cell wall (GO:0005199). We find that the enrichment of terms related to iron binding (GO:0005506) was possibly driven by the upregulation of members of the high-affinity iron permease complex (2 of 3 genes and 1 of 2 genes upregulated in *A. ostoyae* and *A. cepistipes*, respectively, see below). Consistent with the lower number of DEGs in R*vs*NIR, we observed much fewer enriched GO terms in the genes upregulated in rhizomorphs.

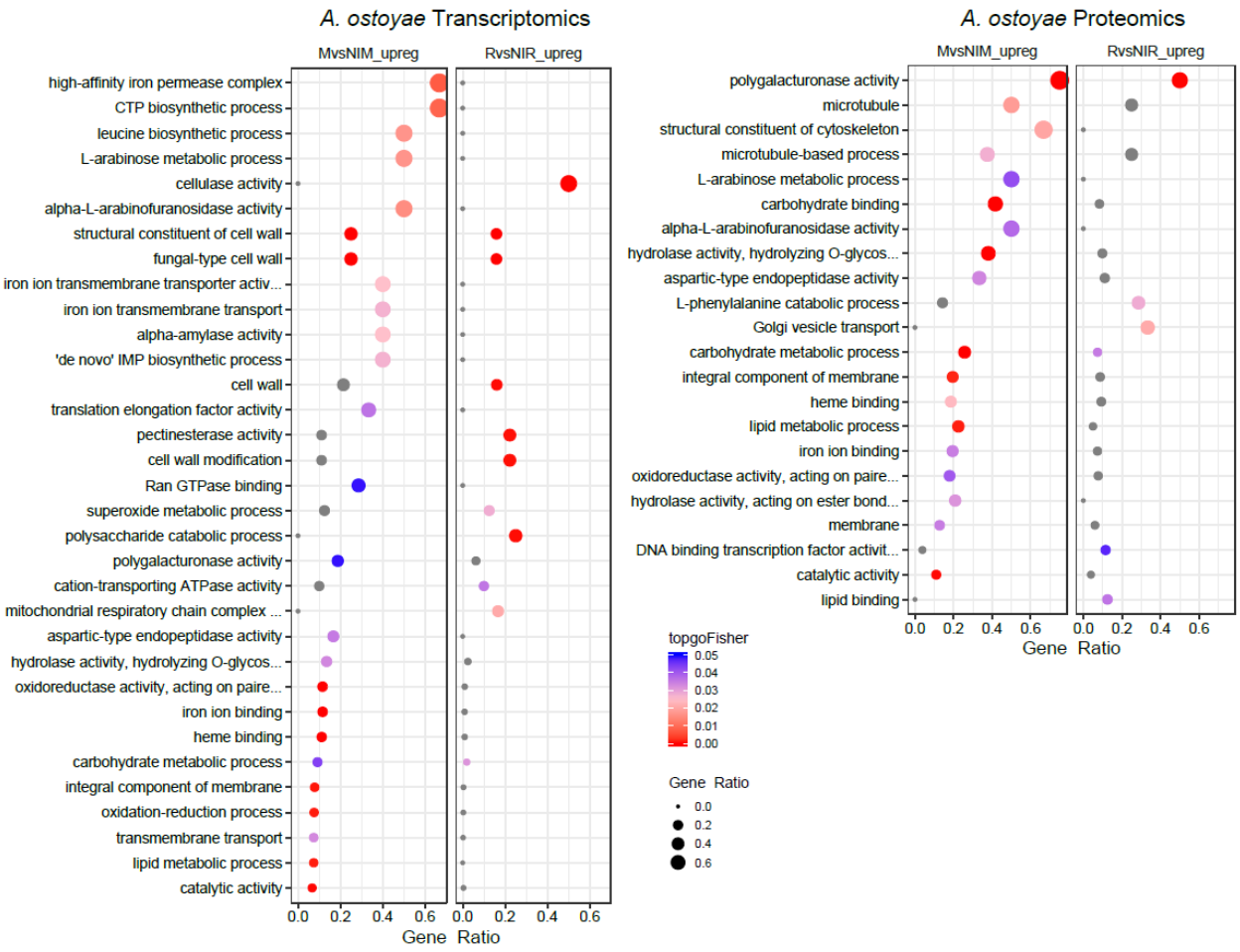

Figure 10: Enriched GO terms in MvsNIM and RvsNIR of A. ostoyae for transcriptomics (left) and proteomics (right). The ratio of the number of a GO term in a specific comparison to the total number of that GO term for a species was used to plot gene ratios for enriched GO terms ($p<0.05$, Fisher's exact test). Size of the dot is directly proportional to the gene ratio, and the color of the dots corresponds to p-values. Grey dots represent GO terms, enriched in only one of the comparisons i.e either MvsNIM or RvsNIR. (MvsNIM: mycelium vs non-invasive mycelium or in RvsNIR: rhizomorphs vs non-invasive rhizomorphs)

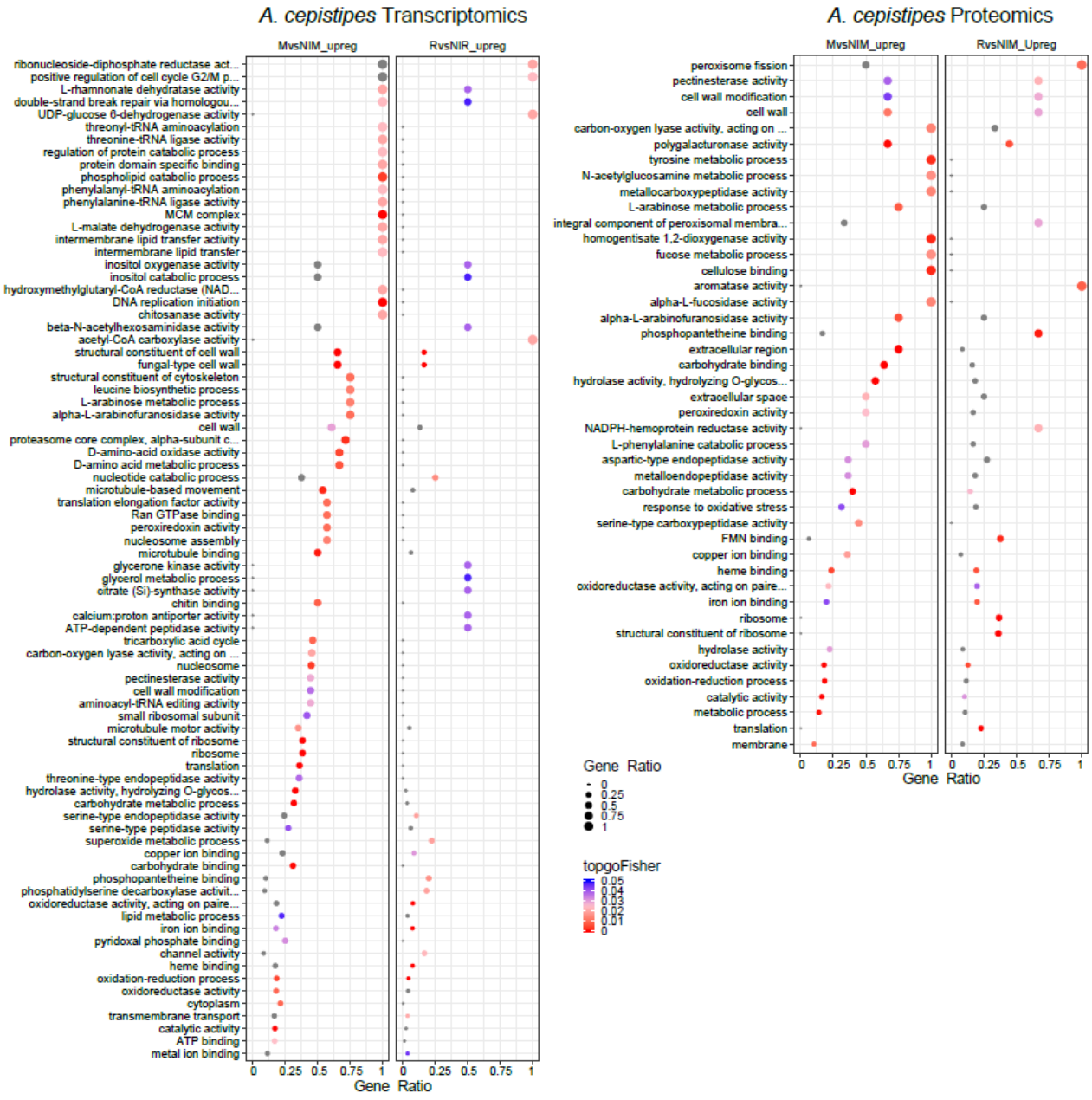

Figure 11: Enriched GO terms in MvsNIM and RvsNIR of A. cepistipes for transcriptomics (left) and proteomics (right). The ratio of the number of a GO term in a specific comparison to the total number of that GO term for a species was used to plot gene ratios for enriched GO terms ($p<0.05$, Fisher's exact test). Size of the dot is directly proportional to the gene ratio, and the color of the dots corresponds to p-values. Grey dots represent GO terms, enriched in only one of the comparisons i.e either MvsNIM or RvsNIR. (MvsNIM: mycelium vs non-invasive mycelium or in RvsNIR: rhizomorphs vs non-invasive rhizomorphs)

4.1.4. Global transcriptome and proteome similarity

We measured global similarity between transcriptomes and proteomes within and between species based on the Pearson correlation coefficient. The similarity between the sample types was assessed based on 11,630 co-orthologous genes in *A. ostoyae* and *A. cepistipes* identified with OrthoFinder (Emms and Kelly, 2015), with transcriptomic and proteomic data covering 10,675 and 2,404 co-orthologous genes, respectively. A surprisingly high correlation was observed between the invasive mycelia of *A. ostoyae* and *A. cepistipes* (Figure 12), whereas the correlation was comparatively lower for all other combinations. This observation was similar for both transcriptomic and proteomic data and was even more pronounced when we considered only genes/proteins that were DEG or DAP in at least one of the species (Figure 13).

Within species, we observed limited differences among transcriptomes, with the highest global transcriptome similarity values observed between invasive tissue types (Figure 13A). For instance, in *A. ostoyae*, the two most similar sample types were invasive mycelium and invasive rhizomorphs (mean Pearson coefficient: 0.92), slightly higher than in other combinations of samples (0.83-0.88). A similar but stronger pattern was observed in *A. cepistipes* (Figure 13A). This suggests that contact with wood induces similar expression changes regardless of tissue type. In support of this, we identified 4 genes that were upregulated in both invasive mycelium and invasive rhizomorphs of *A. ostoyae* and 127 genes upregulated in both invasive mycelium and invasive rhizomorphs of *A. cepistipes*. The majority of these genes were annotated as hydrophobin-domain-containing proteins, cytochrome P450s, galactose-binding domain-like proteins, and a number of CAZymes among others.

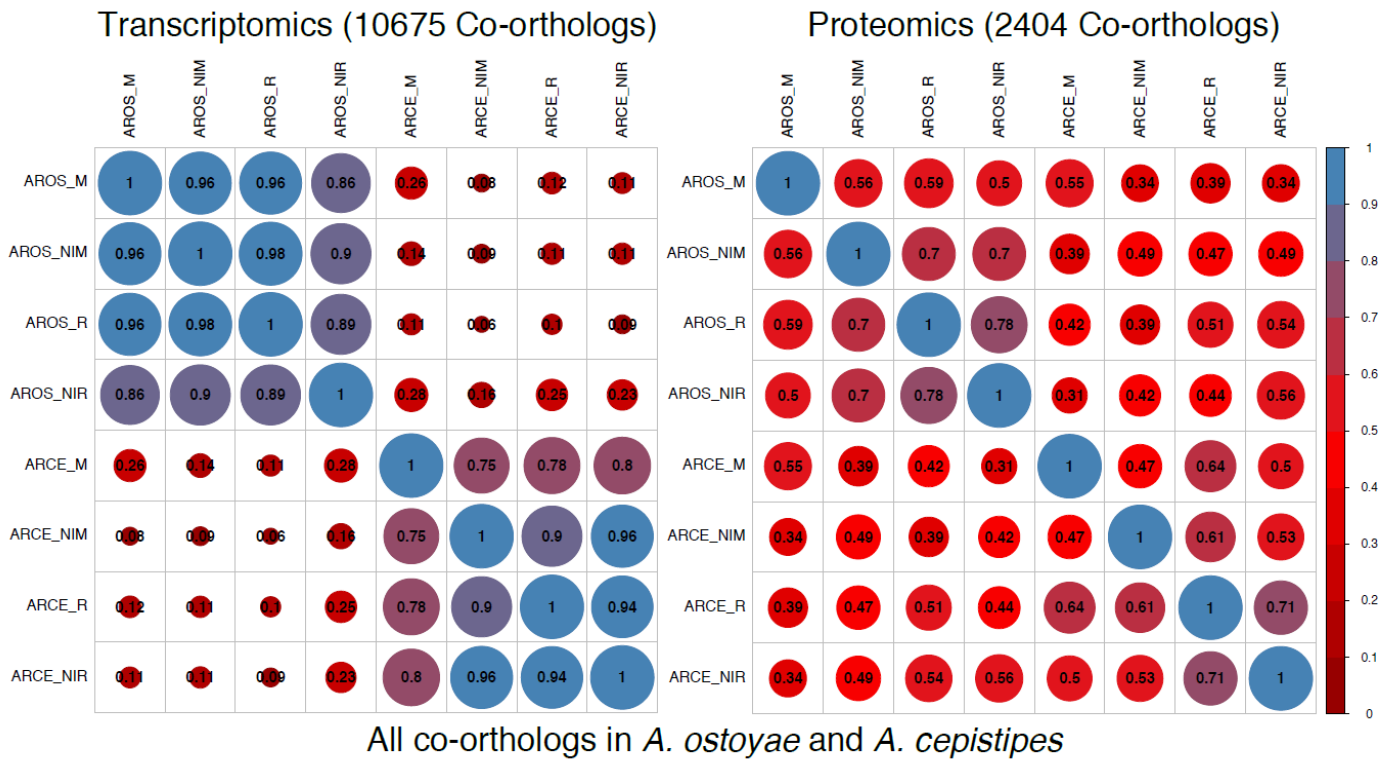

Figure 12: Correlogram for all co-orthologs in the two species, showing the correlation between samples across the two species. Blue represents a higher correlation and red represents lower. The size of the circle is directly proportional to a higher correlation. Pairwise mean Pearson correlation coefficients are indicated as numbers in the circles. .(AROS: A. ostoyae, ARCE: A. cepistipes, M: invasive mycelium, NIM: non-invasive mycelium, R: invasive rhizomorphs, NIR: non-invasive rhizomorphs)

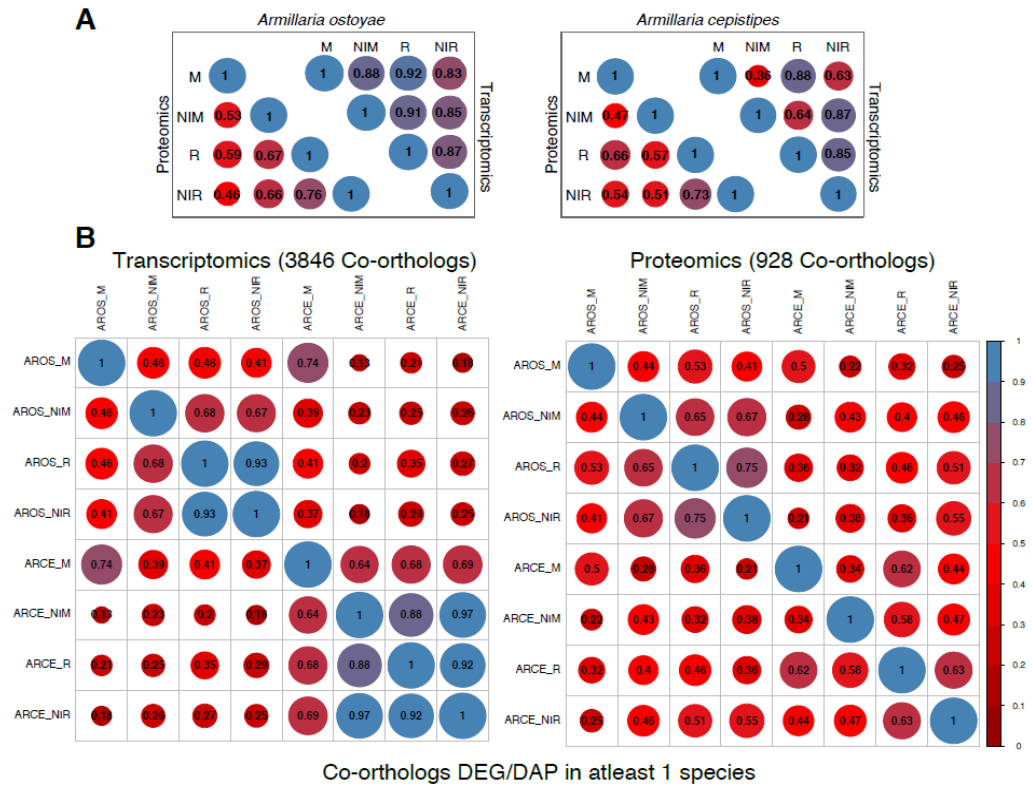

Figure 13: Global omics similarity between A. ostoyae and A. cepistipes. A) Correlation between the 4 tissue types for proteomics and transcriptomics data in A. ostoyae (left) and A. cepistipes (right). B) Correlation between co-orthologs differentially expressed/abundant in at least one species. Size of the circle is proportional to the correlation and correlation coefficients are written as numbers in the circles. (AROS: A. ostoyae, ARCE: A. cepistipes, M: invasive mycelium, NIM: non-invasive mycelium, R: invasive rhizomorphs, NIR: non-invasive rhizomorphs)

4.1.5. Shared transcriptomic response of mycelia

We interpret the between-species correlation of gene expression pattern in the invasive mycelium of both species in response to spruce roots, as the shared response. We further investigated the gene families accounting for the observed shared response to wood, by focusing on co-orthologous gene pairs that showed up- or down-regulated in invasive mycelia of both species. We found a total of 779 co-orthologous genes with similar differential gene expression patterns in invasive mycelium, with 372 genes being significantly up-regulated and 407 genes being significantly down-regulated in the invasive mycelium of *A. ostoyae* as well as *A. cepistipes*. Among the 372 shared up-regulated co-orthologs, we observed higher overall fold changes and expression levels in *A. cepistipes* than in *A. ostoyae* (Figure 14, Figure 15), again highlighting a stronger response of *A. cepistipes* to wood.

Among the top 20 up-regulated co-orthologs with the highest fold changes between M*vs*NIM in the transcriptomic analyses, we found oxoglutarate/iron-dependent dioxygenases, galactose-binding-like domain superfamily proteins, ricin B lectins, hydrophobins, intradiol ring cleavage dioxygenases, GMC oxidoreductases, cytochrome P450-s, and 10 conserved transcription factors several unannotated genes (Figure 15). The most highly induced genes in both species were oxoglutarate/iron-dependent dioxygenases. This superfamily is widely distributed in microorganisms, fungi, plants, and mammals (Bhattacharya et al., 2012; Farrow and Facchini, 2014; Kawai et al., 2014; Korvald et al., 2011) but their versatility makes them difficult to interpret in terms of their precise biological significance in the mechanisms of wood rot. However, this superfamily has been speculated to have roles in organic substrate oxidation, mycotoxin production, and secondary metabolite biosynthesis (Arvind and Koonin, 2001; Korvald et al., 2011; Martinez and Hausinger, 2015) and were reported to be upregulated in white rot and brown rot wood decay studies (Moody et al., 2017; Shah et al., 2016; Young et al., 2015). We found 46 oxoglutarate/iron-dependent dioxygenase genes in both species, of which 5 and 9 were upregulated in the invasive mycelium of *A. ostoyae* and *A. cepistipes*,

respectively (but not in invasive rhizomorphs). In proteomics, we found one and four genes in the invasive mycelium and one and two genes in the invasive rhizomorphs with increased abundance in *A. ostoyae* and *A. cepistipes*, respectively.

In the proteomics data, we found 89 co-orthologs with increased abundance and 45 with decreased abundance in both species (Figure 14, Figure 15), of which those with the highest abundance in both species included the CAZy families GH31, GH3, GH88, GH92, as well as aspartic peptidases, fungal lipases, and FCW-associated Kre9/Knh1. Proteins detectable only in the M and not in NIM, included several CAZymes such as pectin lyases, GH28, carbohydrate-binding modules (CBMs), polysaccharide lyases (PL8), glycoside hydrolases (GH3, GH35), galactosidases, carboxylesterases, and several other gene families such as GMC oxidoreductases, various transporters, and cytochrome P450s.

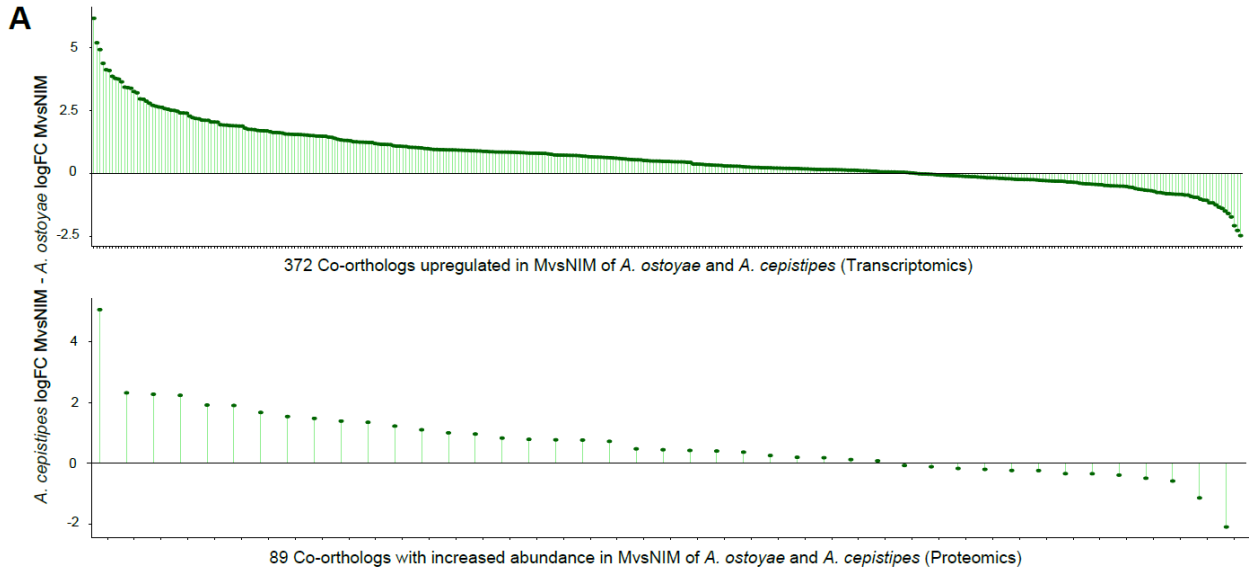

Figure 14: Expression dynamics of shared upregulated co-orthologous genes in mycelia of both species towards the spruce roots (MvsNIM. logFC differences of co-orthologs DEG (up) and DAP (down) in both species, For proteomics, only genes for which a fold change could be calculated are shown (43 out of 89 orthologs).(MvsNIM: insavive mycelium vs non-invasive mycelium)

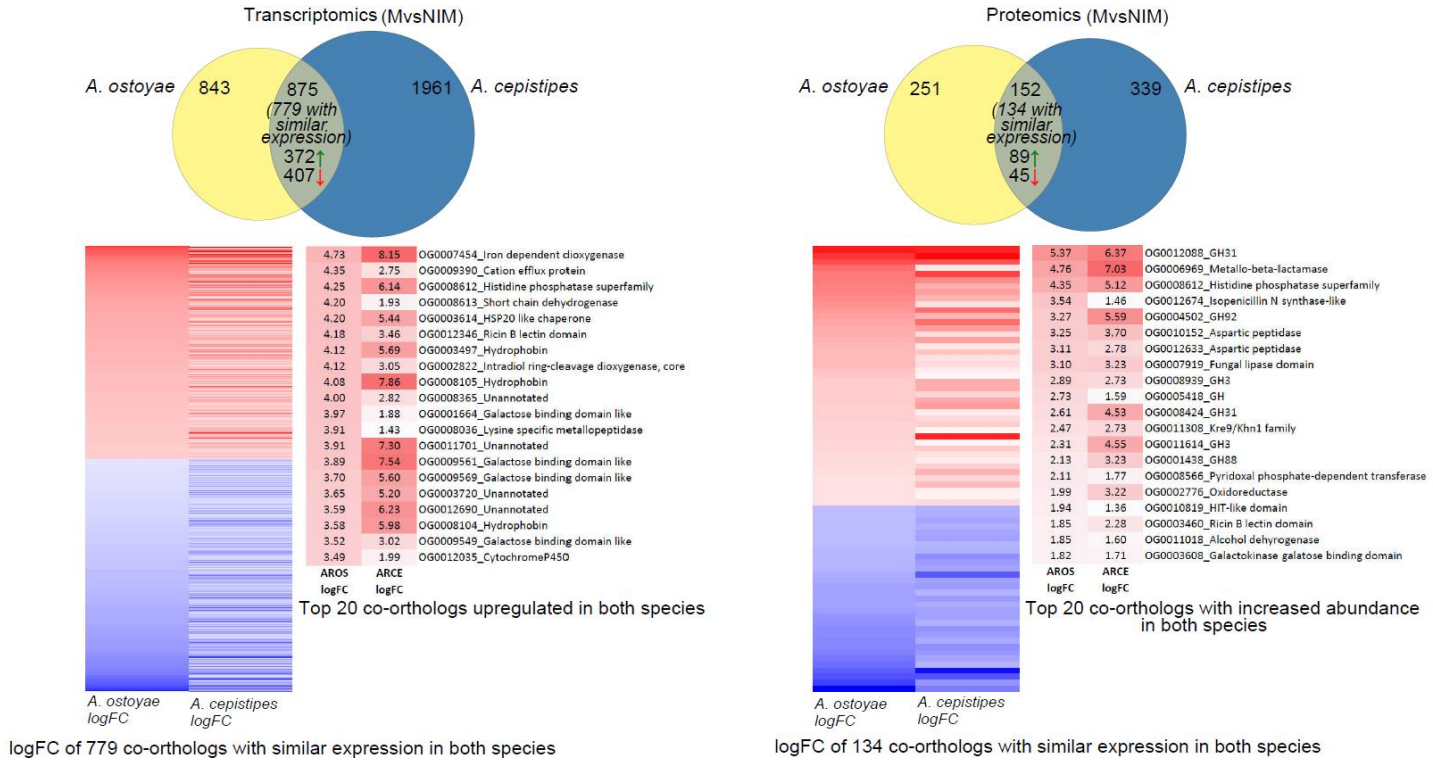

Figure 15: Shared response between mycelia of A. ostoyae and A. cepistipes in response to spruce roots in transcriptomics (left) and proteomics (right) analyses. Venn diagram represents species-specific and common DEG/DAPs in A. ostoyae and A. cepistipes. Heatmap below represents co-orthologs with similar expression patterns (upregulated/downregulated in both species). Next to the heatmap are the top 20 upregulated proteins (red) in the two species. (MvsNIM: mycelium vs non-invasive mycelium)

4.1.6. Characteristic PCWDE expression in invasive mycelia

A diverse array of plant PCWDEs were found to be differentially expressed in the invasive tissues of both species. Overall, the number of up-regulated PCWDEs was much higher in the invasive mycelium than in the invasive rhizomorphs compared to their non-invasive counterparts (Figure 16). The saprotrophic *A. cepistipes* had a higher number of DEG /DAP PCWDEs than the pathogenic *A. ostoyae* (Figure 16). Among the differentially expressed PCWDEs in the mycelium compared to the NIM, up-regulated pectinases were the most numerous, accounting for 17% and 37% of all pectinases in *A. ostoyae* and *A. cepistipes*, respectively. These were followed by cellulases (9%, 27%), hemicellulases (11%, 30%), and expansins (12%, 10%) (Figure 16). We found that most genes related to lignin degradation (Table 1) were down-regulated in both species, with none up-regulated in *A. ostoyae* and six genes up-regulated in *A. cepistipes* (Figure 16). In the invasive mycelia of *A. ostoyae* and *A. cepistipes*, we found one and eight upregulated LPMOs/GH61, respectively, which have been reported to promote cellulose degradation together with cellobiohydrolases (Beeson et al., 2012; Bey et al., 2013; Levasseur et al., 2013; Li et al., 2012; Morgenstern et al., 2014; Quinlan et al., 2011).

Our analyses also revealed upregulation of both pectinolytic PCWDEs and expansins (Figure 16), indicating hallmarks of early- stage of wood decay. In previous time series studies, strong expression of pectinase expression was observed in the early stages of wood decomposition, suggesting that early pectinolytic "pretreatment" (Presley et al., 2018; Zhang et al., 2016) is required to make plant cell wall structure accessible, followed by a wave of expression of non-pectinolytic GHs. Previous studies (Zhang et al., 2016) also observed that early stages of wood rot were characterized by increased expression of expansins and GH28 pectinases, suggesting enzymatic and mechanical loosening of plant cell walls for easier access to cellulose and hemicellulose components. Our observations of pectinolytic PCWDE and expansin expression are consistent with this.

In contrast, we detected less lignin-degrading AAs to be DEG /DAP in the two

species, most of which were down-regulated, suggesting that lignin was not significantly targeted by *Armillaria* in our experiments. The chemical composition of spruce roots was reported to have high lignin content (25–28%) followed by cellulose, hemicellulose, and extractives (Wang et al., 2018), yet our study revealed a general downregulation of LDEs. Based on our literature-based assignment of CAZymes to their respective substrate preferences (Table S1), we identified 39 genes each in *A. ostoyae* and *A. cepistipes*, that were annotated as lignin-degrading genes. These genes belonged to various enzyme families, including class II peroxidases (AA2, AA2_dist), laccases (AA1, AA1_1, AA1_2, AA1_3, AA1_dist), and other alcohol oxidases (AA3, AA5). Of the 39 lignin-degrading genes in *A. ostoyae*, we found 6 genes to be downregulated in the mycelium in response to spruce roots (MvsNIM). No genes were upregulated in *A. ostoyae*. In *A. cepistipes*, we found 12 downregulated and six upregulated lignin-degrading genes under the same conditions (MvsNIM). The modest induction and overall downregulation of ligninolytic genes are notable for white-rot fungi, especially in light of previous studies reporting measurable laccase or peroxidase enzyme activities only at the early stage of wood decay by white-rot fungi (Presley et al., 2018; Qin et al., 2018). On the other hand, the absence of a ligninolytic burst is consistent with the underrepresentation of ligninolytic gene families in *Armillaria* compared to other white-rot Agaricales (Sipos et al., 2017).

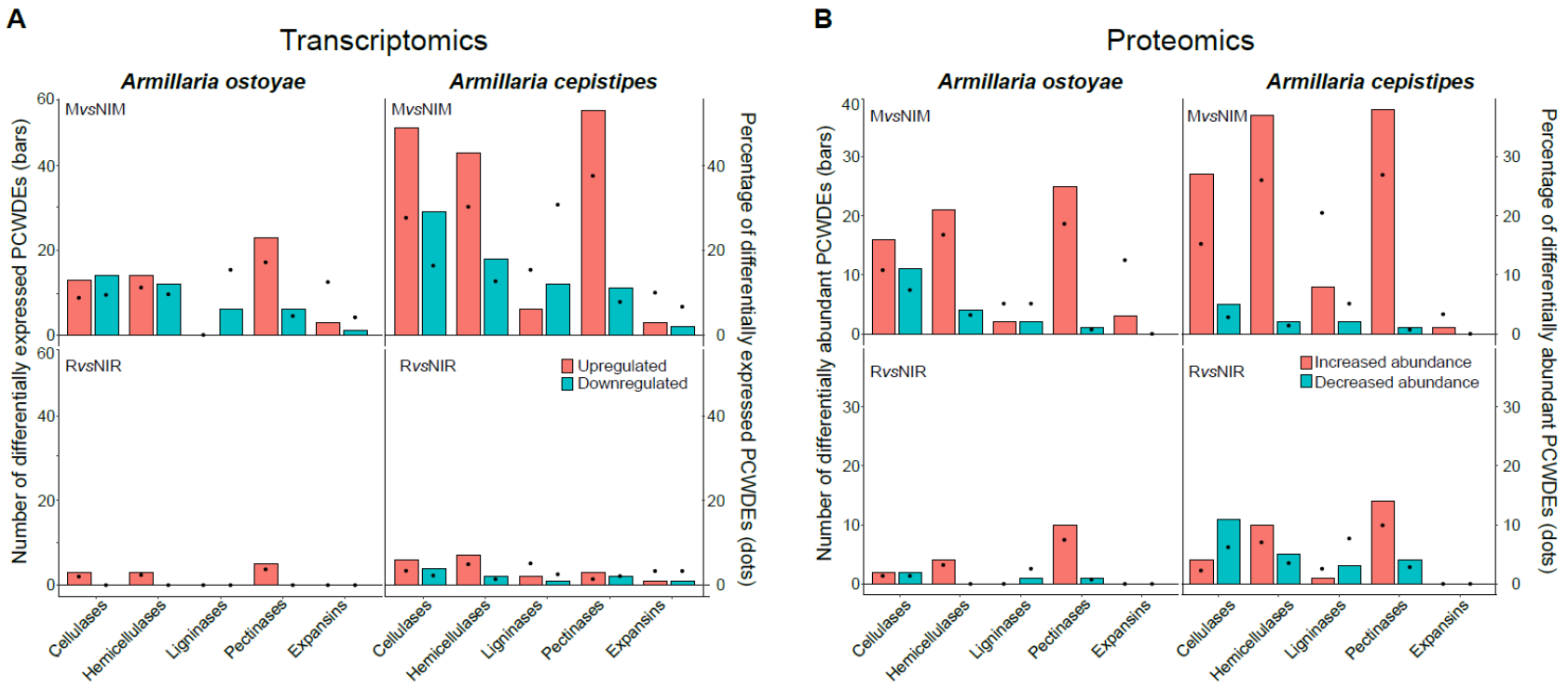

Figure 16. Differentially expressed/abundant plant cell wall degrading enzymes in the two species. Barplot showing number, and dots showing the percentage of DEG/DAP PCWDEs in the two species in MvsNIM (top) and RvsNIR (bottom) in transcriptomics (A) and proteomics (B) data. CAZYmes are classified on the basis of their substrate in the plant cell wall (Table S1) showing the number of genes upregulated/increased abundance (orange) and downregulated/decreased (green) in the two species. (MvsNIM: mycelium vs non-invasive mycelium or in RvsNIR: rhizomorphs vs non-invasive rhizomorphs)

Table 1: Log_2 fold changes of differentially expressed genes in MvsNIM with putative roles in lignin degradation

Armillaria ostoyae

ProtID	logFC	Status
Armosto1_253375	*-3.37*	*Downreg*
Armosto1_256681	*-2.60*	*Downreg*
Armosto1_264507	*-2.39*	*Downreg*
Armosto1_256317	*-1.26*	*Downreg*
Armosto1_268395	*-1.23*	*Downreg*
Armosto1_266072	*-1.21*	*Downreg*

Armillaria cepistipes

ProtID	logFC	Status
Armcep1_22260	*-5.39*	*Downreg*
Armcep1_14336	*-5.38*	*Downreg*
Armcep1_11212	*-5.16*	*Downreg*
Armcep1_11216	*-3.34*	*Downreg*
Armcep1_1253	*-2.83*	*Downreg*
Armcep1_237	*-2.76*	*Downreg*
Armcep1_22148	*-1.96*	*Downreg*
Armcep1_18106	*-1.85*	*Downreg*
Armcep1_15173	*-1.63*	*Downreg*
Armcep1_13155	*-1.17*	*Downreg*
Armcep1_3961	*-1.09*	*Downreg*
Armcep1_18768	*-1.05*	*Downreg*
Armcep1_18865	*1.07*	*Upreg*
Armcep1_7635	*2.79*	*Upreg*
Armcep1_11572	*2.81*	*Upreg*
Armcep1_8298	*3.32*	*Upreg*
Armcep1_18554	*3.32*	*Upreg*
Armcep1_6915	*6.42*	*Upreg*

MvsNIM: Invasive mycelium vs Non-invasive mycelium

4.1.7. Upregulation of transporters in rhizomorphs

To investigate the expression of transporters in our wood-decay system, we identified putative transporters from *A. ostoyae* and *A. cepistipes* that were localized to the plasma membrane and has transport related IPR annotations. We identified 612 and 602 transporters in *A. ostoyae* and *A. cepistipes*, respectively, majorly comprising genes with annotations like MFS domain, ABC transporters, sugar transporters, amino acid/polyamine transporters, and P-type ATPases. Transcriptomics provided dynamics for a much larger number of transporters than proteomics, possibly due to the difficulties in extracting membrane proteins for LC /MS analyses. In the RNA-Seq data, we found 45 and 84 up-regulated, and 96 and 105 down-regulated transporters in the M*vs*NIM of *A. ostoyae* and *A. cepistipes*, respectively (Figure 17). The majority of transporters up-regulated in M*vs*NIM belonged to the MFS and the sugar transporter family. Considerably lower numbers of upregulated transporters were found in rhizomorphs: 2 and 20 upregulated in *A. ostoyae* and *A. cepistipes*, respectively, from the same families.

A striking difference in the expression of transporters was found in the rhizomorphs when compared to invasive mycelium (RvsM) (Figure 17). We found 120 transporters in *A. ostoyae* and 100 transporters in *A. cepistipes* that were upregulated in the RvsM condition. The number of downregulated transporters in the case of R*vs*M were much fewer number in both *A. ostoyae* and *A. cepistipes*. Compared to the total number of these transporters, the most upregulated transporters in R*vs*M were those potentially involved in sugar transport, such as Major Facilitator Sugar Transport-like (IPR005828), Sugar/Inositol Transporter (IPR003663), Sugar Transporters (IPR005829). Several aquaporin-like proteins reported to be involved in fungal development (Krizsán et al., 2019) and ectomycorrhizal function (Peter et al., 2016) were also up-regulated in R*vs*M. The upregulation of transporters in rhizomorphs might suggest their role in the transfer of decomposition intermediates between different parts of the colony, rather than their involvement in active wood decay.

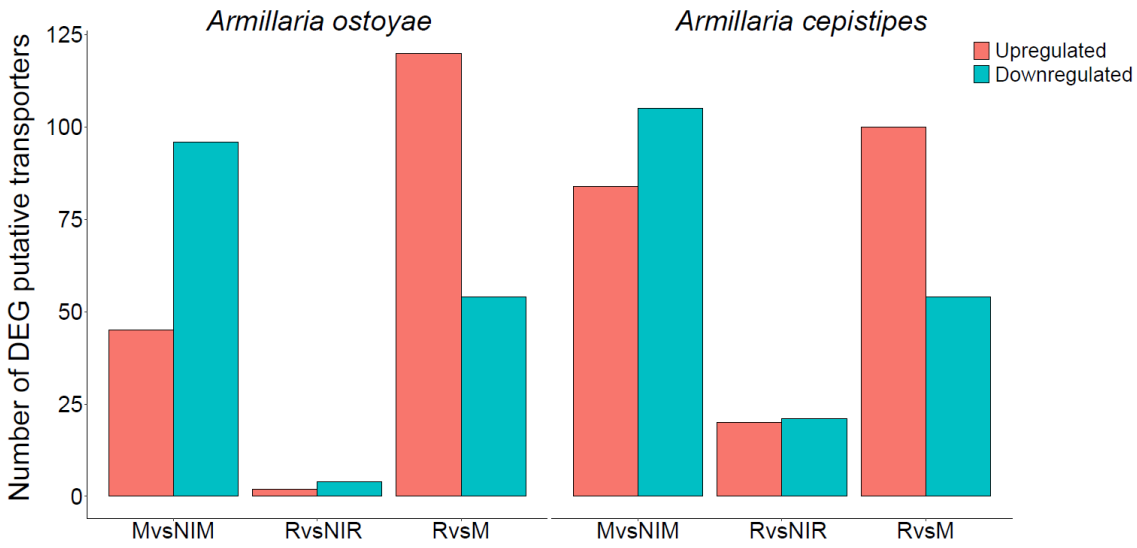

Figure 17. Number of differentially expressed putative transporters in the two species. The number of upregulated (orange) and downregulated (green) genes are shown for MvsNIM, RvsNIR, and RvsM comparisons in the two species. (MvsNIM: mycelium vs non-invasive mycelium or in RvsNIR: rhizomorphs vs non-invasive rhizomorphs)

Overall, our objective in this sub-chapter was to explore the wood-decay patterns employed by *Armillaria* species. To this end, we investigated the colonization of sterilized spruce roots by *A. ostoyae* and *A. cepistipes* using morphological observations and transcriptomic and proteomic techniques. Our results showed that spruce roots were colonized primarily by mycelium, which had a higher number of differentially expressed genes and DAPs compared to rhizomorphs of both species. Whereas, the upregulation of transporters in the rhizomorphs of both species indicated their possible role in the nutrient transfer. In addition, the saprotrophic species *A. cepistipes* showed a stronger transcription response with a higher number of DEG/DAP PCWDEs than the pathogenic (necrotroph) *A. ostoyae*, reflecting a general difference in wood decay strategies between saprotrophic and pathogenic species, with saprotrophs facing more intense competition from other microbes and therefore adapting a more rapid colonization and substrate degradation strategy. We also found a shared gene expression response to spruce root colonization, with a total of 779 co-

orthologous genes showing similar DEG patterns in the invasive mycelium of both species. These included gene families such as oxoglutarate/iron-dependent dioxygenases, galactose-binding-like domain superfamily proteins, and intradiol ring cleavage dioxygenases, as well as several families involved in plant cell wall degradation, among which pectinases were the most abundant. Unexpectedly, the two *Armillaria* species were found to exhibit a wood-decay profile that, unlike that of white rot fungi, largely bypassed the expression of lignin-degrading genes and was characterized by the upregulation of other PCWDEs such as pectinases and cellulases. These expression patterns are more suggestive of soft rot, a known rot type in Ascomycota. Together with *Armillaria*, this appears to be a common wood decay approach among early-diverging developing Agaricomycetes that contain lignin-degrading genes in their genome, but still produce soft rot-like traits or decay patterns not necessarily fitting into the traditional white and BR dichotomy. We hypothesize that WR fungi evolved in an early ancestor of Agaricomycetes that inherited soft-rot machinery from its common ancestors with the Ascomycota, leading to the combination of WR and SR toolkits in Armillaria and other unusual WR fungi. The evolution of such a rot apparatus may allow these fungi to selectively employ either strategy for wood rot. To put our findings in an evolutionary perspective and understand the evolution of the wood-decay apparatus in *Armillaria* species, we used a comparative phylogenomic approach with new *Armillaria* genomes, as detailed in the next subchapter.

4.2. Phylogenomics reveal genomic innovations

4.2.1. Description of new *Armillaria* genomes

We report the high-quality annotated *de novo* genomes of seven *Armillaria* species, including *A. borealis, A. ectypa, A. fumosa, A. mellea, A. nabsnona, A. novaezealandiae*, and *A. tabescens*. The new genomes were assembled into 33-864 scaffolds of 40-79 Mbp using Falcon (v.1.8.8), with 12,228-19,984 predicted gene models *(performed by collaborators at JGI Mycocosm)*. The benchmarking universal single copy orthologs (BUSCO) completeness values range from 97.7% to 99.7%. Sequencing statistics for the new genomes are summarized in Table 2.

We examined all currently known major clades (Koch et al., 2017), including the Northern Hemisphere clade (*A. borealis, A. ostoyae, A. gallica, A. cepistipes, A. solidipes, A. nabsnona*), the Australasian/Southern American clade (*A. luteobubalina, A. fumosa, A. novaezelandiae*), African (*A. fuscipes*), and the melleoid clade (*A. mellea*). In addition, we included the genomes of two exannulated species from the subgenus *Desarmillaria* (*A. tabescens* and *A. ectypa*), of which the moss-associated *A. ectypa* had the smallest genome among *Armillaria* species. We also included *Guyanagaster necrorhizus* (Koch et al., 2021), which belongs to the sister genus of *Armillaria* (Koch et al., 2017). Other species of Physalacriaceae were included as outgroups (Figure 18).

Table 2: List of Armillaria genomes used.

Name	Host Preference	Assembly Length	# of Genes	BUSCO (fungi)	# of Scaffolds	Scaffold N50	Reference
Armillaria gallica 21-2 v1.0	Weak pathogen of Angiosperms	8,53,36,812	25,704	100	319	22	(Sipos et al., 2017)
Armillaria cepistipes B5	Saprobe	7,58,28,441	23,460	95.9	287	8	(Sipos et al., 2017)
Armillaria nabsnona CMW6904 v1.0	Saprobe	6,27,18,798	19,015	99.7	85	9	This study
Armillaria solidipes 28-4 v1.0	Pathogen of Gymnosperms	5,80,09,494	20,811	95.5	229	21	(Sipos et al., 2017)
Armillaria ostoyae C18/9	Pathogen of Gymnosperms	6,01,06,801	22,705	99	106	9	(Sipos et al., 2017)
Armillaria borealis FPL87.14 v1.0	Weak pathogen of Angiosperms	7,16,89,880	19,984	99.4	864	50	This study
Armillaria fumosa CBS 122221 v1.0	Saprobe	5,58,24,865	16,095	99.6	54	7	This study
Armillaria luteobubalina HWK02 v1.0	Pathogen of Angiosperms	9,71,06,278	20,318	98.6	439	28	This study

Armillaria novae-zelandiae 2840 v1.0	Weak pathogen of Gymnosperms	7,93,34,843	18,551	97.6	427	26	This study
Armillaria mellea DSM 3731	Pathogen of Angiosperms	7,95,45,241	14473	82.8	29300	680	(Collins et al., 2013)
Armillaria mellea ELDO17 v1.0	Pathogen of Angiosperms	7,08,56,304	15,646	99	474	8	This study
Armillaria fuscipes strain CMW2740	Pathogen of Gymnosperms	5,29,84,320	16,267	87.6	24403	4876	(Wingfield et al., 2016)
Armillaria tabescens CCBAS 213 v1.0	Pathogen of Angiosperms	7,48,75,987	19,032	98.6	659	33	This study
Armillaria ectypa FPL83.16 v1.0	Mosses	4,05,98,130	12,228	99.3	33	5	This study
Guyanagaster necrorhiza MCA 3950 v1.0	NA	5,36,86,691	14,276	99	168	15	(Koch et al., 2021)

BUSCO: Benchmarking Universal Single Copy Orthologs

For further comparative analysis, we annotated the CAZymes, with *A. luteobubalina* having the highest (716) and *G. necrorhizus* the lowest (497) number of CAZymes. CAZymes were sub-categorized into gene families related to the PCWDEs, such as the ones acting on celluloses, hemicelluloses, pectin and lignin, and gene families related to the FCW such as the ones acting on chitin, glucans, galactans and mannans among others (Table S1). Studies have shown that pathogenic fungi encode more PCWDEs in their genomes than saprobes (Hill et al., 2022; Zhao et al., 2013). However, the new *Armillaria* genomes did not reveal a significant difference in the PCWDE or CAZy repertoires of pathogenic and saprobic species (Figure 18).

We also annotated the secreted and SSPs (<300 amino acids), which include cysteine-rich proteins with diverse functions, such as the colonization of the host, modulation of the host immune response (Plett and Plett, 2022), and regulation of development (Almási et al., 2019). Overall, *Armillaria* genomes encode 270-507 putative SSPs (with the exception of *Guyanagaster* encoding 262 SSPs), with *A. fuscipes* having the lowest number and *A. luteobubalina* the highest. Based on IPR annotations, 45-57% of the SSPs had no known functional domains, which we hereafter refer to as unannotated SSPs. In plant pathogenic fungi, this latter class of SSPs are typically referred to as candidate secreted effector proteins (Lo Presti et al., 2015; O'Connell et al., 2012; Sonah et al., 2016).

Figure 18: General genome statistics and reconstruction of ancestral genome size dynamics for 15 Armillaria species and five outgroups in the Physalacriaceae. Numbers and dots at nodes represent ancestral proteome sizes in the Physalacriaceae tree. Blue dots represent benchmarking universal single copy orthologs(BUSCO) scores for each species. For proteome sizes, darker color shows proteins with no known functional domains (unannotated proteins). Carbohydrate active enzymes (CAZymes) - darker color shows plant cell wall degrading enzymes (PCWDEs), lighter color shows other CAZymes. Secretomes and small secreted proteins (SSPs) - darker color shows unannotated proteins, and lighter color shows proteins with known functional domains.

4.2.2. Genetic innovations in *Armillaria* clade

To analyze the genomic innovations associated with the rise of *Armillaria* in more detail than previously, we combined the genomes of 15 *Armillaria* species with those of other Agaricales with different lifestyles, resulting in a dataset of 66 species (Table S2). Reconstruction of genome-wide gene gain/loss patterns revealed genome expansion in *Armillaria*, consistent with results reported by Sipos et al. (2017) using four *Armillaria* species. The estimated ancient gene set at the root node comprised 9,929 genes, suggesting an early origin of most genes (Figure 19). The *Armillaria* clade showed net genome expansion with 18,662 protein-coding genes inferred for the MRCA of *Armillaria* (2,913 duplications, 189 losses), in contrast to 15,938 for the MRCA of *Armillaria* and *Guyanagaster* (2,158 duplications, 4,375 losses) and 18,155 for the MRCA of *Armillaria*, Guyanagaster, and Hymenopellis (653 duplications, 5,187 losses) (Figure 19). The MRCA of the Northern Hemisphere clade was inferred to 23,736 genes (3,140 duplications, 1,525 losses). These data suggest that the large repertoires of protein-coding genes of *Armillaria* spp. can be explained by genus-specific gene duplications early in their history, as previously proposed (Sipos et al., 2017).

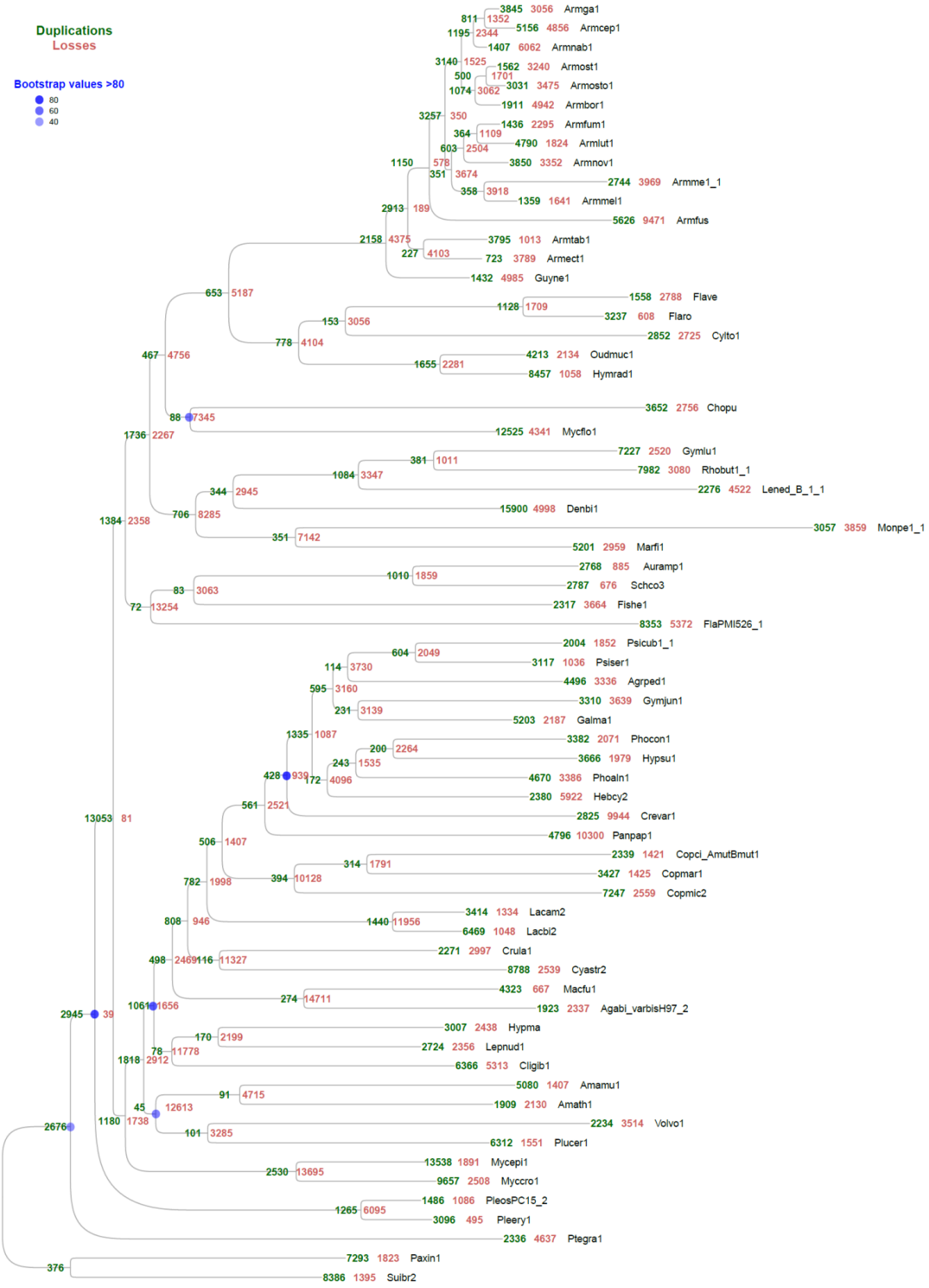

Figure 19: Summary of gene losses and gains from COMPARE mappings. Duplications (green) and losses (red) at each node for Dataset 1. Bootstrap support values less than 80 are shown in blue.

4.2.3. Enriched functions among gene duplication events

The 2,913 duplications in the MRCA of *Armillaria* were inferred to a total of 1,473 orthogroups. GO and IPR enrichment analyses revealed a significant overrepresentation of 55 molecular functions, 18 biological processes, and three cellular component terms (topGO, weight01 algorithm, $p < 0.05$) (Figure 20) and 733 IPR terms in these orthogroups. These included gene families with functions related to plant biomass utilization, such as pectin degradation (pectate lyases, pectin lyases, pectinesterases, GH28), cellulose binding, and gene families putatively related to the degradation of extracellular and aromatic compounds (e.g. intradiol ring cleavage dioxygenase, multi copper oxidases), and several other broader functions (Figure 20).

Duplicated genes were also enriched in putative pathogenesis-related gene families. For instance, we found a significant overrepresentation of deuterolysins, aspartic peptidases, chitin deacetylases, and Golgi-associated pathogenesis-related proteins in *Armillaria* expansions. Ceratoplatanins and LysM domains, which have been reported to support infection in pathogenic fungi (Baccelli, 2015; Li et al., 2019; Muraosa et al., 2019), were also enriched in *Armillaria*.

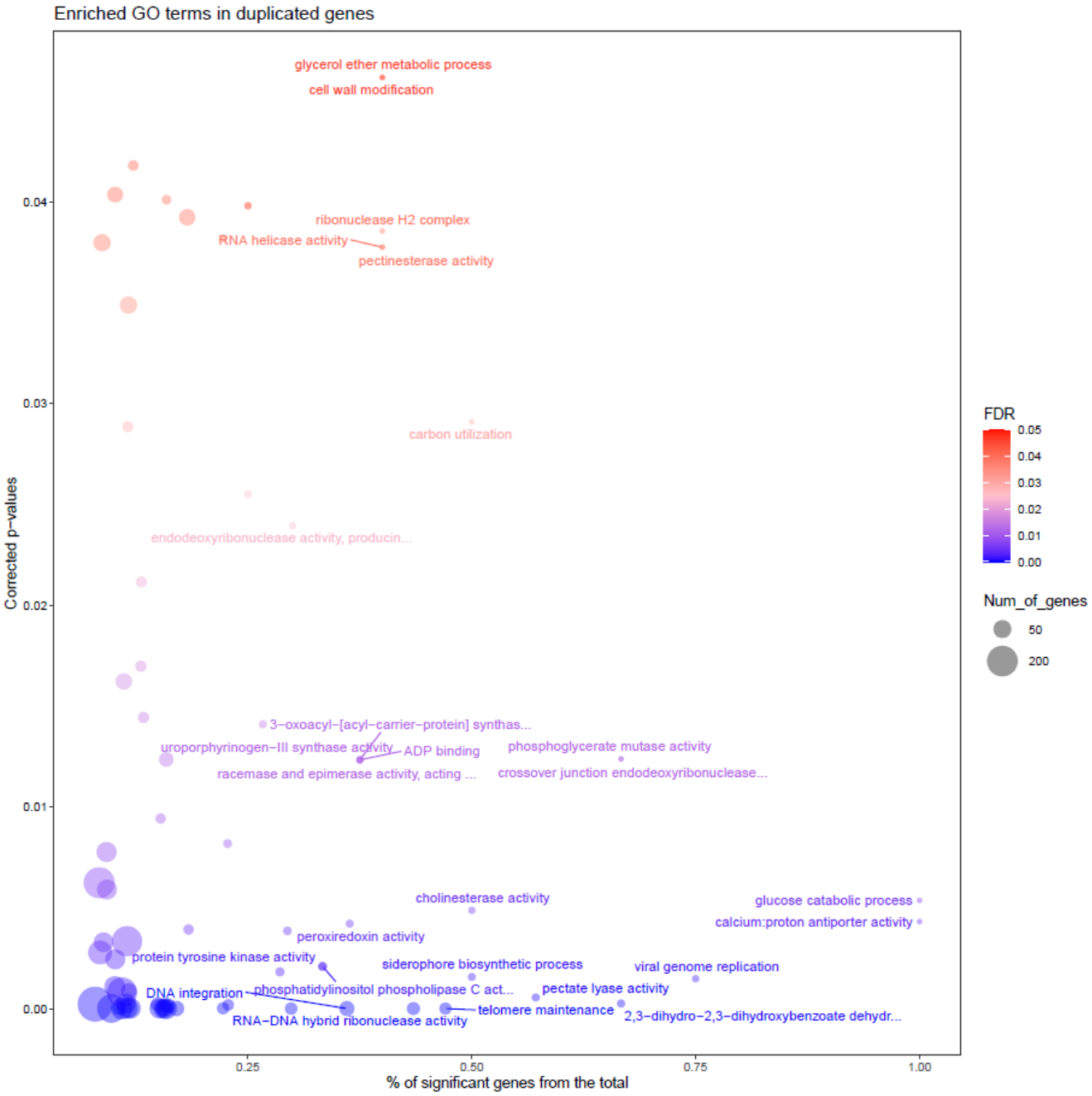

Figure 20: GO terms enriched in duplicated genes. Significantly enriched GO terms in the 1473 orthogroups, inferred by 2913 duplications at Armillaria MRCA. The x-axis shows the percentage of significant genes from the total number of genes, y-axis shows p-values. Blue shows lower and red shows higher p-values. GO terms that had at least 30% of genes significant from the total number of genes are mentioned in the plot.

4.2.4. Novel-core genes in *Armillaria*

Gene families that have evolved within and are conserved in most *Armillaria* species are referred to as novel core orthogroups and may be particularly relevant for explaining the plethora of *Armillaria*-specific innovations such as genome expansions, the enrichment of certain genes related to pathogenicity and pectin degradation, the production of underground rhizomorphs, the ability to reach extreme colony sizes, low mutation rates, diploidy, and bioluminescence. We, therefore, analyzed novel core orthogroups and found 212 shared by at least twelve *Armillaria* species, including *G. necrorhizus* (Figure 21). Of these, 116 consisted of proteins for which no functional annotations are known. The remaining orthogroups were dominated by gene families such as F-box domains, Leucine-rich repeats, Cytochrome P450s, Zinc-finger C2H2 type transcription factors, protein kinases, and other rapidly evolving gene families.

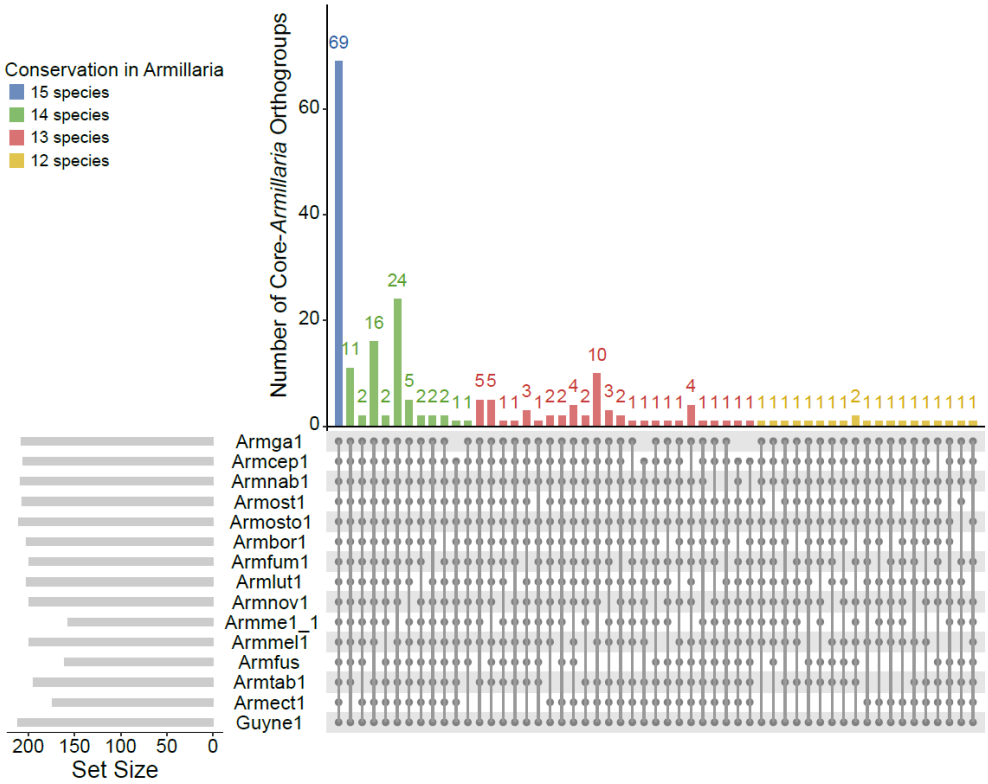

Figure 21: Novel-core genes in Armillaria. UpsetR plot showing novel-core orthogroups present exclusively in at least 12 Armillaria species (including Guynagaster necrorhizus)

(Armga1: Armillaria gallica, Armcep1: A. cepistipes, Armnab1: A. nabsnona, Armost1: A. solidipes, Armosto1: A. ostoyae, Armbor1: A. borealis, Armfum1: A. fumosa, Armlut1 A. luteobubalina, Armnov1: A. novae zealandiae, Armme1_1: A. mellea (old), Armmel1: A. mellea (new), Armfus1: A, fuscipes, Armtab1: A. tabescens, Armect1: A. ectypa, Guyne1: Guynagaster necrorhizus)

4.2.5. Plant biomass-degrading enzymes in *Armillaria* and the Physalacriaceae

Ecologically, *Armillaria* species are reported to be facultative necrotrophs that first kill the host, then utilize its biomass during the saprotrophic phase. The new genomes allowed us to make predictions on the wood decay strategy of *Armillaria*, relative to other wood-decaying fungi based on their PCWDEs. Similar to WR fungi and necrotrophs (Nagy et al., 2017; Shao et al., 2021), *Armillaria* species possess the complete enzymatic repertoire for degrading woody plant biomass (Figure 18). We generated phylogenetic PCAs for *Armillaria* species, other Physalacriaceae and other fungi with different nutritional lifestyles (Dataset 2 in Table S2). Based on the gene copy numbers of cellulases, pectinases, *Armillaria* and other Physalacriaceae showed clear separation from both WR and LD fungi (Figure 22). In the case of ligninases, *Armillaria* and other Physalacriaceae were separated from WR species, however, were still grouped together with the LDs (Figure 22). Further, to achieve a finer-scale resolution and the loading factors that govern the separation between lifestyles, we restricted our phylogenetic PCAs to only wood-decay lifestyles - WR and LD fungi, along with the Physalacriaceae (Figure 23).

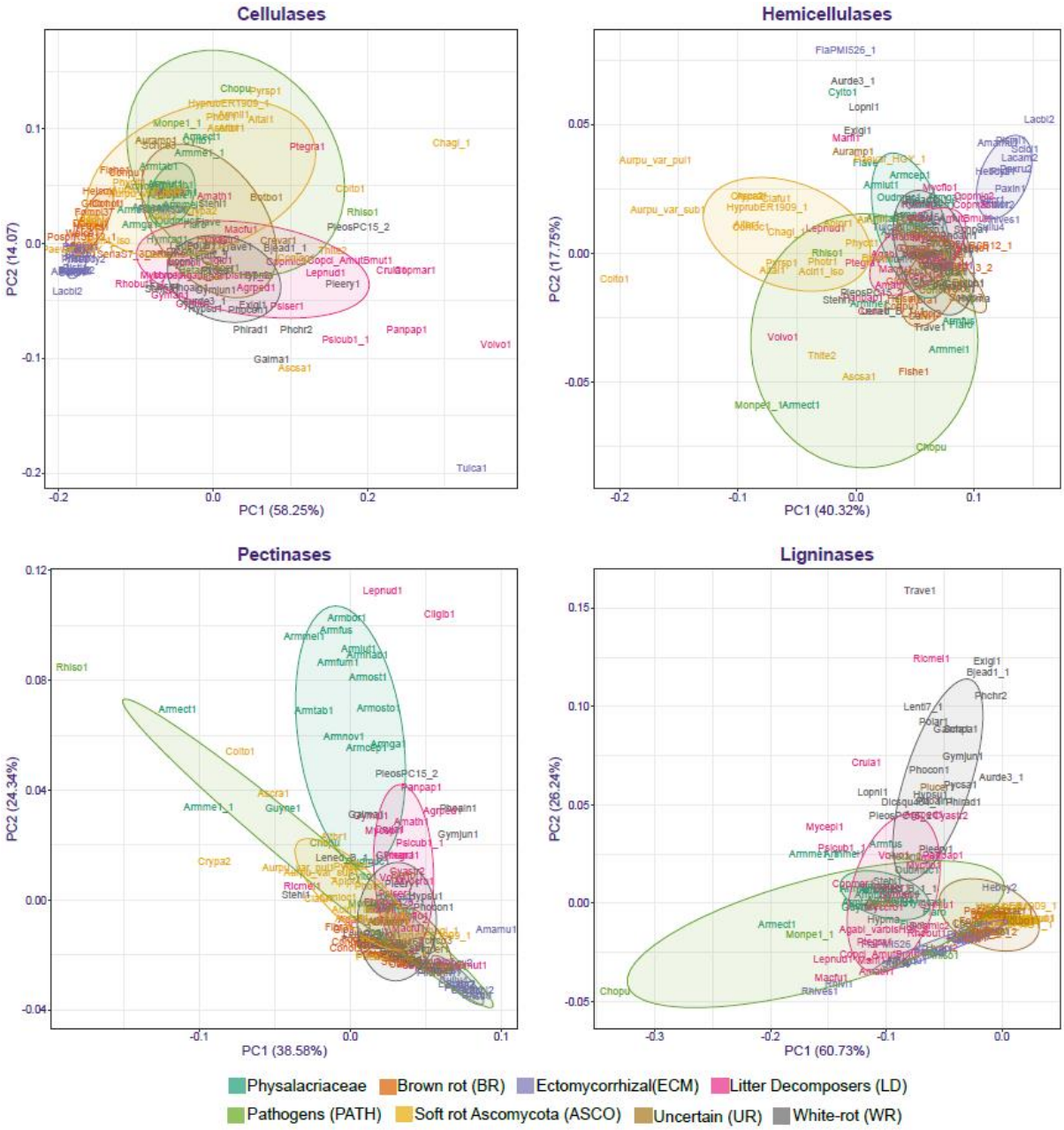

Figure 22: Plant biomass degradation genes in Armillaria and other Agaricales. Phylogenetic PCAs for PCWDE gene families in Armillaria and other fungi from Dataset 2 (Table S2). Species abbreviations are colored based on nutritional mode. (ASCO: Ascomycota, BR: brown-rot, ECM: ectomycorrhizal, LD: litter decomposer, UR: uncertain, WR: white-rot)

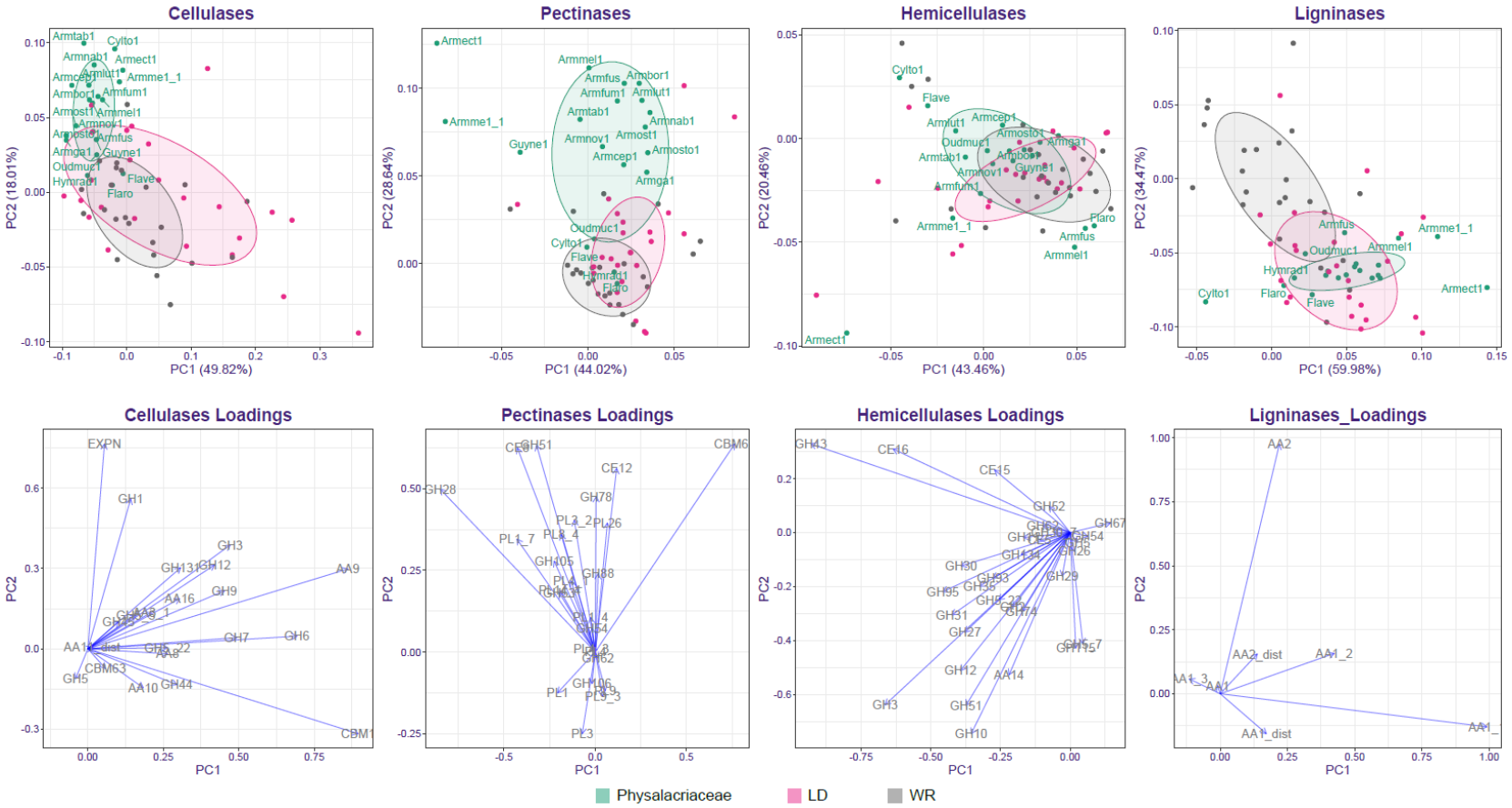

Figure 23: Plant biomass degradation genes in Armillaria. Phylogenetic PCAs (above) and their respective loading factors (below) for PCWDE gene families. Species abbreviations are colored according to nutritional modes. (LD: litter decomposer, WR: white-rot)

Cellulases and pectinases clearly separated *Armillaria* spp. and other Physalacriaceae from WR and LD fungi (Figure 23), while hemicellulase and ligninase PCA-s grouped them with LD and WR fungi. The loading factors for cellulases indicate that this segregation is mainly driven by expansins, AA16, AA8, and AA3_1 auxiliary activity families, and the GH1 and GH45 glycoside hydrolase (GH) families. Consistent with the loading factors, the AA3_1, GH1, and GH45 families have noticeably more copies in *Armillaria* and other Physalacriaceae than in WR and LD (Figure 24). On the other hand, *Armillaria* and other Physalacriaceae were depleted of CBM1 and GH5_5, with an average of 12 and five genes, respectively, compared with WR and LD, whose genomes encode 20-60 CBM1 and 4-10 GH5_5 genes. We found that the GH44 family, which is specific to Basidiomycota (Sun et al., 2022), was absent in Physalacriaceae and *Armillaria*, suggesting that gene losses could have also driven the trophic mode evolution of these fungi toward an Ascomycota-like lifestyle.

In pectinase PCA, the highest loading family was CBM67 (rhamnose-binding modules), which were enriched in *Armillaria* species and absent in most WR species in our dataset (Figure 25). CBM67s are frequently associated with GH78 and PL1 (Resl et al., 2022). Of these, the PL1 family is present in all Physalacriaceae species but is absent in many WR and LD fungi (with the exception of two *Pleurotus* species, which have even more copies than Physalacriaceae) (Figure 25). Other pectin-related gene families such as GH28, GH53, GH88, CE8, and CE12 were present in higher numbers in *Armillaria* and other Physalacriaceae than in WR and LD fungi, while PL1_7, PL26, PL3_2, PL4_1 were more abundant in *Armillaria* species and absent in most WR species but present in some LDs.

As for hemicellulases, Physalacriaceae species grouped with WR and LD fungi. However, there were two families, GH29 with an average of 3 genes and GH93 with 1-2 genes in each Physalacriaceae species, which were absent in 40-50% of WR and LD species (Figure 26). For ligninases, we found that Physalaciaceae species grouped with LDs, and apart from white rotters. The separation from the WRs was mainly caused by class II peroxidases (AA2), which averaged 14 copies in the WRs, but only

7-8 copies in *Armillaria*, Physalacriaceae, and LD fungi. Other lignin modification-related gene families, such as the multicopper oxidase subfamilies AA1_1 (laccases) and AA1_2 (ferroxidases), had an average of 20 and 2-3 copies, respectively, in Physalacriaceae, compared to on average of nine AA1_1 and one AA1_2 genes in WR fungi (Figure 27). We also analyzed the H_2O_2-producing CAZy families AA3 and AA5; these showed a similar pattern to ligninases, with *Armillaria* grouping with the LD fungi and distant from WR species (Figure 27).

These analyses portray *Armillaria* and the Physalacriaceae as versatile wood decayers that are nevertheless distinct from WR, despite previous classifications as such (C. Collins et al., 2017; Collins et al., 2013; Floudas et al., 2015; Sipos et al., 2018, 2017). This is consistent with microscopy, chemical as well as our transcriptomic analyses (Campbell, 1932, 1931; Daniel et al., 1992; Floudas et al., 2015; Schwarze, 2007), which indicated that their decay chemistry is similar to soft rot (Campbell, 1931; Schwarze, 2007), which is known only in the Ascomycota. These observations prompted us to systematically look for similarities between PCWDE repertoires of the Physalacriaceae and the Ascomycota. We found 16 CAZy orthogroups that were significantly overrepresented in both groups with respect to WR+LD fungi (BH-corrected p-value >0.05, Fisher's exact test (Figure 28). These included several of the high-loading families from the PCAs, as well as other PCWDEs acting on cellulose (AA3_1, AA8, CBM1), pectin (PL3_2, PL1_7, PL9_3), cellulose/chitin (AA16), and hemicellulose (GH31, GH43, GH93, CE4). These families could either be the result of co-expansion in both the Ascomycota and the Physalacriaceae or represent HGT events. Blast searches with *Armillaria* GH28 genes suggested the latter scenario to be more likely, which led us to systematically evaluate the role of HGTs.

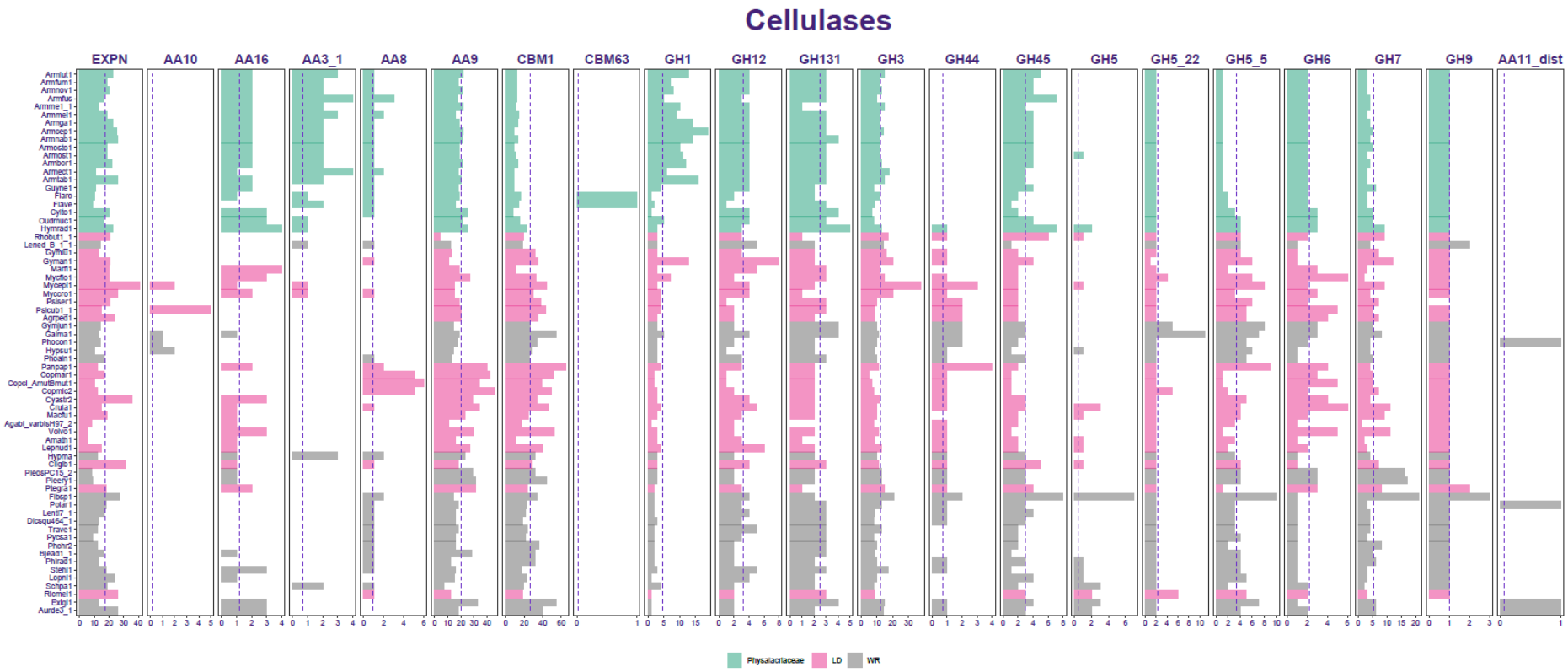

Figure 24: Barplots for cellulase genes. Gene copy numbers of cellulose-acting CAZymes. Bars are colored according to nutritional mode. X-axis shows gene copy numbers and Y-axis depicts species from selected lifestyles, sorted according to their phylogeny. Dashed vertical line depicts average gene copies for each family. (LD: litter decomposer, WR: white-rot)

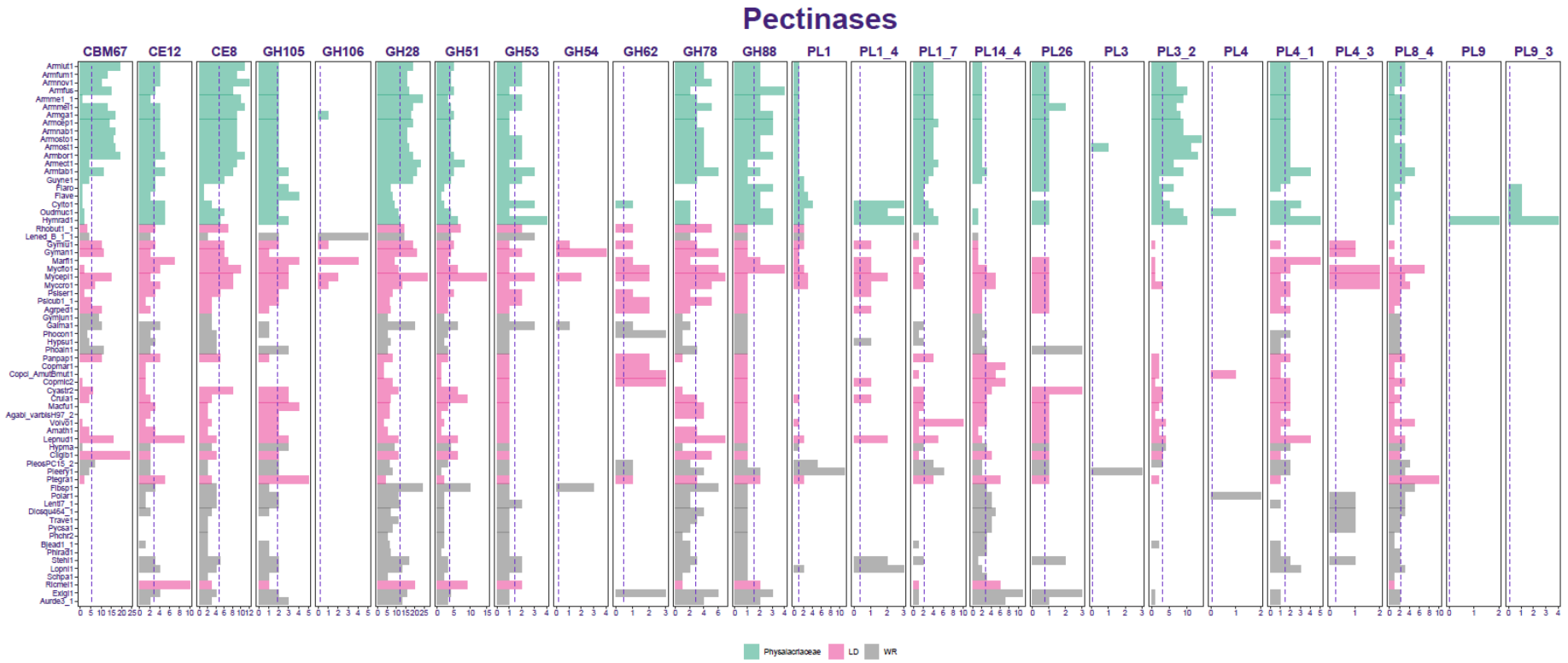

Figure 25: Barplots for pectinase genes. Gene copy numbers of pectin-acting CAZymes. Bars are colored according to nutritional mode. X-axis shows gene copy numbers and Y-axis depicts species from selected lifestyles, sorted according to their phylogeny. Dashed vertical line depicts average gene copies for each family. (LD: litter decomposer, WR: white-rot)

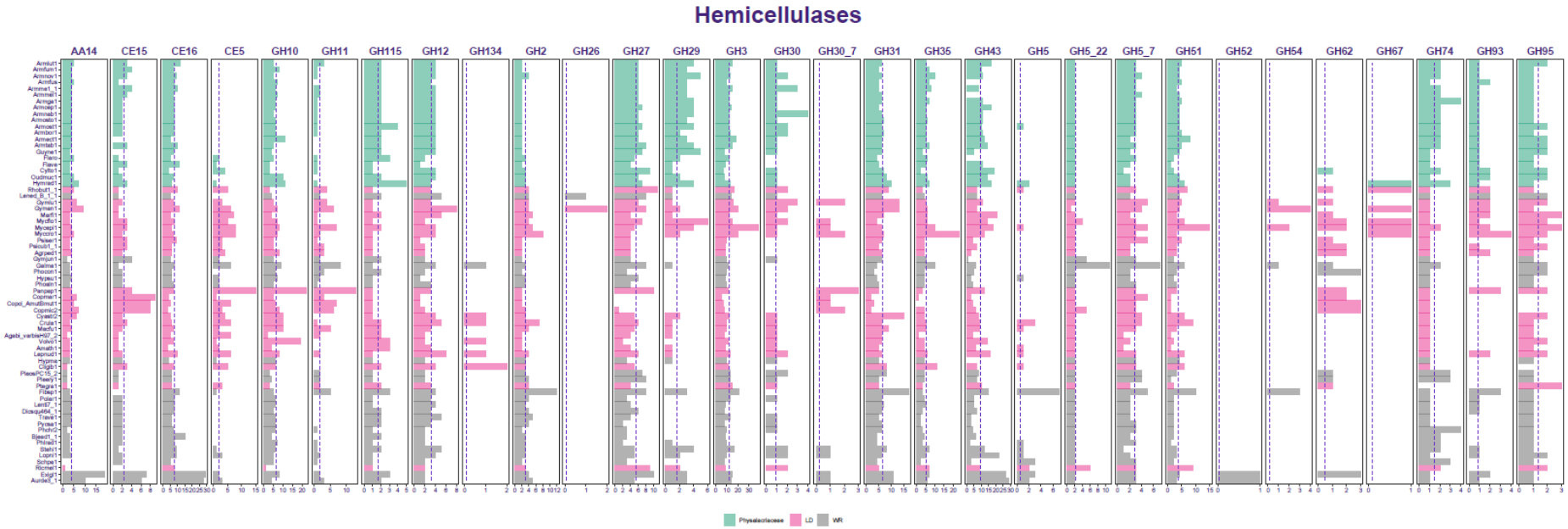

Figure 26: Barplots for hemicellulase genes. Gene copy numbers of CAZymes for specific substrates. Bars are colored according to nutritional mode. X-axis shows gene copy numbers and Y-axis depicts species from selected lifestyles, sorted according to their phylogeny. Dashed vertical line depicts average gene copies for each family. (LD: litter decomposer, WR: white-rot)

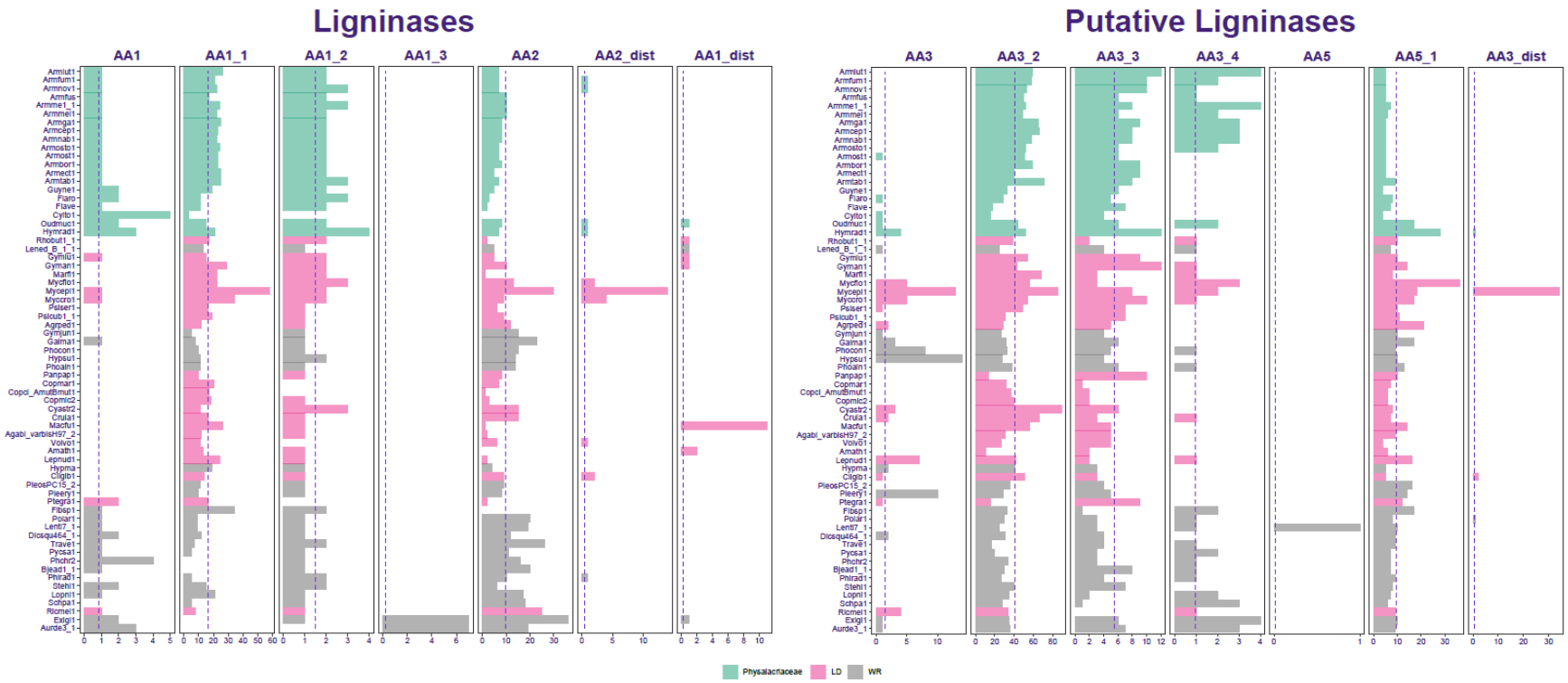

Figure 27: Barplots for ligninase genes and other gene families putatively involved in the degradation of lignin monomers. Gene copy numbers of CAZymes for specific substrates. Bars are colored according to nutritional mode. X-axis shows gene copy numbers and Y-axis depicts species from selected lifestyles, sorted according to their phylogeny. Dashed vertical line depicts average gene copies for each family. (LD: litter decomposer, WR: white-rot)

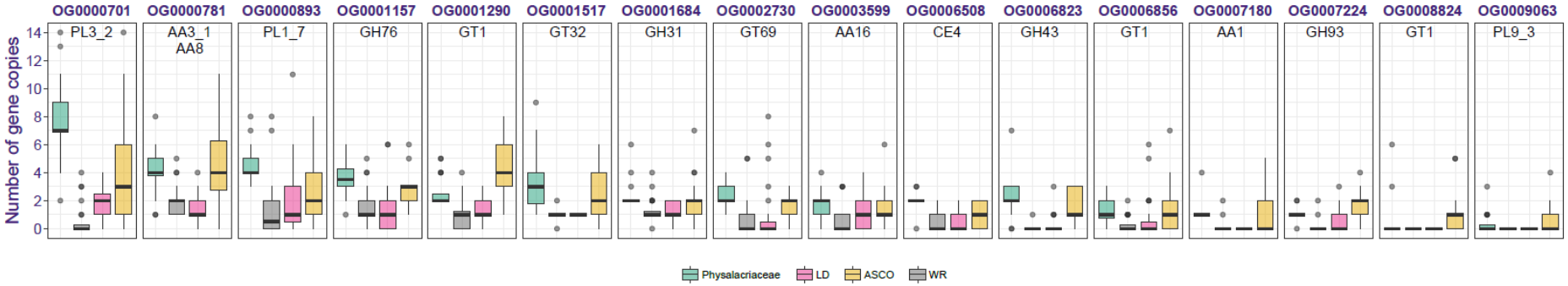

Figure 28: Co-shared CAZy orthogroups in Physalacriaceae and Ascomycota. Boxplot of copy numbers of 16 CAZy orthogroups co-enriched in Physalacriaceae and in Ascomycota with respect to WR and LD fungi. Scale limits for the boxplot were set to 14, losing one sample point (Conioc1 in OG0000781 with 18 genes). Predominant CAZy families for each orthogroup are mentioned in the boxes. Lifestyles of the species used are denoted by colors. (ASCO: Ascomycota, LD: litter decomposer, WR: white-rot)

4.2.6. Widespread horizontal transfer of genes from Ascomycota

To identify HT gene candidates, we calculated the AI (Gladyshev et al., 2008) for each *Armillaria* and Physalacriaceae protein based on a phylogenetically broad set of 942 species from the Ascomycota, Mucoromycota, early-diverging fungi as well as plants and bacteria. Based on AI>1, we identified 99-195 HT gene candidates per species, with *A. gallica* having the most and *A. ectypa* the fewest in *Armillaria*. Among Physalacriaceae, *H. radicata* had the highest estimated number of HT genes (247), and *F. velutipes* had the lowest (88) (Figure 29).

Based on the top putative donor species from the AI data, we assembled a dataset comprising 20 Physalacriaceae, 90 Basidiomycota, 210 Ascomycota, 7 Mucoromycota, and 2 Zoopagomycota species. Using OrthoFinder (v.2.5.4), we identified 649 orthogroups containing at least one gene predicted as HT by AI. Due to the similarity of the CAZy repertoires of Physalacriaceae to Ascomycota (see above), we also included all CAZy orthogroups in these analyses. In total, we analyzed 675 orthogroups by combining phylogenetic support (at least 70% bootstrap in ML gene trees), and top hits against the UniRef100 database (Suzek et al., 2015). Overall we recovered 101 strongly supported HGT events (Figure 29) into Physalacriaceae, corresponding to 1089 individual genes, consistent with estimates based on the AI. Multiple internal nodes of the Physalacriaceae tree were identified as putative recipients, most of which were deep in the family. 88 HGT events were confidently associated with Ascomycota as donors, in particular the Sordariomycetes and Dothideomycetes (28 transfers each). We find that ~45% of HT genes have undergone one or multiple rounds of duplication (a total of 488 duplicated genes) within the Physalacriaceae, indicating that HT genes were likely integrated into the life history of Physalacriaceae and *Armillaria* therein. Expression levels of HT genes support their functionality (Figure 30).

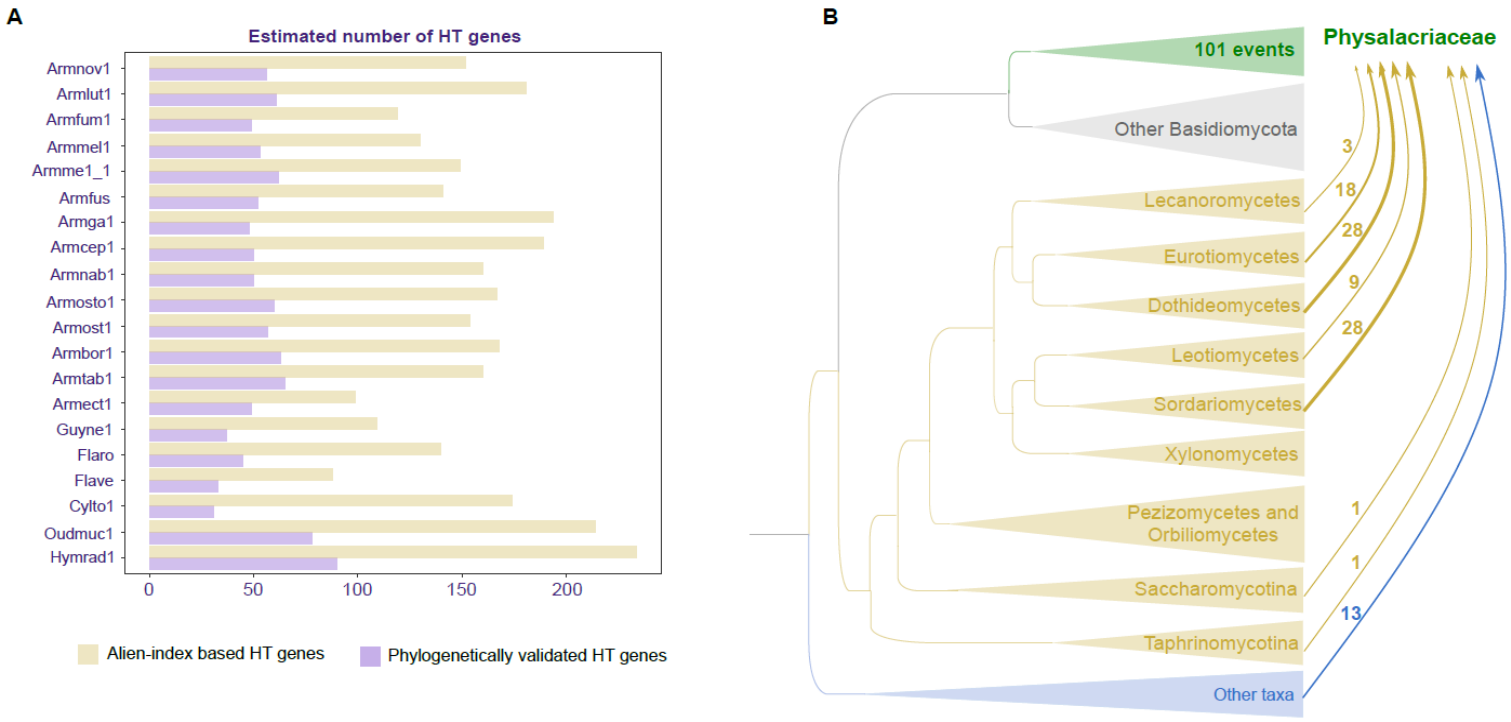

Figure 29. Horizontal gene transfers into Armillaria and the Physalacriaceae family. A) Barplot showing the number of HT genes identified in each genome using AI calculations (yellow) and by phylogenetic validation (purple). B) Schematic representation of donor and recipient relationships for HT events after phylogenetic validation. Size of the arrow is proportional to the number of transfer events inferred from all the nodes belonging to a specific donor group. The number of events for each donor group are listed along the arrows.(HT: Horizontally transferred)

Among proteins descended from phylogenetically validated HT events, we found 164 CAZymes, of which 117 belonged to families that were co-enriched in Ascomycota and Physalacriaceae compared to WR and LD species (AA3_1, AA8, GH43, GH93, GT1, PL3_2 and PL9_3). This indicates that the co-enrichment signal detected using the simple copy-number-based analyses above was likely created by HGT events. In addition to CAZymes, HT genes included intradiol ring-cleavage dioxygenases, CAP domain proteins, Pyr1-like SCP domains, as well as gene families with broad functional roles such as cytochrome P450, peptidases, transporters, and transcription factors.

Based on gene function annotations, we find that horizontal transfer affected several families associated with wood-decay (e.g. AA3_1, GH43, PL3_2), as well as plant-fungal interactions (e.g. CAP domain proteins, peptidases), which suggests that it might have shaped the plant biomass-degrading and pathogenic abilities of the genus. Given that Physalacriaceae species have been reported to cause soft-rot-like decay on wood (Campbell, 1932, 1931; Floudas et al., 2015; Schwarze, 2007) and that soft-rot is classically restricted to the Ascomycota (Worrall et al., 1997), we hypothesize that HGT contributed to the evolution of plant biomass-degrading ability of these species. We speculate that the large number of putative HGT events from Sordariomycetes and Dothideomycetes might stem from the extensive contact of *Armillaria* spp. with other plant pathogens in these classes and/or their peculiar niche and longevity. Their rhizomorphs can reach several meters in length and can contact numerous other soil microbes, perhaps providing time windows for gene exchange. Additionally, other idiosyncrasies of *Armillaria*, such as diploidy or the - as yet uncovered - mechanisms that ensure a low mutation rate (Anderson et al., 2018), could also be factored in the successful incorporation of foreign DNA in their genomes.

4.2.7 Distinct expression profiles for plant infection, necrotrophy and wood decay

During infection, *Armillaria* enters the host through the root system, colonizes and kills the cambium cells, which leads to death of the plant and onset of the necrotrophic phase (Baumgartner et al., 2011). Molecular aspects associated with this process are not well explored known, with the most information available on the wood-decaying phase (Collins et al., 2013; Devkota and Hammerschmidt, 2020; Ross-Davis et al., 2013; Sipos et al., 2017). To obtain a molecular perspective on these strategies and better understand how *Armillaria* spp. utilize expanding, novel core and HT genes, PCWDEs and gene groups frequently associated with pathogenicity, we analyzed the above-mentioned wood-decay transcriptomics in *A. ostoyae* and *A. cepistipes*, new RNA-Seq data for two *in vitro* pathosystems (for *A. ostoyae, A. borealis* and *A. luteobubalina*) obtained from our collaborators and re-analyzed published data (Sipos et al., 2017). We examined the data generated for an *in planta* time-series experiment of *A. luteobubalina* infecting *Eucalyptus grandis* seedlings from 24 hours to 2 weeks and *in vitro* fresh stem invasion assays with highly and less-virulent isolates of both *A. ostoyae* and *A. borealis* (Figure 31). The latter experiment emulated the cambium-killing phase of the fungus. Published studies covered rhizomorph and fruiting body development in *A. ostoyae* (Sipos et al., 2017). To obtain an overall species-independent picture, we aggregated differential gene expression data across experiments and calculated DEG enrichment ratios in each of the 24 gene groups we defined (see Methods 3.2.6). These enrichment ratios reflect the proportion of differentially expressed genes in a given gene group in a given experiment and are shown as a heatmap in Figure 32 and see Figure 33).

In planta infection, wood-decay and stem colonization as well as fruiting body/rhizomorph development showed distinct enrichment patterns. Cellulose-, hemicellulose-, pectin- and lignin-related PCWDE genes showed a clear enrichment in stem invasion and wood-decay experiments, as expected based on known functions of these genes (Floudas et al., 2015; Sipos et al., 2017). Among genes upregulated

on fresh stems, pectinases were most dominant, which possibly enables the fungus to spread between the bark and the sapwood. At the same time, PCWDEs were depleted in the *in planta* time series experiment, indicating that *A. luteobubalina* did not induce these genes during the infection phase. This is consistent with most necrotrophs expressing a limited set of PCWDEs for plant penetration and a larger battery of enzymes during the necrotrophic phase (O'Connell et al., 2012; Olson et al., 2012). Other virulence-related genes include cerato-platanins (Baccelli, 2015; Yang et al., 2018), which showed an enriched upregulation at 24 h and 48 h in *A. luteobubalina* and in stem invasion by *A. borealis* (but not *A. ostoyae*).

Phylogenetically validated HT genes, including intradiol ring-cleavage dioxygenases, PCWDEs, peptidases and transporters, showed enrichment in wood-decay and stem-invasion experiments and were differentially expressed in all the 6 RNASeq datasets (Figure 30). Bioluminescence genes (Ke et al., 2020) were enriched in root-invading mycelium and rhizomorph (*A. ostoyae*) samples. In the developmental dataset SSPs, expanded, novel core and stress-related genes were found to be enriched in various developmental stages of the fungus (Figure 33). Genes related to oxidative stress were upregulated in various stages of *in planta* infection and in stem invasion assays (Figure 31, Figure 32). Superoxide dismutases, catalases and members of the glutathione system and ergothioneine pathway were enriched among upregulated genes in the *in planta* invasion assays, whereas Glutathione-S-transferases and catalases were enriched in wood-decay-related experiments.

It is also evident from Figure 32, that there are species- and strain-specific enrichment patterns among up- and downregulated genes. For example, the virulent *A. borealis* A6 strain had a unique enrichment of pathogenicity-related LysM proteins and cerato-platanins, which was not seen in the less-virulent A4 strain or in *A. ostoyae*. Nevertheless, in both *A. borealis* and *A. ostoyae*, the virulent strains (A6 and C18, respectively) showed more enrichment across most gene categories tested. The species- and strain-specific enrichment patterns also suggest that each species mount

a different response under the examined conditions, which might correlate with differences in lifestyle or virulence.

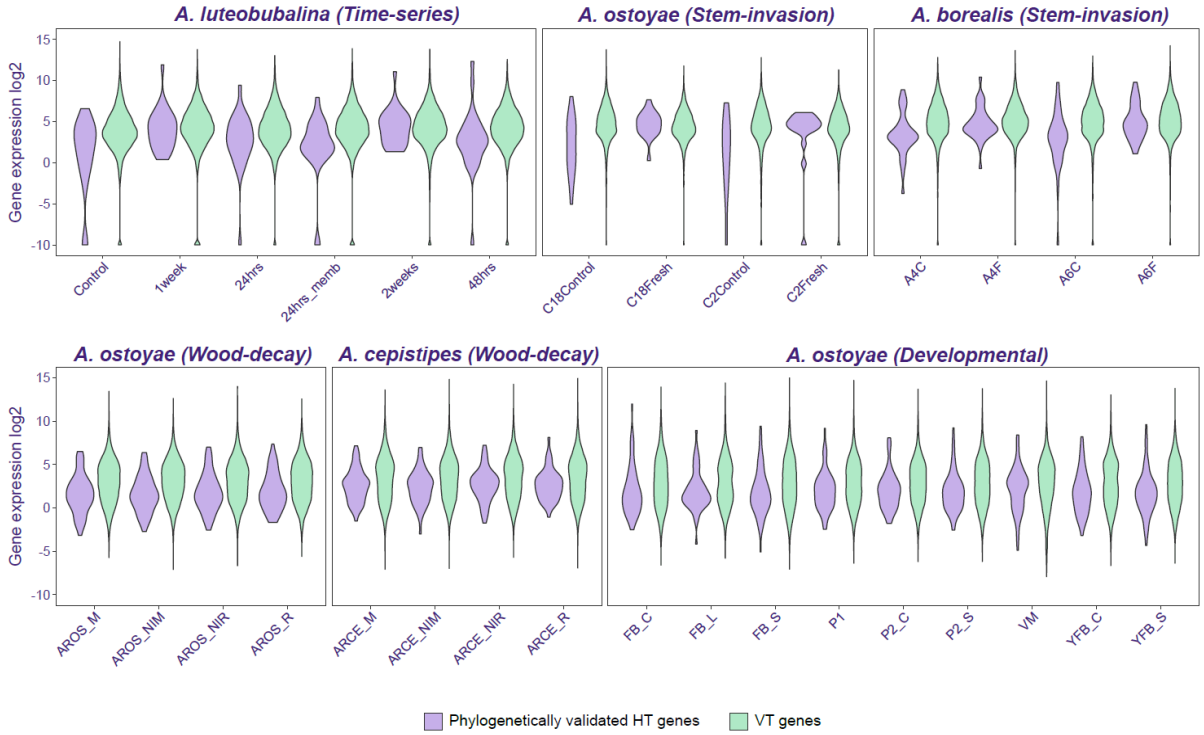

Figure 30: Expression of HT and VT genes in six RNA-Seq datasets Violin plot showing gene expression of phylogenetically validated HT and VT genes in A. ostoyae fruiting body development transcriptome. Y-axis shows log_2 transformed expression values, and x-axis shows the sample comparisons for each experiment. (HT: horizontally transferred, VT: vertically transferred)

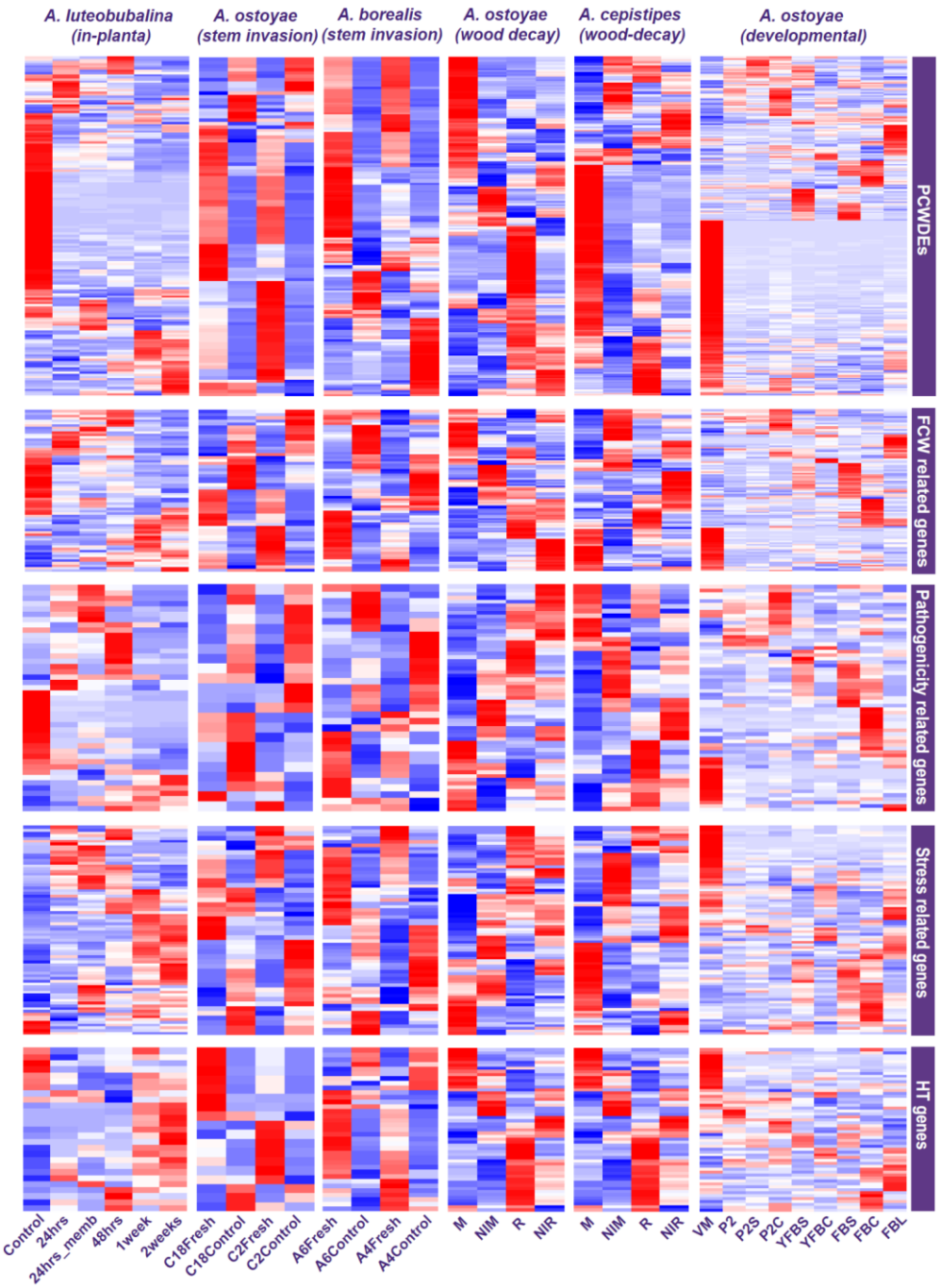

Figure 31: Heatmaps for different gene groups showing gene expression in samples from the six RNA-Seq datasets. Blue and red colors correspond to low and high gene expression, respectively.(PCWDE: plant cell wall degrading genes, FCW: fungal cell wall, HT: horizontally transferred)

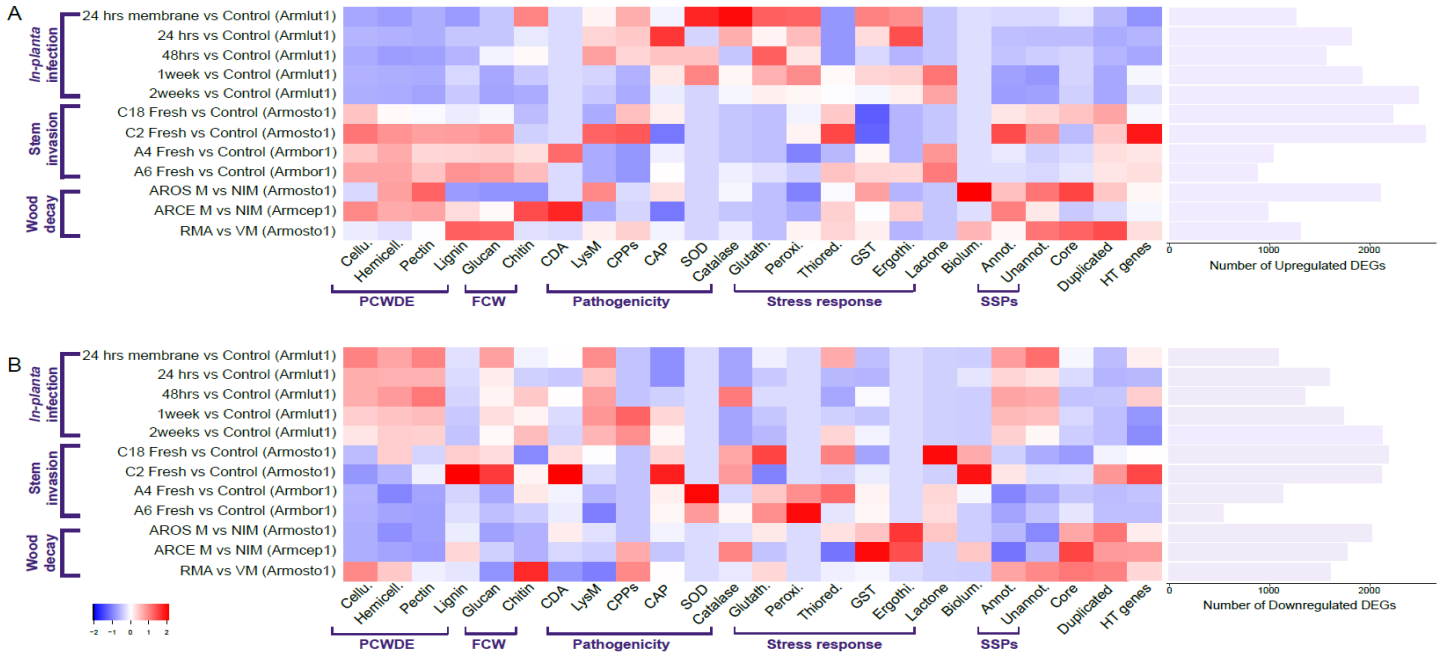

Figure 32: Enrichment of DEGs of wood-decay, pathogenicity, stress-response and other gene families in 6 RNA-Seq datasets. The heatmap shows enrichment ratios for 24 gene groups (x-axis) from aggregated differential gene expression data in six experiments (A - upregulated, B - downregulated genes). Y-axis shows the sample comparison for each dataset, with the number of DEGs shown as a barplot. In the heatmaps, warmer colors mean higher enrichment ratios. (Cellu: cellulases, Hemicell.: hemicellulases, PCWDE: plant cell wall degrading enzymes, FCW: fungal cell wall, CDA: chitin deacetylase, LysM: lysine binding module, CPPs: cerato-platanins, SOD: superoxide dismutase, Glutath.: glutathione system, Peroxi.: peroxidases, Thiored: thioreductases, GST: glutathione-S-tranferase, Ergothi.: ergothione, Biolum: bioluminiscence, Anot.: annotated , Unannot.: unannotated, SSPs: small secreted proteins, HT: horizontally transferred)

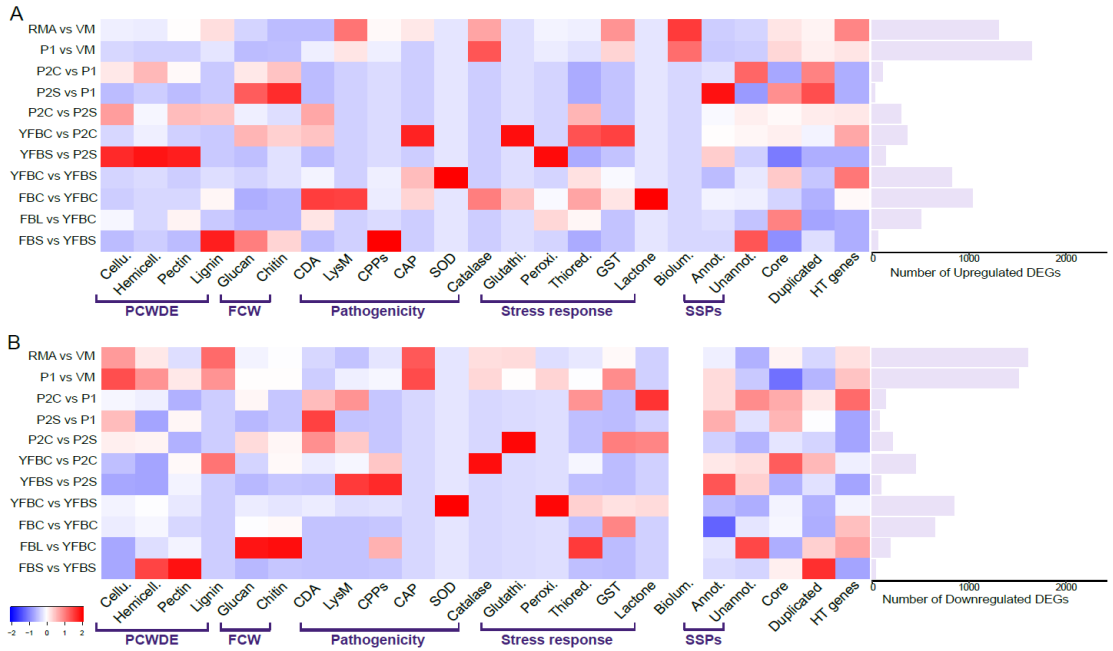

Figure 33: Enrichment of DEGs of selected gene families in the developmental dataset from Sipos et al 2017. The heatmap shows enrichment ratios for 23 gene groups ("Ergothione: removed due to no enrichment) from aggregated differential gene expression (A - upregulated, B - downregulated genes). Y-axis shows the sample comparison for each dataset, with the number of DEGs shown as a barplot. In the heatmap, warmer colors mean higher enrichment ratios. (Cellu: cellulases, Hemicell.: hemicellulases, PCWDE: plant cell wall degrading enzymes, FCW: fungal cell wall, CDA: chitin deacetylase, LysM: lysine binding module, CPPs: cerato-platanins, SOD: superoxide dismutase, Glutath.: glutathione system, Peroxi.: peroxidases, Thiored: thioreductases, GST: glutathione-S-tranferase, Ergothi.: ergothione, Biolum: bioluminiscence, Anot.: annotated , Unannot.: unannotated, SSPs: small secreted proteins, HT: horizontally transferred)

Chapter 5. Discussion

To better understand the genetic basis of the unique biology of *Armillaria* species, we analyzed transcriptomic and proteomic profiling of wood-decay systems in two *Armillaria* species and perfomed phylogenomic comparisons using new and previously published *Armillaira* genomes.

The transcriptomic and proteomic profiling of wood-decay systems in two *Armillaria* species indicated that *A. cepistipes*, a saprotroph, induces a higher number of PCWDEs than *A. ostoyae*, a pathogen. This suggests that saprotrophs may induce a wider array of wood-decay enzymes, which helps them to compete with other microbes and break down their substrates more quickly. In comparison, pathogens may not face as much pressure to induce these enzymes. The study's findings were consistent with those of gene expression studies in saprotrophic and pathogenic phases of other fungi, such as *Heterobasidion irregulare* (Olson et al., 2012). Co-orthologs of the pathogenic and saprobe *Armillaria* species showed similar differential gene expression patterns in the invasive mycelium, with an upregulated genes associated with iron acquisition, hydrophobins, CBM67s, cytochrome P450s, and plant PCWDEs. Among PCWDEs, cellulose- and hemicellulose-degrading enzyme genes, expansins, and pectinolytic genes were upregulated in M*vs*NIM, whereas lignin-degrading genes were mainly downregulated. Additionally, the underrepresentation of lignin-degrading genes (AA1, AA2, and AA5) in *Armillaria* genomes (Sipos et al., 2017) and earlier research that questioned the WR nature of these species (Campbell, 1932, 1931; Floudas et al., 2015; Schwarze, 2007) are also consistent with the downregulation of lignin-degrading genes among the DEGs/DAPs.

Several early-diverging Agaricomycetes, which predate the emergence of lignin-degrading class II peroxidases, have been associated with SR-type decay. Despite the fact that SR is a decay type known to be widespread in Ascomycota, studies have linked this type of decay in *Cylindrobasidium torrendii* (type II SR(Floudas et al., 2015)), *Armillaria* spp. (type I SR (Schwarze, 2007)), as well as *Oudemansiella*

mucida (Agaricales) (Daniel et al., 1992) and *Meripilus giganteus* (Polyporales) (Schwarze and Fink, 1998), suggesting a selective deployment of lignin-degrading enzymes. These species have all the PCWDEs required for breaking down cellulose and hemicellulose, however, they have fewer gene copies required for lignin degradation. Given these studies and the observations of our wood-decay omics analysis, we presume that these along with early diverging Agaricomycetes, and later evolved species that have fewer gene copies and capacity for lignin degradation (e.g., *Jaapia, Botryobasidium* and *Schizophyllum* (Nagy et al., 2016)), are able to revert to a plesiomorphic SR type mechanism, in which cellulolytic and pectinolytic activities predominate. Overall, this decay profile appears to be spread across the Agaricomycetes clade, and we propose that these species represent secondarily SR fungi, possessing a reduced repertoire of class-II peroxidases, that based on the gene expression regulation could allow these species to switch between SR and WR to follow a selective mode of lignin degradation.

To put our findings into an evolutionary perspective, we further, using new and previously published *Armillaria* genomes, along with other Agaricales, in phylogenomic comparisons to explore genomic innovations and gene repertoire variations in *Armillaria*. Our results confirmed that *Armillaria* spp. have an expanded repertoire of protein-coding genes (Figure 18), several novel gene families (Figure 21), and a plethora of lignocellulose degrading PCWDEs (including lignin) (Figure 18) (Collins et al., 2013, 2017; Ross-Davis et al., 2013; Sipos et al., 2017, 2018). Genes related to pectin-degradation, cellulose binding, and other putative extracellular and aromatic compound breakdown processes were enriched in *Armillaria* species. We also found an over-representation of putative pathogenesis-related gene families such as ceratoplatanins, LysM domains, deuterolysins, aspartic peptidases, chitin deacetylases, and Golgi-like pathogenesis-related proteins in *Armillaria* genomes.

Using the new genomes, we were able to make prediction whether variations in the plant cell wall degrading gene repertoire are responsible for the functional diversity of wood-decay strategies in *Armillaria*. Phylogenetic PCAs revealed that

Armillaria and the Physalacriaceae differ from WR, particularly based on their cellulase and pectinase gene families. For instance, *Armillaria* and Physalacriaceae lack the GH44 family, which is unique to Basidiomycota, and the CBM67 family (rhamnose-binding modules), which were enriched in *Armillaria* species, were not only absent in the majority of WR species but also had the highest loading in the pectinase PCA. In addition, all Physalacriaceae species contain members of the PL1 family, but many WR and LD fungi lack the PL1 family. This suggests that both gene gains and losses have played a role in the evolution of trophic modes in these fungi. Our observations are consistent with previous microscopy and chemical studies, as well as our wood-decay transcriptomics, indicating that the strategy of wood decay in *Armillaria* hints towards SR in Ascomycota. In addition, we found CAZy orthogroups that were significantly overrepresented in both Physalacriaceae and Ascomycota with respect to WR and LD fungi. These included some of the high-loading families from the phylogenetic PCAs such as PCWDEs acting on cellulose (AA3_1, AA8, CBM1), pectin (PL3_2, PL1_7, PL9_3), and hemicellulose (GH31, GH43, GH93, CE4), respectively. These families may arise as a consequence of co-expansion in both Ascomycota and Physalacriaceae or via HGT events.

We systematically evaluated HGT events into Physalacriaceae using a two-step method. Firstly, using the AI method with a phylogenetically diverse dataset including fungi from different taxonomic orders as well as bacteria and plants, we identified the candidate HT genes. Secondly, these were followed by phylogenetic validation, revealing 101 strongly supported HGT events into Physalacriaceae. Out of these, 88 HGT events had Ascomycota donors, predominantly from the Sordariomycetes and Dothideomycetes. The phylogenetically verified HT events had 164 CAZymes, of which 117 belonged to families that were co-enriched among Ascomycota and Physalacriaceae in comparison to white-rot and litter-decomposing fungi (AA3 1, AA8, GH43, GH93, GT1, PL3 2 and PL9 3). As a result, it is likely that HGT events were responsible for the co-enrichment signal that was described above. Along with CAZymes, HT genes also comprised cytochrome P450, peptidases, transporters, transcription factors, CAP domain proteins, intradiol ring-cleavage

dioxygenases, and Pyr1-like SCP domains. Based on the multiple expression data, the substantial influx of Ascomycota genes via HGT appears to have influenced both the ability to degrade plant biomass and the pathogenic attributes of *Armillaria* (Figure 30). Our analyses provided evidence that horizontal transfer affects families related to wood-decay (e.g. AA3 1, GH43, PL3 2) and plant-fungal interactions (e.g. CAP - domain proteins, Pyr1-like SCP domains, peptidases), raising the possibility that it might have shaped evolution of these strategies in *Armillaria* species.

In addition, we checked the molecular mechanisms underlying the infection process by a comprehensive analysis using different transcriptomic datasets related to wood decay, cambium killing (from Prof. György Sipos), root-colonization (from Jonathan Plett) and fruiting body development (Sipos et al., 2017). This allowed us to gain molecular perspectives into how *Armillaria* spp. use the expanded, novel core, HT genes, PCWDEs and pathogenicity-related gene families. We combined the DEG data across these studies and estimated the DEG enrichment ratios for several gene groups to get an overall perspective on the behavior of different *Armillaria* species. Our analysis showed that wood decay, stem colonization, in-planta assay, and fruiting body/rhizomorph growth all displayed distinctive enrichment patterns. In stem invasion and wood-decay experiments, PCWDE genes associated with cellulose, hemicellulose, pectin, and lignin displayed a distinct enrichment pattern, as would be predicted given their known activities. Pectinases were the most predominant genes among those upregulated on fresh stems, which may help the fungus loosen the plant cell wall and structure and spread between the sapwood and the bark. The *in planta* time series experiment however showed downregulation of PCWDEs, indicating that these genes were not induced by *A. luteobubalina* during host infection. Instead, other genes involved in virulence such as cerato-platanins, CAP domains, catalases and genes related to oxidative stress were upregulated at different time points in *A. luteobubalina*. This is in line with the majority of necrotrophs that express more virulence genes than PCWDEs during plant colonization. We also found that, in the stem invasion assay, the more virulent strain when compared to the less virulent strain, displays a distinctive enrichment of pathogenicity-related LysM proteins and cerato-

platanins, suggesting that the enrichment patterns for up- and downregulated genes differ according to species and strain. Additionally, such a subsequent analysis of the species- and strain-specific enrichment patterns revealed that species may respond differently to the substrates/hosts, which may be related to variations in lifestyle or pathogenicity.

Overall, the gene expression pattern of PCWDEs during wood-decay by two conifer-colonizing *Armillaria* spp., hinted towards a SR type decay. The existence of SR-like decay in Basidiomycota has previously been suggested (Campbell, 1932, 1931; Daniel et al., 1992; Floudas et al., 2015; Schwarze, 2007; Schwarze and Fink, 1998), but was not proven or examined at a gene expression level. This decay pattern, however, stands out from the conventional WR and BR decays and may offer an evolutionary explanation for unique decay types prevalent among the diversity of wood-decay fungi. In comparative phylogenomics, we found that phylogenetic PCAs distinguished *Armillaria* from WR species, which is surprising considering that Agaricales normally decay wood in this manner (Ruiz-Dueñas et al., 2021). Additionally, using new genomic data, we show that *Armillaria* species have acquired horizontally transferred genes from the Ascomycota. Consequently, HGT could be a source of novelty in the evolution of fungal systems for decomposing plant biomass, explaining the decay type. Further, functional and expression data suggest that HGT could have affected two key aspects of *Armillaria* lifestyle - plant biomass-degrading and pathogenicity. During root and cambium colonization, horizontally acquired genes as well as genes related to putative virulence factors and wood decay were expressed. Based on our results, we find that the evolution of *Armillaria* genomes was marked with multiple types of genetic innovations, including horizontal gene transfer from Ascomycota. The findings of this work, in combination with existing and emerging pathosystems (Adelberg et al., 2021; Ford et al., 2017), could improve research into the molecular mechanisms of plant colonization.

Acknowledegment

First and foremost, I would like to express my sincere gratitude to my PhD supervisor, Dr. László G. Nagy, for his invaluable guidance and support throughout my doctoral studies. Your constant encouragement and positive attitude have been truly inspiring. I am especially grateful for your ability to clarify complex concepts through effective communication, and for the opportunity to learn from your extensive expertise and knowledge in the field. It has been an incredible experience to have learned so much from you over the years and I am still learning more. Thank you for everything. I could not have wished for a better mentor.

Similar thanks go to each and every current and former member of the Fungal Evolution and Genomics Lab for the mushroom forays, cooking sessions, lab gatherings, extending my Hungarian vocabulary, the endless supply of homegrown goodies and all the other amazing moments and memories. You are all truly wonderful colleagues and friends.

I would like to thank all of my co-authors for their contributions to this project. In particular, I want to thank Dr. Zsolt Merényi and Dr. Balázs Bálint for their invaluable input and support during our brainstorming sessions. Your expertise in coding and HPC has been a tremendous asset and has helped me to grow as a computational biologist. I feel fortunate to have had the opportunity to work with and learn from experts like you.

Additionally, I would like to extend my gratitude to Prof. György Sipos, Dr. Jonathan Plett, Prof. Jason C. Slot, Dr. Rebecca Owens and many others for their successful scientific collaboration and publications.

I am also grateful to my reviewing committee for their valuable suggestions that helped to bring this work to its current form.

I would like to thank the administrative staff of the Institute of Biochemistry at the Biological Research Centre, and the Faculty of Science and Informatics, University of Szeged for their help and support during my studies.

I am grateful for the wonderful time I spent with friends such as Kaushik Nath Bhaumik, Gaurav Sharma, Kamal Kant, Paras Gaur, and others who made my stay here memorable.

Last but not the least, I would like to thank my parents and my brother for their kind support and understanding.

List of References

Aanen, D.K., 2014. How a long-lived fungus keeps mutations in check. Science 346, 922–923. https://doi.org/10.1126/science.1261401

Akcapinar, G.B., Kappel, L., Sezerman, O.U., Seidl-Seiboth, V., 2015. Molecular diversity of LysM carbohydrate-binding motifs in fungi. Curr. Genet. 61, 103–113. https://doi.org/10.1007/s00294-014-0471-9

Alexa, A., Rahenfuhrer, J., 2016. topGO: Enrichement Analysis for Gene Ontology.

Alexander, W.G., Wisecaver, J.H., Rokas, A., Hittinger, C.T., 2016. Horizontally acquired genes in early-diverging pathogenic fungi enable the use of host nucleosides and nucleotides. Proc. Natl. Acad. Sci. 113, 4116–4121. https://doi.org/10.1073/pnas.1517242113

Allan, J., Regmi, R., Denton-Giles, M., Kamphuis, L.G., Derbyshire, M.C., 2019. The host generalist phytopathogenic fungus *Sclerotinia sclerotiorum* differentially expresses multiple metabolic enzymes on two different plant hosts. Sci. Rep. 9, 19966. https://doi.org/10.1038/s41598-019-56396-w

Almagro Armenteros, J.J., Sønderby, C.K., Sønderby, S.K., Nielsen, H., Winther, O., 2017. DeepLoc: prediction of protein subcellular localization using deep learning. Bioinformatics 33, 3387–3395. https://doi.org/10.1093/bioinformatics/btx431

Almási, É., Sahu, N., Krizsán, K., Bálint, B., Kovács, G.M., Kiss, B., Cseklye, J., Drula, E., Henrissat, B., Nagy, I., Chovatia, M., Adam, C., LaButti, K., Lipzen, A., Riley, R., Grigoriev, I.V., Nagy, L.G., 2019. Comparative genomics reveals unique wood- decay strategies and fruiting body development in the Schizophyllaceae. New Phytol. 224, 902–915. https://doi.org/10.1111/nph.16032

Alveshere, B.C., Bennett, P., Kim, M.-S., Klopfenstein, N.B., LeBoldus, J.M., 2021. First Report of *Armillaria cepistipes* Causing Root Disease on *Populus trichocarpa* (Black Cottonwood) in Oregon, U.S.A. Plant Dis. 105, 2729. https://doi.org/10.1094/PDIS-09-20-1993-PDN

Anderson, J.B., Bruhn, J.N., Kasimer, D., Wang, H., Rodrigue, N., Smith, M.L., 2018. Clonal evolution and genome stability in a 2500-year-old fungal individual. Proc. R. Soc. B Biol. Sci. 285, 20182233. https://doi.org/10.1098/rspb.2018.2233

Anderson, J.B., Catona, S., 2014. Genomewide mutation dynamic within a long-lived individual of *Armillaria gallica*. Mycologia 106, 642–648. https://doi.org/10.3852/13-367

Anderson, J.B., Ullrich, R.C., 1982. Translocation in rhizomorphs of *Armillaria mellea*. Exp. Mycol. 6, 31–40. https://doi.org/10.1016/0147-5975(82)90061-5

Arvind, L., Koonin, V.E., 2001. The DNA-repair protein AlkB, EGL-9, and leprecan define new families of 2-oxoglutarate- and iron-dependent dioxygenases. Genome Biol., research0007.1 (2001) 2. https://doi.org/doi:10.1186/gb-2001-2-3-research0007

Ayuso-Fernández, I., Rencoret, J., Gutiérrez, A., Ruiz-Dueñas, F.J., Martínez, A.T., 2019. Peroxidase evolution in white-rot fungi follows wood lignin evolution in plants. Proc. Natl. Acad. Sci. 116, 17900–17905. https://doi.org/10.1073/pnas.1905040116

Baccelli, I., 2015. Cerato-platanin family proteins: one function for multiple biological roles? Front. Plant Sci. 5. https://doi.org/10.3389/fpls.2014.00769

Bahram, M., Netherway, T., 2022. Fungi as mediators linking organisms and ecosystems. FEMS Microbiol. Rev. 46, fuab058. https://doi.org/10.1093/femsre/fuab058

Baldrian, P., Valášková, V., 2008. Degradation of cellulose by basidiomycetous fungi. FEMS Microbiol. Rev. 32, 501–521. https://doi.org/10.1111/j.1574-6976.2008.00106.x

Bass, A.J., Robinson, D.G., Storey, J.D., 2019. Determining sufficient sequencing depth in

RNA-Seq differential expression studies (preprint). Genomics. https://doi.org/10.1101/635623
Baumgartner, K., 2004. Root Collar Excavation for Postinfection control of Armillaria root disease of grapevine. Plant Dis. 88, 1235–1240. https://doi.org/10.1094/PDIS.2004.88.11.1235
Baumgartner, K., Coetzee, M.P.A., Hoffmeister, D., 2011. Secrets of the subterranean pathosystem of *Armillaria*: Subterranean pathosystem of *Armillaria*. Mol. Plant Pathol. 12, 515–534. https://doi.org/10.1111/j.1364-3703.2010.00693.x
Bautista, D., Guayazan-Palacios, N., Buitrago, M.C., Cardenas, M., Botero, D., Duitama, J., Bernal, A.J., Restrepo, S., 2021. Comprehensive time-series analysis of the gene expression profile in a susceptible cultivar of tree tomato (*Solanum betaceum*) during the infection of phytophthora betacei. Front. Plant Sci. 12, 730251. https://doi.org/10.3389/fpls.2021.730251
Beeson, W.T., Phillips, C.M., Cate, J.H.D., Marletta, M.A., 2012. Oxidative Cleavage of Cellulose by Fungal Copper-Dependent Polysaccharide Monooxygenases. J. Am. Chem. Soc. 134, 890–892. https://doi.org/10.1021/ja210657t
Bendel, M., Kienast, F., Rigling, D., 2006. Genetic population structure of three *Armillaria* species at the landscape scale: a case study from Swiss *Pinus mugo* forests. Mycol. Res. 110, 705–712. https://doi.org/10.1016/j.mycres.2006.02.002
Bey, M., Zhou, S., Poidevin, L., Henrissat, B., Coutinho, P.M., Berrin, J.-G., Sigoillot, J.-C., 2013. Cello-Oligosaccharide Oxidation Reveals Differences between Two Lytic Polysaccharide Monooxygenases (Family GH61) from *Podospora anserina*. Appl. Environ. Microbiol. 79, 488–496. https://doi.org/10.1128/AEM.02942-12
Bhattacharya, A., Kourmpetli, S., Ward, D.A., Thomas, S.G., Gong, F., Powers, S.J., Carrera, E., Taylor, B., de Caceres Gonzalez, F.N., Tudzynski, B., Phillips, A.L., Davey, M.R., Hedden, P., 2012. Characterization of the Fungal Gibberellin Desaturase as a 2-Oxoglutarate-Dependent Dioxygenase and Its Utilization for Enhancing Plant Growth. Plant Physiol. 160, 837–845. https://doi.org/10.1104/pp.112.201756
Blanchette, R.A., Held, B.W., Jurgens, J.A., McNew, D.L., Harrington, T.C., Duncan, S.M., Farrell, R.L., 2004. Wood-Destroying Soft Rot Fungi in the Historic Expedition Huts of Antarctica. Appl. Environ. Microbiol. 70, 1328–1335. https://doi.org/10.1128/AEM.70.3.1328-1335.2004
Bonfante, P., Genre, A., 2010. Mechanisms underlying beneficial plant–fungus interactions in mycorrhizal symbiosis. Nat. Commun. 1, 48. https://doi.org/10.1038/ncomms1046
Bourras, S., McNally, K.E., Müller, M.C., Wicker, T., Keller, B., 2016. Avirulence Genes in Cereal Powdery Mildews: The Gene-for-Gene Hypothesis 2.0. Front. Plant Sci. 7. https://doi.org/10.3389/fpls.2016.00241
Brownlee, C., Jennings, D.H., 1982a. Pathway of translocation in *Serpula lacrimans*. Trans. Br. Mycol. Soc. 79, 401–407. https://doi.org/10.1016/S0007-1536(82)80033-8
Brownlee, C., Jennings, D.H., 1982b. Long distance translocation in *Serpula lacrimans*: Velocity estimates and the continuous monitoring of induced perturbations. Trans. Br. Mycol. Soc. 79, 143–148. https://doi.org/10.1016/S0007-1536(82)80200-3
Caballero, J.R.I., Lalande, B.M., Hanna, J.W., Klopfenstein, N.B., Kim, M.-S., Stewart, J.E., 2022. Genomic Comparisons of Two *Armillaria* Species with Different Ecological Behaviors and Their Associated Soil Microbial Communities. Microb. Ecol. https://doi.org/10.1007/s00248-022-01989-8
Cairney, J.W.G., 1991. Rhizomorphs: Organs of exploration or exploitation? Mycologist 5, 5–10. https://doi.org/10.1016/S0269-915X(09)80325-X
Cairney, J.W.G., Jennings, D.H., Ratcliffe, R.G., Southon, T.E., 1988. The physiology of

basidiomycete linear organs II. Phosphate uptake by rhizomorphs of *Armillaria mellea*. New Phytol. 109, 327–333. https://doi.org/10.1111/j.1469-8137.1988.tb04202.x
Campbell, W.G., 1932. The chemistry of the white rots of wood. Biochem. J. 26, 1829–1838. https://doi.org/10.1042/bj0261829
Campbell, W.G., 1931. The chemistry of the white rots of wood. Biochem. J. 25, 2023–2027. https://doi.org/10.1042/bj0252023
Canam, T., Dumonceaux, T.J., Record, E., Li, Y., 2013. White-rot fungi: the key to sustainable biofuel production? Biofuels 4, 247–250. https://doi.org/10.4155/bfs.13.6
Capella-Gutierrez, S., Silla-Martinez, J.M., Gabaldon, T., 2009. trimAl: a tool for automated alignment trimming in large-scale phylogenetic analyses. Bioinformatics 25, 1972–1973. https://doi.org/10.1093/bioinformatics/btp348
Chen, H., He, S., Zhang, S., A, R., Li, W., Liu, S., 2022. The Necrotroph Botrytis cinerea BcSpd1 Plays a Key Role in Modulating Both Fungal Pathogenic Factors and Plant Disease Development. Front. Plant Sci. 13, 820767. https://doi.org/10.3389/fpls.2022.820767
Chen, L., Bóka, B., Kedves, O., Nagy, V.D., Szűcs, A., Champramary, S., Roszik, R., Patocskai, Z., Münsterkötter, M., Huynh, T., Indic, B., Vágvölgyi, C., Sipos, G., Kredics, L., 2019. Towards the Biological Control of Devastating Forest Pathogens from the Genus *Armillaria*. Forests 10, 1013. https://doi.org/10.3390/f10111013
Choi, J., Lee, G.-W., Kim, K.-T., Jeon, J., Détry, N., Kuo, H.-C., Sun, H., Asiegbu, F.O., Lee, Y.-H., 2017. Comparative analysis of genome sequences of the conifer tree pathogen, *Heterobasidion annosum* s.s . Genomics Data 14, 106–113. https://doi.org/10.1016/j.gdata.2017.10.003
Clipson, N.J.W., Cairney, J.W.G., Jennings, D.H., 1987. The physiology of basidiomycete linear organs. I. Phosphate uptake by cords and mycelium in the laboratory and the field. New Phytol. 105, 449–157. https://doi.org/10.1111/j.1469-8137.1987.tb00882.x
Collins, B.C., Hunter, C.L., Liu, Y., Schilling, B., Rosenberger, G., Bader, S.L., Chan, D.W., Gibson, B.W., Gingras, A.-C., Held, J.M., Hirayama-Kurogi, M., Hou, G., Krisp, C., Larsen, B., Lin, L., Liu, S., Molloy, M.P., Moritz, R.L., Ohtsuki, S., Schlapbach, R., Selevsek, N., Thomas, S.N., Tzeng, S.-C., Zhang, H., Aebersold, R., 2017. Multi-laboratory assessment of reproducibility, qualitative and quantitative performance of SWATH-mass spectrometry. Nat. Commun. 8. https://doi.org/10.1038/s41467-017-00249-5
Collins, C., Hurley, R., Almutlaqah, N., O'Keeffe, G., Keane, T., Fitzpatrick, D., Owens, R., 2017. Proteomic Characterization of *Armillaria mellea* Reveals Oxidative Stress Response Mechanisms and Altered Secondary Metabolism Profiles. Microorganisms 5, 60. https://doi.org/10.3390/microorganisms5030060
Collins, C., Keane, T.M., Turner, D.J., O'Keeffe, G., Fitzpatrick, D.A., Doyle, S., 2013. Genomic and Proteomic Dissection of the Ubiquitous Plant Pathogen, *Armillaria mellea* : Toward a New Infection Model System. J. Proteome Res. 12, 2552–2570. https://doi.org/10.1021/pr301131t
Cox, J., Hein, M.Y., Luber, C.A., Paron, I., Nagaraj, N., Mann, M., 2014. Accurate Proteome-wide Label-free Quantification by Delayed Normalization and Maximal Peptide Ratio Extraction, Termed MaxLFQ. Mol. Cell. Proteomics 13, 2513–2526. https://doi.org/10.1074/mcp.M113.031591
Cox, K.D., Scherm, H., 2006. Interaction dynamics between saprobic lignicolous fungi and Armillaria in controlled environments: Exploring the potential for competitive exclusion of Armillaria on peach. Biol. Control 37, 291–300. https://doi.org/10.1016/j.biocontrol.2006.01.012

Dance, A., 2017. Special relationship between fungi and plants may have spurred changes to ancient climate. Proc. Natl. Acad. Sci. 114, 12089–12091. https://doi.org/10.1073/pnas.1716319114

Daniel, G., Volc, J., Nilsson, T., 1992. Soft rot and multiple T-branching by the basidiomycete *Oudemansiella mucida*. Mycol. Res. 96, 49–54. https://doi.org/10.1016/S0953-7562(09)80995-7

de Jonge, R., Peter van Esse, H., Kombrink, A., Shinya, T., Desaki, Y., Bours, R., van der Krol, S., Shibuya, N., Joosten, M.H.A.J., Thomma, B.P.H.J., 2010. Conserved Fungal LysM Effector Ecp6 Prevents Chitin-Triggered Immunity in Plants. Science 329, 953–955. https://doi.org/10.1126/science.1190859

Devkota, P., Hammerschmidt, R., 2020. The infection process of Armillaria mellea and Armillaria solidipes. Physiol. Mol. Plant Pathol. 112, 101543. https://doi.org/10.1016/j.pmpp.2020.101543

Dodds, P.N., Lawrence, G.J., Catanzariti, A.-M., Teh, T., Wang, C.-I.A., Ayliffe, M.A., Kobe, B., Ellis, J.G., 2006. Direct protein interaction underlies gene-for-gene specificity and coevolution of the flax resistance genes and flax rust avirulence genes. Proc. Natl. Acad. Sci. 103, 8888–8893. https://doi.org/10.1073/pnas.0602577103

Dodds, P.N., Rafiqi, M., Gan, P.H.P., Hardham, A.R., Jones, D.A., Ellis, J.G., 2009. Effectors of biotrophic fungi and oomycetes: pathogenicity factors and triggers of host resistance. New Phytol. 183, 993–1000. https://doi.org/10.1111/j.1469-8137.2009.02922.x

Duplessis, S., Cuomo, C.A., Lin, Y.-C., Aerts, A., Tisserant, E., Veneault-Fourrey, C., Joly, D.L., Hacquard, S., Amselem, J., Cantarel, B.L., Chiu, R., Coutinho, P.M., Feau, N., Field, M., Frey, P., Gelhaye, E., Goldberg, J., Grabherr, M.G., Kodira, C.D., Kohler, A., Kües, U., Lindquist, E.A., Lucas, S.M., Mago, R., Mauceli, E., Morin, E., Murat, C., Pangilinan, J.L., Park, R., Pearson, M., Quesneville, H., Rouhier, N., Sakthikumar, S., Salamov, A.A., Schmutz, J., Selles, B., Shapiro, H., Tanguay, P., Tuskan, G.A., Henrissat, B., Van de Peer, Y., Rouzé, P., Ellis, J.G., Dodds, P.N., Schein, J.E., Zhong, S., Hamelin, R.C., Grigoriev, I.V., Szabo, L.J., Martin, F., 2011. Obligate biotrophy features unraveled by the genomic analysis of rust fungi. Proc. Natl. Acad. Sci. 108, 9166–9171. https://doi.org/10.1073/pnas.1019315108

Eastwood, D.C., Floudas, D., Binder, M., Majcherczyk, A., Schneider, P., Aerts, A., Asiegbu, F.O., Baker, S.E., Barry, K., Bendiksby, M., Blumentritt, M., Coutinho, P.M., Cullen, D., de Vries, R.P., Gathman, A., Goodell, B., Henrissat, B., Ihrmark, K., Kauserud, H., Kohler, A., LaButti, K., Lapidus, A., Lavin, J.L., Lee, Y.-H., Lindquist, E., Lilly, W., Lucas, S., Morin, E., Murat, C., Oguiza, J.A., Park, J., Pisabarro, A.G., Riley, R., Rosling, A., Salamov, A., Schmidt, O., Schmutz, J., Skrede, I., Stenlid, J., Wiebenga, A., Xie, X., Kues, U., Hibbett, D.S., Hoffmeister, D., Hogberg, N., Martin, F., Grigoriev, I.V., Watkinson, S.C., 2011. The Plant Cell Wall-Decomposing Machinery Underlies the Functional Diversity of Forest Fungi. Science 333, 762–765. https://doi.org/10.1126/science.1205411

Emms, D.M., Kelly, S., 2019. OrthoFinder: phylogenetic orthology inference for comparative genomics. Genome Biol. 20, 238. https://doi.org/10.1186/s13059-019-1832-y

Emms, D.M., Kelly, S., 2015. OrthoFinder: solving fundamental biases in whole genome comparisons dramatically improves orthogroup inference accuracy. Genome Biol. 16. https://doi.org/10.1186/s13059-015-0721-2

Farrow, S.C., Facchini, P.J., 2014. Functional diversity of 2-oxoglutarate/Fe(II)-dependent dioxygenases in plant metabolism. Front. Plant Sci. 5. https://doi.org/10.3389/fpls.2014.00524

Filip, G.M., Fitzgerald, S.A., Chadwick, K.L., Max, T.A., 2009. Thinning Ponderosa Pine Affected by *Armillaria* Root Disease: 40 Years of Growth and Mortality on an Infected Site in Central Oregon. West. J. Appl. For. 24, 88–94. https://doi.org/10.1093/wjaf/24.2.88

Flor, H.H., 1971. Current Status of the Gene-For-Gene Concept. Annu. Rev. Phytopathol. 9, 275–296. https://doi.org/10.1146/annurev.py.09.090171.001423

Floudas, D., 2021. Evolution of lignin decomposition systems in fungi, in: Advances in Botanical Research. Elsevier, pp. 37–76. https://doi.org/10.1016/bs.abr.2021.05.003

Floudas, D., Bentzer, J., Ahrén, D., Johansson, T., Persson, P., Tunlid, A., 2020. Uncovering the hidden diversity of litter-decomposition mechanisms in mushroom-forming fungi. ISME J. 14, 2046–2059. https://doi.org/10.1038/s41396-020-0667-6

Floudas, D., Binder, M., Riley, R., Barry, K., Blanchette, R.A., Henrissat, B., Martinez, A.T., Otillar, R., Spatafora, J.W., Yadav, J.S., Aerts, A., Benoit, I., Boyd, A., Carlson, A., Copeland, A., Coutinho, P.M., de Vries, R.P., Ferreira, P., Findley, K., Foster, B., Gaskell, J., Glotzer, D., Gorecki, P., Heitman, J., Hesse, C., Hori, C., Igarashi, K., Jurgens, J.A., Kallen, N., Kersten, P., Kohler, A., Kues, U., Kumar, T.K.A., Kuo, A., LaButti, K., Larrondo, L.F., Lindquist, E., Ling, A., Lombard, V., Lucas, S., Lundell, T., Martin, R., McLaughlin, D.J., Morgenstern, I., Morin, E., Murat, C., Nagy, L.G., Nolan, M., Ohm, R.A., Patyshakuliyeva, A., Rokas, A., Ruiz-Duenas, F.J., Sabat, G., Salamov, A., Samejima, M., Schmutz, J., Slot, J.C., St. John, F., Stenlid, J., Sun, H., Sun, S., Syed, K., Tsang, A., Wiebenga, A., Young, D., Pisabarro, A., Eastwood, D.C., Martin, F., Cullen, D., Grigoriev, I.V., Hibbett, D.S., 2012. The Paleozoic Origin of Enzymatic Lignin Decomposition Reconstructed from 31 Fungal Genomes. Science 336, 1715–1719. https://doi.org/10.1126/science.1221748

Floudas, D., Held, B.W., Riley, R., Nagy, L.G., Koehler, G., Ransdell, A.S., Younus, H., Chow, J., Chiniquy, J., Lipzen, A., Tritt, A., Sun, H., Haridas, S., LaButti, K., Ohm, R.A., Kües, U., Blanchette, R.A., Grigoriev, I.V., Minto, R.E., Hibbett, D.S., 2015. Evolution of novel wood decay mechanisms in Agaricales revealed by the genome sequences of *Fistulina hepatica* and *Cylindrobasidium torrendii*. Fungal Genet. Biol. 76, 78–92. https://doi.org/10.1016/j.fgb.2015.02.002

Foley, R.C., Kidd, B.N., Hane, J.K., Anderson, J.P., Singh, K.B., 2016. Reactive Oxygen Species Play a Role in the Infection of the Necrotrophic Fungi, Rhizoctonia solani in Wheat. PLOS ONE 11, e0152548. https://doi.org/10.1371/journal.pone.0152548

Ford, K.L., Henricot, B., Baumgartner, K., Bailey, A.M., Foster, G.D., 2017. A faster inoculation assay for *Armillaria* using herbaceous plants. J. Hortic. Sci. Biotechnol. 92, 39–47. https://doi.org/10.1080/14620316.2016.1223528

Fox, E.M., Howlett, B.J., 2008. Secondary metabolism: regulation and role in fungal biology. Curr. Opin. Microbiol. 11, 481–487. https://doi.org/10.1016/j.mib.2008.10.007

Friesen, T.L., Meinhardt, S.W., Faris, J.D., 2007. The Stagonospora nodorum-wheat pathosystem involves multiple proteinaceous host-selective toxins and corresponding host sensitivity genes that interact in an inverse gene-for-gene manner: SNB of wheat is induced by multiple toxins. Plant J. 51, 681–692. https://doi.org/10.1111/j.1365-313X.2007.03166.x

Gadd, G.M., 2013. Fungi and Their Role in the Biosphere, in: Reference Module in Earth Systems and Environmental Sciences. Elsevier, p. B9780124095489010000. https://doi.org/10.1016/B978-0-12-409548-9.00933-7

Gaskell, J., Marty, A., Mozuch, M., Kersten, P.J., Splinter BonDurant, S., Sabat, G., Azarpira, A., Ralph, J., Skyba, O., Mansfield, S.D., Blanchette, R.A., Cullen, D., 2014. Influence of Populus Genotype on Gene Expression by the Wood Decay Fungus *Phanerochaete*

chrysosporium. Appl. Environ. Microbiol. 80, 5828–5835. https://doi.org/10.1128/AEM.01604-14
Gladyshev, E.A., Meselson, M., Arkhipova, I.R., 2008. Massive Horizontal Gene Transfer in Bdelloid Rotifers. Science 320, 1210–1213. https://doi.org/10.1126/science.1156407
Graham-Taylor, C., Kamphuis, L.G., Derbyshire, M.C., 2020. A detailed in silico analysis of secondary metabolite biosynthesis clusters in the genome of the broad host range plant pathogenic fungus Sclerotinia sclerotiorum. BMC Genomics 21, 7. https://doi.org/10.1186/s12864-019-6424-4
Granlund, H.I., Jennings, D.H., Thompson, W., 1985. Translocation of solutes along rhizomorphs of *Armillaria mellea*. Trans. Br. Mycol. Soc. 84, 111–119. https://doi.org/10.1016/S0007-1536(85)80224-2
Grigoriev, I.V., Nikitin, R., Haridas, S., Kuo, A., Ohm, R., Otillar, R., Riley, R., Salamov, A., Zhao, X., Korzeniewski, F., Smirnova, T., Nordberg, H., Dubchak, I., Shabalov, I., 2014. MycoCosm portal: gearing up for 1000 fungal genomes. Nucleic Acids Res. 42, D699-704. https://doi.org/10.1093/nar/gkt1183
Guillaumin, J.-J., Mohammed, C., Anselmi, N., Courtecuisse, R., Gregory, S.C., Holdenrieder, O., Intini, M., Lung, B., Marxmüller, H., Morrison, D., Rishbeth, J., Termorshuizen, A.J., Tirró, A., Dam, B., 1993. Geographical distribution and ecology of the *Armillaria* species in western Europe. For. Pathol. 23, 321–341. https://doi.org/10.1111/j.1439-0329.1993.tb00814.x
Guo, T., Wang, H.C., Xue, W.Q., Zhao, J., Yang, Z.L., 2016. Phylogenetic Analyses of Armillaria Reveal at Least 15 Phylogenetic Lineages in China, Seven of Which Are Associated with Cultivated Gastrodia elata. PLOS ONE 11, e0154794. https://doi.org/10.1371/journal.pone.0154794
Hao, H., Zhang, J., Wang, H., Wang, Q., Chen, M., Juan, J., Feng, Z., Chen, H., 2019. Comparative transcriptome analysis reveals potential fruiting body formation mechanisms in Morchella importuna. AMB Express 9, 103. https://doi.org/10.1186/s13568-019-0831-4
He, K., Wu, Y., 2016. Receptor-Like Kinases and Regulation of Plant Innate Immunity, in: The Enzymes. Elsevier, pp. 105–142. https://doi.org/10.1016/bs.enz.2016.09.003
Heinzelmann, R., Dutech, C., Tsykun, T., Labbé, F., Soularue, J.-P., Prospero, S., 2019. Latest advances and future perspectives in *Armillaria* research. Can. J. Plant Pathol. 41, 1–23. https://doi.org/10.1080/07060661.2018.1558284
Heinzelmann, R., Prospero, S., Rigling, D., 2017. Virulence and Stump Colonization Ability of *Armillaria borealis* on Norway Spruce Seedlings in Comparison to Sympatric *Armillaria* Species. Plant Dis. 101, 470–479. https://doi.org/10.1094/PDIS-06-16-0933-RE
Heinzelmann, R., Rigling, D., Sipos, G., Münsterkötter, M., Croll, D., 2020. Chromosomal assembly and analyses of genome-wide recombination rates in the forest pathogenic fungus Armillaria ostoyae. Heredity 124, 699–713. https://doi.org/10.1038/s41437-020-0306-z
Hill, R., Buggs, R.J.A., Vu, D.T., Gaya, E., 2022. Lifestyle Transitions in Fusarioid Fungi are Frequent and Lack Clear Genomic Signatures. Mol. Biol. Evol. 39, msac085. https://doi.org/10.1093/molbev/msac085
Hood, I.A., Redfern, D.B., Kile, G.A., 1991. *Armillaria* Root Disease, in: Armilalria Root Disease, Agriculture Handbook No. 691. USDA Forest Service, Washington, D.C, pp. 122–149.
Houterman, P.M., Cornelissen, B.J.C., Rep, M., 2008. Suppression of Plant Resistance Gene-Based Immunity by a Fungal Effector. PLoS Pathog. 4, e1000061. https://doi.org/10.1371/journal.ppat.1000061

Huang, J., Si, W., Deng, Q., Li, P., Yang, S., 2014. Rapid evolution of avirulence genes in rice blast fungus Magnaporthe oryzae. BMC Genet. 15, 45. https://doi.org/10.1186/1471-2156-15-45

Hyde, K.D., Xu, J., Rapior, S., Jeewon, R., Lumyong, S., Niego, A.G.T., Abeywickrama, P.D., Aluthmuhandiram, J.V.S., Brahamanage, R.S., Brooks, S., Chaiyasen, A., Chethana, K.W.T., Chomnunti, P., Chepkirui, C., Chuankid, B., de Silva, N.I., Doilom, M., Faulds, C., Gentekaki, E., Gopalan, V., Kakumyan, P., Harishchandra, D., Hemachandran, H., Hongsanan, S., Karunarathna, A., Karunarathna, S.C., Khan, S., Kumla, J., Jayawardena, R.S., Liu, J.-K., Liu, N., Luangharn, T., Macabeo, A.P.G., Marasinghe, D.S., Meeks, D., Mortimer, P.E., Mueller, P., Nadir, S., Nataraja, K.N., Nontachaiyapoom, S., O'Brien, M., Penkhrue, W., Phukhamsakda, C., Ramanan, U.S., Rathnayaka, A.R., Sadaba, R.B., Sandargo, B., Samarakoon, B.C., Tennakoon, D.S., Siva, R., Sriprom, W., Suryanarayanan, T.S., Sujarit, K., Suwannarach, N., Suwunwong, T., Thongbai, B., Thongklang, N., Wei, D., Wijesinghe, S.N., Winiski, J., Yan, J., Yasanthika, E., Stadler, M., 2019. The amazing potential of fungi: 50 ways we can exploit fungi industrially. Fungal Divers. 97, 1–136. https://doi.org/10.1007/s13225-019-00430-9

Jennings, D.H., 1987. Translocation of solutes in fungi. Biol. Rev. 62, 215–243. https://doi.org/10.1111/j.1469-185X.1987.tb00664.x

Jones, P., Binns, D., Chang, H.-Y., Fraser, M., Li, W., McAnulla, C., McWilliam, H., Maslen, J., Mitchell, A., Nuka, G., Pesseat, S., Quinn, A.F., Sangrador-Vegas, A., Scheremetjew, M., Yong, S.-Y., Lopez, R., Hunter, S., 2014. InterProScan 5: genome-scale protein function classification. Bioinformatics 30, 1236–1240. https://doi.org/10.1093/bioinformatics/btu031

Jwa, N.-S., Hwang, B.K., 2017. Convergent Evolution of Pathogen Effectors toward Reactive Oxygen Species Signaling Networks in Plants. Front. Plant Sci. 8, 1687. https://doi.org/10.3389/fpls.2017.01687

Kanyuka, K., Igna, A.A., Solomon, P.S., Oliver, R.P., 2022. The rise of necrotrophic effectors. New Phytol. 233, 11–14. https://doi.org/10.1111/nph.17811

Katoh, K., Standley, D.M., 2013. MAFFT multiple sequence alignment software version 7: improvements in performance and usability. Mol. Biol. Evol. 30, 772–780. https://doi.org/10.1093/molbev/mst010

Kawai, Y., Ono, E., Mizutani, M., 2014. Evolution and diversity of the 2-oxoglutarate-dependent dioxygenase superfamily in plants. Plant J. 78, 328–343. https://doi.org/10.1111/tpj.12479

Ke, H.-M., Lee, H.-H., Lin, C.-Y.I., Liu, Y.-C., Lu, M.R., Hsieh, J.-W.A., Chang, C.-C., Wu, P.-H., Lu, M.J., Li, J.-Y., Shang, G., Lu, R.J.-H., Nagy, L.G., Chen, P.-Y., Kao, H.-W., Tsai, I.J., 2020. *Mycena* genomes resolve the evolution of fungal bioluminescence. Proc. Natl. Acad. Sci. 117, 31267–31277. https://doi.org/10.1073/pnas.2010761117

Kedves, O., Shahab, D., Champramary, S., Chen, L., Indic, B., Bóka, B., Nagy, V.D., Vágvölgyi, C., Kredics, L., Sipos, G., 2021. Epidemiology, Biotic Interactions and Biological Control of Armillarioids in the Northern Hemisphere. Pathogens 10, 76. https://doi.org/10.3390/pathogens10010076

Kim, M.-S., Heinzelmann, R., Labbé, F., Ota, Y., Elías-Román, R.D., Pildain, M.B., Stewart, J.E., Woodward, S., Klopfenstein, N.B., 2022. Armillaria root diseases of diverse trees in wide-spread global regions, in: Forest Microbiology. Elsevier, pp. 361–378. https://doi.org/10.1016/B978-0-323-85042-1.00004-5

Koch, R.A., Herr, J.R., 2021. Global Distribution and Richness of Armillaria and Related Species Inferred From Public Databases and Amplicon Sequencing Datasets. Front.

Microbiol. 12, 733159. https://doi.org/10.3389/fmicb.2021.733159
Koch, R.A., Wilson, A.W., Séné, O., Henkel, T.W., Aime, M.C., 2017. Resolved phylogeny and biogeography of the root pathogen *Armillaria* and its gasteroid relative, *Guyanagaster*. BMC Evol. Biol. 17. https://doi.org/10.1186/s12862-017-0877-3
Koch, R.A., Yoon, G.M., Aryal, U.K., Lail, K., Amirebrahimi, M., LaButti, K., Lipzen, A., Riley, R., Barry, K., Henrissat, B., Grigoriev, I.V., Herr, J.R., Aime, M.C., 2021. Symbiotic nitrogen fixation in the reproductive structures of a basidiomycete fungus. Curr. Biol. 31, 3905-3914.e6. https://doi.org/10.1016/j.cub.2021.06.033
Koeck, M., Hardham, A.R., Dodds, P.N., 2011. The role of effectors of biotrophic and hemibiotrophic fungi in infection: Effectors of biotrophic fungi. Cell. Microbiol. 13, 1849–1857. https://doi.org/10.1111/j.1462-5822.2011.01665.x
Köhl, L., Lukasiewicz, C.E., van der Heijden, M.G.A., 2016. Establishment and effectiveness of inoculated arbuscular mycorrhizal fungi in agricultural soils: Mycorrhizal inoculation in agricultural soils. Plant Cell Environ. 39, 136–146. https://doi.org/10.1111/pce.12600
Kohler, A., Kuo, A., Nagy, L.G., Morin, E., Barry, K.W., Buscot, F., Canbäck, B., Choi, C., Cichocki, N., Clum, A., Colpaert, J., Copeland, A., Costa, M.D., Doré, J., Floudas, D., Gay, G., Girlanda, M., Henrissat, B., Herrmann, S., Hess, J., Högberg, N., Johansson, T., Khouja, H.-R., LaButti, K., Lahrmann, U., Levasseur, A., Lindquist, E.A., Lipzen, A., Marmeisse, R., Martino, E., Murat, C., Ngan, C.Y., Nehls, U., Plett, J.M., Pringle, A., Ohm, R.A., Perotto, S., Peter, M., Riley, R., Rineau, F., Ruytinx, J., Salamov, A., Shah, F., Sun, H., Tarkka, M., Tritt, A., Veneault-Fourrey, C., Zuccaro, A., Tunlid, A., Grigoriev, I.V., Hibbett, D.S., Martin, F., 2015. Convergent losses of decay mechanisms and rapid turnover of symbiosis genes in mycorrhizal mutualists. Nat. Genet. 47, 410–415. https://doi.org/10.1038/ng.3223
Kolesnikova, A.I., Putintseva, Y.A., Simonov, E.P., Biriukov, V.V., Oreshkova, N.V., Pavlov, I.N., Sharov, V.V., Kuzmin, D.A., Anderson, J.B., Krutovsky, K.V., 2019. Mobile genetic elements explain size variation in the mitochondrial genomes of four closely-related Armillaria species. BMC Genomics 20, 351. https://doi.org/10.1186/s12864-019-5732-z
Korvald, H., Mølstad Moe, A.M., Cederkvist, F.H., Thiede, B., Laerdahl, J.K., Bjørås, M., Alseth, I., 2011. *Schizosaccharomyces pombe* Ofd2 Is a Nuclear 2-Oxoglutarate and Iron Dependent Dioxygenase Interacting with Histones. PLoS ONE 6, e25188. https://doi.org/10.1371/journal.pone.0025188
Krizsán, K., Almási, É., Merényi, Z., Sahu, N., Virágh, M., Kószó, T., Mondo, S., Kiss, B., Bálint, B., Kües, U., Barry, K., Cseklye, J., Hegedüs, B., Henrissat, B., Johnson, J., Lipzen, A., Ohm, R.A., Nagy, I., Pangilinan, J., Yan, J., Xiong, Y., Grigoriev, I.V., Hibbett, D.S., Nagy, L.G., 2019. Transcriptomic atlas of mushroom development reveals conserved genes behind complex multicellularity in fungi. Proc. Natl. Acad. Sci. 116, 7409–7418. https://doi.org/10.1073/pnas.1817822116
Kuo, A., Bushnell, B., Grigoriev, I.V., 2014. Fungal Genomics, in: Advances in Botanical Research. Elsevier, pp. 1–52. https://doi.org/10.1016/B978-0-12-397940-7.00001-X
Lacaze, A., Joly, D.L., 2020. Structural specificity in plant–filamentous pathogen interactions. Mol. Plant Pathol. 21, 1513–1525. https://doi.org/10.1111/mpp.12983
Lanver, D., Müller, A.N., Happel, P., Schweizer, G., Haas, F.B., Franitza, M., Pellegrin, C., Reissmann, S., Altmüller, J., Rensing, S.A., Kahmann, R., 2018. The Biotrophic Development of *Ustilago maydis* Studied by RNA-Seq Analysis. Plant Cell 30, 300–323. https://doi.org/10.1105/tpc.17.00764
Leach, R., 1937. Observations on the parasitism and control of *Armillaria mellea*. Proc. R. Soc. Lond. Ser. B - Biol. Sci. 121, 561–573. https://doi.org/10.1098/rspb.1937.0003

Lebreton, A., Zeng, Q., Miyauchi, S., Kohler, A., Dai, Y.-C., Martin, F.M., 2021. Evolution of the Mode of Nutrition in Symbiotic and Saprotrophic Fungi in Forest Ecosystems. Annu. Rev. Ecol. Evol. Syst. 52, 385–404. https://doi.org/10.1146/annurev-ecolsys-012021-114902

Levasseur, A., Drula, E., Lombard, V., Coutinho, P.M., Henrissat, B., 2013. Expansion of the enzymatic repertoire of the CAZy database to integrate auxiliary redox enzymes. Biotechnol. Biofuels 6, 41. https://doi.org/10.1186/1754-6834-6-41

Li, H., Wei, H., Hu, J., Lacey, E., Sobolev, A.N., Stubbs, K.A., Solomon, P.S., Chooi, Y.-H., 2020. Genomics-Driven Discovery of Phytotoxic Cytochalasans Involved in the Virulence of the Wheat Pathogen *Parastagonospora nodorum*. ACS Chem. Biol. 15, 226–233. https://doi.org/10.1021/acschembio.9b00791

Li, X., Beeson, W.T., Phillips, C.M., Marletta, M.A., Cate, J.H.D., 2012. Structural Basis for Substrate Targeting and Catalysis by Fungal Polysaccharide Monooxygenases. Structure 20, 1051–1061. https://doi.org/10.1016/j.str.2012.04.002

Liang, X., Rollins, J.A., 2018. Mechanisms of Broad Host Range Necrotrophic Pathogenesis in *Sclerotinia sclerotiorum*. Phytopathology® 108, 1128–1140. https://doi.org/10.1094/PHYTO-06-18-0197-RVW

Liu, W., Liu, J., Ning, Y., Ding, B., Wang, X., Wang, Z., Wang, G.-L., 2013. Recent Progress in Understanding PAMP- and Effector-Triggered Immunity against the Rice Blast Fungus Magnaporthe oryzae. Mol. Plant 6, 605–620. https://doi.org/10.1093/mp/sst015

Liu, X., Zhang, Z., 2022. A double- edged sword: reactive oxygen species (ROS) during the rice blast fungus and host interaction. FEBS J. 289, 5505–5515. https://doi.org/10.1111/febs.16171

Lombard, V., Golaconda Ramulu, H., Drula, E., Coutinho, P.M., Henrissat, B., 2014. The carbohydrate-active enzymes database (CAZy) in 2013. Nucleic Acids Res. 42, D490–D495. https://doi.org/10.1093/nar/gkt1178

Lorrain, C., Feurtey, A., Möller, M., Haueisen, J., Stukenbrock, E., 2021. Dynamics of transposable elements in recently diverged fungal pathogens: lineage-specific transposable element content and efficiency of genome defenses. G3 GenesGenomesGenetics 11, jkab068. https://doi.org/10.1093/g3journal/jkab068

Lundell, T.K., Mäkelä, M.R., Hildén, K., 2010. Lignin-modifying enzymes in filamentous basidiomycetes - ecological, functional and phylogenetic review. J. Basic Microbiol. 50, 5–20. https://doi.org/10.1002/jobm.200900338

Marañón-Jiménez, S., Radujković, D., Verbruggen, E., Grau, O., Cuntz, M., Peñuelas, J., Richter, A., Schrumpf, M., Rebmann, C., 2021. Shifts in the Abundances of Saprotrophic and Ectomycorrhizal Fungi With Altered Leaf Litter Inputs. Front. Plant Sci. 12, 682142. https://doi.org/10.3389/fpls.2021.682142

Martinez, S., Hausinger, R.P., 2015. Catalytic Mechanisms of Fe(II)- and 2-Oxoglutarate-dependent Oxygenases. J. Biol. Chem. 290, 20702–20711. https://doi.org/10.1074/jbc.R115.648691

McDowell, J.M., 2013. Genomic and transcriptomic insights into lifestyle transitions of a hemi-biotrophic fungal pathogen. New Phytol. 197, 1032–1034. https://doi.org/10.1111/nph.12141

McKelvey, S.M., Murphy, R.A., 2017. Biotechnological Use of Fungal Enzymes, in: Kavanagh, K. (Ed.), Fungi. John Wiley & Sons, Inc., Hoboken, NJ, USA, pp. 201–225. https://doi.org/10.1002/9781119374312.ch8

Meinhardt, L.W., Costa, G.G., Thomazella, D.P., Teixeira, P.J.P., Carazzolle, M., Schuster, S.C., Carlson, J.E., Guiltinan, M.J., Mieczkowski, P., Farmer, A., Ramaraj, T., Crozier,

J., Davis, R.E., Shao, J., Melnick, R.L., Pereira, G.A., Bailey, B.A., 2014. Genome and secretome analysis of the hemibiotrophic fungal pathogen, *Moniliophthora roreri*, which causes frosty pod rot disease of cacao: mechanisms of the biotrophic and necrotrophic phases. BMC Genomics 15, 164. https://doi.org/10.1186/1471-2164-15-164

Mihail, J.D., Bruhn, J.N., 2007. Dynamics of bioluminescence by *Armillaria gallica, A. mellea* and *A. tabescens*. Mycologia 99, 341–350. https://doi.org/10.1080/15572536.2007.11832558

Miyara, I., Shafran, H., Davidzon, M., Sherman, A., Prusky, D., 2010. pH Regulation of Ammonia Secretion by *Colletotrichum gloeosporioides* and Its Effect on Appressorium Formation and Pathogenicity. Mol. Plant-Microbe Interactions® 23, 304–316. https://doi.org/10.1094/MPMI-23-3-0304

Miyara, I., Shafran, H., Kramer Haimovich, H., Rollins, J., Sherman, A., Prusky, D., 2008. Multi- factor regulation of pectate lyase secretion by *Colletotrichum gloeosporioides* pathogenic on avocado fruits. Mol. Plant Pathol. 9, 281–291. https://doi.org/10.1111/j.1364-3703.2007.00462.x

Miyauchi, S., Kiss, E., Kuo, A., Drula, E., Kohler, A., Sánchez-García, M., Morin, E., Andreopoulos, B., Barry, K.W., Bonito, G., Buée, M., Carver, A., Chen, C., Cichocki, N., Clum, A., Culley, D., Crous, P.W., Fauchery, L., Girlanda, M., Hayes, R.D., Kéri, Z., LaButti, K., Lipzen, A., Lombard, V., Magnuson, J., Maillard, F., Murat, C., Nolan, M., Ohm, R.A., Pangilinan, J., Pereira, M. de F., Perotto, S., Peter, M., Pfister, S., Riley, R., Sitrit, Y., Stielow, J.B., Szöllősi, G., Žifčáková, L., Štursová, M., Spatafora, J.W., Tedersoo, L., Vaario, L.-M., Yamada, A., Yan, M., Wang, P., Xu, J., Bruns, T., Baldrian, P., Vilgalys, R., Dunand, C., Henrissat, B., Grigoriev, I.V., Hibbett, D., Nagy, L.G., Martin, F.M., 2020. Large-scale genome sequencing of mycorrhizal fungi provides insights into the early evolution of symbiotic traits. Nat. Commun. 11, 5125. https://doi.org/10.1038/s41467-020-18795-w

Miyauchi, S., Navarro, D., Grisel, S., Chevret, D., Berrin, J.-G., Rosso, M.-N., 2017. The integrative omics of white-rot fungus *Pycnoporus coccineus* reveals co-regulated CAZymes for orchestrated lignocellulose breakdown. PLOS ONE 12, e0175528. https://doi.org/10.1371/journal.pone.0175528

Möller, M., Stukenbrock, E.H., 2017. Evolution and genome architecture in fungal plant pathogens. Nat. Rev. Microbiol. 15, 756–771. https://doi.org/10.1038/nrmicro.2017.76

Moloney, N.M., Owens, R.A., Meleady, P., Henry, M., Dolan, S.K., Mulvihill, E., Clynes, M., Doyle, S., 2016. The iron-responsive microsomal proteome of *Aspergillus fumigatus*. J. Proteomics 136, 99–111. https://doi.org/10.1016/j.jprot.2015.12.025

Money, N.P., 2002. Mushroom stem cells. BioEssays News Rev. Mol. Cell. Dev. Biol. 24, 949–952. https://doi.org/10.1002/bies.10160

Moody, S.C., Dudley, E., Hiscox, J., Boddy, L., Eastwood, D.C., 2017. Interdependence of Primary Metabolism and Xenobiotic Mitigation Characterizes the Proteome of *Bjerkandera adusta* during Wood Decomposition. Appl. Environ. Microbiol. 84. https://doi.org/10.1128/AEM.01401-17

Morgenstern, I., Powlowski, J., Tsang, A., 2014. Fungal cellulose degradation by oxidative enzymes: from dysfunctional GH61 family to powerful lytic polysaccharide monooxygenase family. Brief. Funct. Genomics 13, 471–481. https://doi.org/10.1093/bfgp/elu032

Nagy, L.G., Kovács, G.M., Krizsán, K., 2018. Complex multicellularity in fungi: evolutionary convergence, single origin, or both?: Complex multicellularity in Fungi. Biol. Rev. 93, 1778–1794. https://doi.org/10.1111/brv.12418

Nagy, L.G., Ohm, R.A., Kovács, G.M., Floudas, D., Riley, R., Gácser, A., Sipiczki, M., Davis, J.M., Doty, S.L., de Hoog, G.S., Lang, B.F., Spatafora, J.W., Martin, F.M., Grigoriev, I.V., Hibbett, D.S., 2014. Latent homology and convergent regulatory evolution underlies the repeated emergence of yeasts. Nat. Commun. 5, 4471. https://doi.org/10.1038/ncomms5471

Nagy, L.G., Riley, R., Bergmann, P.J., Krizsán, K., Martin, F.M., Grigoriev, I.V., Cullen, D., Hibbett, D.S., 2017. Genetic Bases of Fungal White Rot Wood Decay Predicted by Phylogenomic Analysis of Correlated Gene-Phenotype Evolution. Mol. Biol. Evol. 34, 35–44. https://doi.org/10.1093/molbev/msw238

Nagy, L.G., Riley, R., Tritt, A., Adam, C., Daum, C., Floudas, D., Sun, H., Yadav, J.S., Pangilinan, J., Larsson, K.-H., Matsuura, K., Barry, K., Labutti, K., Kuo, R., Ohm, R.A., Bhattacharya, S.S., Shirouzu, T., Yoshinaga, Y., Martin, F.M., Grigoriev, I.V., Hibbett, D.S., 2016. Comparative Genomics of Early-Diverging Mushroom-Forming Fungi Provides Insights into the Origins of Lignocellulose Decay Capabilities. Mol. Biol. Evol. 33, 959–970. https://doi.org/10.1093/molbev/msv337

Newman, T.E., Derbyshire, M.C., 2020. The Evolutionary and Molecular Features of Broad Host-Range Necrotrophy in Plant Pathogenic Fungi. Front. Plant Sci. 11, 591733. https://doi.org/10.3389/fpls.2020.591733

Nguyen, L.-T., Schmidt, H.A., von Haeseler, A., Minh, B.Q., 2015. IQ-TREE: A Fast and Effective Stochastic Algorithm for Estimating Maximum-Likelihood Phylogenies. Mol. Biol. Evol. 32, 268–274. https://doi.org/10.1093/molbev/msu300

O'Connell, R.J., Thon, M.R., Hacquard, S., Amyotte, S.G., Kleemann, J., Torres, M.F., Damm, U., Buiate, E.A., Epstein, L., Alkan, N., Altmüller, J., Alvarado-Balderrama, L., Bauser, C.A., Becker, C., Birren, B.W., Chen, Z., Choi, J., Crouch, J.A., Duvick, J.P., Farman, M.A., Gan, P., Heiman, D., Henrissat, B., Howard, R.J., Kabbage, M., Koch, C., Kracher, B., Kubo, Y., Law, A.D., Lebrun, M.-H., Lee, Y.-H., Miyara, I., Moore, N., Neumann, U., Nordström, K., Panaccione, D.G., Panstruga, R., Place, M., Proctor, R.H., Prusky, D., Rech, G., Reinhardt, R., Rollins, J.A., Rounsley, S., Schardl, C.L., Schwartz, D.C., Shenoy, N., Shirasu, K., Sikhakolli, U.R., Stüber, K., Sukno, S.A., Sweigard, J.A., Takano, Y., Takahara, H., Trail, F., van der Does, H.C., Voll, L.M., Will, I., Young, S., Zeng, Q., Zhang, J., Zhou, S., Dickman, M.B., Schulze-Lefert, P., Ver Loren van Themaat, E., Ma, L.-J., Vaillancourt, L.J., 2012. Lifestyle transitions in plant pathogenic *Colletotrichum* fungi deciphered by genome and transcriptome analyses. Nat. Genet. 44, 1060–1065. https://doi.org/10.1038/ng.2372

Oghenekaro, A.O., Raffaello, T., Kovalchuk, A., Asiegbu, F.O., 2016. De novo transcriptomic assembly and profiling of *Rigidoporus microporus* during saprotrophic growth on rubber wood. BMC Genomics 17. https://doi.org/10.1186/s12864-016-2574-9

Olson, Å., Aerts, A., Asiegbu, F., Belbahri, L., Bouzid, O., Broberg, A., Canbäck, B., Coutinho, P.M., Cullen, D., Dalman, K., Deflorio, G., van Diepen, L.T.A., Dunand, C., Duplessis, S., Durling, M., Gonthier, P., Grimwood, J., Fossdal, C.G., Hansson, D., Henrissat, B., Hietala, A., Himmelstrand, K., Hoffmeister, D., Högberg, N., James, T.Y., Karlsson, M., Kohler, A., Kües, U., Lee, Y.-H., Lin, Y.-C., Lind, M., Lindquist, E., Lombard, V., Lucas, S., Lundén, K., Morin, E., Murat, C., Park, J., Raffaello, T., Rouzé, P., Salamov, A., Schmutz, J., Solheim, H., Ståhlberg, J., Vélëz, H., de Vries, R.P., Wiebenga, A., Woodward, S., Yakovlev, I., Garbelotto, M., Martin, F., Grigoriev, I.V., Stenlid, J., 2012. Insight into trade-off between wood decay and parasitism from the genome of a fungal forest pathogen. New Phytol. 194, 1001–1013. https://doi.org/10.1111/j.1469-8137.2012.04128.x

Peay, K.G., Kennedy, P.G., Talbot, J.M., 2016. Dimensions of biodiversity in the Earth

mycobiome. Nat. Rev. Microbiol. 14, 434–447. https://doi.org/10.1038/nrmicro.2016.59

Perazzolli, M., Bampi, F., Faccin, S., Moser, M., De Luca, F., Ciccotti, A.M., Velasco, R., Gessler, C., Pertot, I., Moser, C., 2010. *Armillaria mellea* Induces a Set of Defense Genes in Grapevine Roots and One of Them Codifies a Protein with Antifungal Activity. Mol. Plant-Microbe Interactions 23, 485–496. https://doi.org/10.1094/MPMI-23-4-0485

Peter, M., Kohler, A., Ohm, R.A., Kuo, A., Krützmann, J., Morin, E., Arend, M., Barry, K.W., Binder, M., Choi, C., Clum, A., Copeland, A., Grisel, N., Haridas, S., Kipfer, T., LaButti, K., Lindquist, E., Lipzen, A., Maire, R., Meier, B., Mihaltcheva, S., Molinier, V., Murat, C., Pöggeler, S., Quandt, C.A., Sperisen, C., Tritt, A., Tisserant, E., Crous, P.W., Henrissat, B., Nehls, U., Egli, S., Spatafora, J.W., Grigoriev, I.V., Martin, F.M., 2016. Ectomycorrhizal ecology is imprinted in the genome of the dominant symbiotic fungus *Cenococcum geophilum*. Nat. Commun. 7. https://doi.org/10.1038/ncomms12662

Porter, D.L., Bradshaw, A.J., Nielsen, R.H., Newell, P., Dentinger, B.T.M., Naleway, S.E., 2022. The melanized layer of Armillaria ostoyae rhizomorphs: Its protective role and functions. J. Mech. Behav. Biomed. Mater. 125, 104934. https://doi.org/10.1016/j.jmbbm.2021.104934

Presley, G.N., Panisko, E., Purvine, S.O., Schilling, J.S., 2018. Coupling Secretomics with Enzyme Activities To Compare the Temporal Processes of Wood Metabolism among White and Brown Rot Fungi. Appl. Environ. Microbiol. 84. https://doi.org/10.1128/AEM.00159-18

Pronos, J., Patton, R.F., 1978. Penetration and colonization of oak roots by *Armillaria mellea* in Wisconsin. For. Pathol. 8, 259–267. https://doi.org/10.1111/j.1439-0329.1978.tb00632.x

Prospero, S., Holdenrieder, O., Rigling, D., 2004. Comparison of the virulence of *Armillaria cepistipes* and *Armillaria ostoyae* on four Norway spruce provenances. For. Pathol. 34, 1–14. https://doi.org/10.1046/j.1437-4781.2003.00339.x

Prospero, S., Rigling, D., Holdenrieder, O., 2003. Population structure of Armillaria species in managed Norway spruce stands in the Alps. New Phytol. 158, 365–373. https://doi.org/10.1046/j.1469-8137.2003.00731.x

Qin, X., Su, X., Luo, H., Ma, R., Yao, B., Ma, F., 2018. Deciphering lignocellulose deconstruction by the white rot fungus *Irpex lacteus* based on genomic and transcriptomic analyses. Biotechnol. Biofuels 11. https://doi.org/10.1186/s13068-018-1060-9

Quinlan, R.J., Sweeney, M.D., Lo Leggio, L., Otten, H., Poulsen, J.-C.N., Johansen, K.S., Krogh, K.B.R.M., Jorgensen, C.I., Tovborg, M., Anthonsen, A., Tryfona, T., Walter, C.P., Dupree, P., Xu, F., Davies, G.J., Walton, P.H., 2011. Insights into the oxidative degradation of cellulose by a copper metalloenzyme that exploits biomass components. Proc. Natl. Acad. Sci. 108, 15079–15084. https://doi.org/10.1073/pnas.1105776108

Raabe, R.D., 1962. Host list of the root rot fungus, *Armillaria mellea*. Hilgardia 33, 25–88. https://doi.org/10.3733/hilg.v33n02p025

Redfern, D.B., 1978. Infection by *Armillaria mellea* and some Factors Affecting Host Resistance and the Severity of Disease. Forestry 51, 121–135. https://doi.org/10.1093/forestry/51.2.121

Rees, H.J., Bashir, N., Drakulic, J., Cromey, M.G., Bailey, A.M., Foster, G.D., 2021. Identification of native endophytic *Trichoderma* spp. for investigation of *in vitro* antagonism towards *Armillaria mellea* using synthetic- and plant- based substrates. J. Appl. Microbiol. 131, 392–403. https://doi.org/10.1111/jam.14938

Revell, L.J., 2012. phytools: an R package for phylogenetic comparative biology (and other things): phytools: R package. Methods Ecol. Evol. 3, 217–223. https://doi.org/10.1111/j.2041-210X.2011.00169.x

Revell, L.J., 2009. SIZE-CORRECTION AND PRINCIPAL COMPONENTS FOR INTERSPECIFIC COMPARATIVE STUDIES. Evolution 63, 3258–3268. https://doi.org/10.1111/j.1558-5646.2009.00804.x

Riley, R., Salamov, A.A., Brown, D.W., Nagy, L.G., Floudas, D., Held, B.W., Levasseur, A., Lombard, V., Morin, E., Otillar, R., Lindquist, E.A., Sun, H., LaButti, K.M., Schmutz, J., Jabbour, D., Luo, H., Baker, S.E., Pisabarro, A.G., Walton, J.D., Blanchette, R.A., Henrissat, B., Martin, F., Cullen, D., Hibbett, D.S., Grigoriev, I.V., 2014. Extensive sampling of basidiomycete genomes demonstrates inadequacy of the white-rot/brown-rot paradigm for wood decay fungi. Proc. Natl. Acad. Sci. 111, 9923–9928. https://doi.org/10.1073/pnas.1400592111

Rishbeth, J., 1968. The growth rate of Armillaria mellea. Trans. Br. Mycol. Soc. 51, 575–586. https://doi.org/10.1016/S0007-1536(68)80027-0

Ritchie, M.E., Phipson, B., Wu, D., Hu, Y., Law, C.W., Shi, W., Smyth, G.K., 2015. limma powers differential expression analyses for RNA-sequencing and microarray studies. Nucleic Acids Res. 43, e47–e47. https://doi.org/10.1093/nar/gkv007

Robinson, M.D., McCarthy, D.J., Smyth, G.K., 2010. edgeR: a Bioconductor package for differential expression analysis of digital gene expression data. Bioinforma. Oxf. Engl. 26, 139–140. https://doi.org/10.1093/bioinformatics/btp616

Robinson, M.D., Oshlack, A., 2010. A scaling normalization method for differential expression analysis of RNA-seq data. Genome Biol. 11, R25. https://doi.org/10.1186/gb-2010-11-3-r25

Robinson, R.M., Smith, R.H., 2001. Fumigation of regrowth karri stumps with metham-sodium to control *Armillaria luteobubalina*. Aust. For. 64, 209–215. https://doi.org/10.1080/00049158.2001.10676190

Rodriguez-Moreno, L., Ebert, M.K., Bolton, M.D., Thomma, B.P.H.J., 2018. Tools of the crook-infection strategies of fungal plant pathogens. Plant J. 93, 664–674. https://doi.org/10.1111/tpj.13810

Ross-Davis, A.L., Stewart, J.E., Hanna, J.W., Kim, M.-S., Knaus, B.J., Cronn, R., Rai, H., Richardson, B.A., McDonald, G.I., Klopfenstein, N.B., 2013. Transcriptome of an *Armillaria* root disease pathogen reveals candidate genes involved in host substrate utilization at the host-pathogen interface. For. Pathol. 43, 468–477. https://doi.org/10.1111/efp.12056

Rudawska, M., Leski, T., Stasińska, M., 2011. Species and functional diversity of ectomycorrhizal fungal communities on Scots pine (Pinus sylvestris L.) trees on three different sites. Ann. For. Sci. 68, 5–15. https://doi.org/10.1007/s13595-010-0002-x

Ruiz-Dueñas, F.J., Barrasa, J.M., Sánchez-García, M., Camarero, S., Miyauchi, S., Serrano, A., Linde, D., Babiker, R., Drula, E., Ayuso-Fernández, I., Pacheco, R., Padilla, G., Ferreira, P., Barriuso, J., Kellner, H., Castanera, R., Alfaro, M., Ramírez, L., Pisabarro, A.G., Riley, R., Kuo, A., Andreopoulos, W., LaButti, K., Pangilinan, J., Tritt, A., Lipzen, A., He, G., Yan, M., Ng, V., Grigoriev, I.V., Cullen, D., Martin, F., Rosso, M.-N., Henrissat, B., Hibbett, D., Martínez, A.T., 2021. Genomic Analysis Enlightens Agaricales Lifestyle Evolution and Increasing Peroxidase Diversity. Mol. Biol. Evol. 38, 1428–1446. https://doi.org/10.1093/molbev/msaa301

Rytioja, J., Hildén, K., Yuzon, J., Hatakka, A., de Vries, R.P., Mäkelä, M.R., 2014. Plant-Polysaccharide-Degrading Enzymes from Basidiomycetes. Microbiol. Mol. Biol. Rev. 78, 614–649. https://doi.org/10.1128/MMBR.00035-14

Schilling, J.S., Kaffenberger, J.T., Held, B.W., Ortiz, R., Blanchette, R.A., 2020. Using Wood Rot Phenotypes to Illuminate the “Gray” Among Decomposer Fungi. Front. Microbiol. 11, 1288. https://doi.org/10.3389/fmicb.2020.01288

Schmitt, C.L., Tatum, M.L., 2008. The Malheur National Forest Location of the World’s Largest Living Organism [The Humongous Fungus]. USDA.

Schwarze, F.W.M.R., 2007. Wood decay under the microscope. Fungal Biol. Rev. 21, 133–170. https://doi.org/10.1016/j.fbr.2007.09.001

Schwarze, F.W.M.R., Fink, S., 1998. Host and cell type affect the mode of degradation by *Meripilus giganteus*. New Phytol. 139, 721–731. https://doi.org/10.1046/j.1469-8137.1998.00238.x

Shah, F., Nicolás, C., Bentzer, J., Ellström, M., Smits, M., Rineau, F., Canbäck, B., Floudas, D., Carleer, R., Lackner, G., Braesel, J., Hoffmeister, D., Henrissat, B., Ahrén, D., Johansson, T., Hibbett, D.S., Martin, F., Persson, P., Tunlid, A., 2016. Ectomycorrhizal fungi decompose soil organic matter using oxidative mechanisms adapted from saprotrophic ancestors. New Phytol. 209, 1705–1719. https://doi.org/10.1111/nph.13722

Shao, D., Smith, D.L., Kabbage, M., Roth, M.G., 2021. Effectors of Plant Necrotrophic Fungi. Front. Plant Sci. 12, 687713. https://doi.org/10.3389/fpls.2021.687713

Shi, L., Dossa, G.G.O., Paudel, E., Zang, H., Xu, J., Harrison, R.D., 2019. Changes in Fungal Communities across a Forest Disturbance Gradient. Appl. Environ. Microbiol. 85. https://doi.org/10.1128/AEM.00080-19

Sipos, G., Anderson, J.B., Nagy, L.G., 2018. *Armillaria*. Curr. Biol. 28, PR297-R298. https://doi.org/doi:10.1016/j.cub.2018.01.026

Sipos, G., Prasanna, A.N., Walter, M.C., O’Connor, E., Bálint, B., Krizsán, K., Kiss, B., Hess, J., Varga, T., Slot, J., Riley, R., Bóka, B., Rigling, D., Barry, K., Lee, J., Mihaltcheva, S., LaButti, K., Lipzen, A., Waldron, R., Moloney, N.M., Sperisen, C., Kredics, L., Vágvölgyi, C., Patrignani, A., Fitzpatrick, D., Nagy, I., Doyle, S., Anderson, J.B., Grigoriev, I.V., Güldener, U., Münsterkötter, M., Nagy, L.G., 2017. Genome expansion and lineage-specific genetic innovations in the forest pathogenic fungi Armillaria. Nat. Ecol. Evol. 1, 1931–1941. https://doi.org/10.1038/s41559-017-0347-8

Smith, M.L., Bruhn, J.N., Anderson, J.B., 1992. The fungus Armillaria bulbosa is among the largest and oldest living organisms. Nature 356, 428–431. https://doi.org/10.1038/356428a0

Stamatakis, A., 2014. RAxML version 8: a tool for phylogenetic analysis and post-analysis of large phylogenies. Bioinformatics 30, 1312–1313. https://doi.org/10.1093/bioinformatics/btu033

Steinegger, M., Söding, J., 2017. MMseqs2 enables sensitive protein sequence searching for the analysis of massive data sets. Nat. Biotechnol. 35, 1026–1028. https://doi.org/10.1038/nbt.3988

Stergiopoulos, I., Collemare, J., Mehrabi, R., De Wit, P.J.G.M., 2013. Phytotoxic secondary metabolites and peptides produced by plant pathogenic *Dothideomycete* fungi. FEMS Microbiol. Rev. 37, 67–93. https://doi.org/10.1111/j.1574-6976.2012.00349.x

Stoian, V., Vidican, R., Crişan, I., Puia, C., Şandor, M., Stoian, V.A., Păcurar, F., Vaida, I., 2019. Sensitive approach and future perspectives in microscopic patterns of mycorrhizal roots. Sci. Rep. 9, 10233. https://doi.org/10.1038/s41598-019-46743-2

Strullu- Derrien, C., Selosse, M., Kenrick, P., Martin, F.M., 2018. The origin and evolution of mycorrhizal symbioses: from palaeomycology to phylogenomics. New Phytol. 220, 1012–1030. https://doi.org/10.1111/nph.15076

Suzek, B.E., Wang, Y., Huang, H., McGarvey, P.B., Wu, C.H., the UniProt Consortium, 2015.

UniRef clusters: a comprehensive and scalable alternative for improving sequence similarity searches. Bioinformatics 31, 926–932. https://doi.org/10.1093/bioinformatics/btu739
Tanaka, S., Kahmann, R., 2021. Cell wall–associated effectors of plant-colonizing fungi. Mycologia 113, 247–260. https://doi.org/10.1080/00275514.2020.1831293
Teixeira, P.J.P.L., Thomazella, D.P. de T., Reis, O., do Prado, P.F.V., do Rio, M.C.S., Fiorin, G.L., José, J., Costa, G.G.L., Negri, V.A., Mondego, J.M.C., Mieczkowski, P., Pereira, G.A.G., 2014. High-Resolution Transcript Profiling of the Atypical Biotrophic Interaction between *Theobroma cacao* and the Fungal Pathogen *Moniliophthora perniciosa*. Plant Cell 26, 4245–4269. https://doi.org/10.1105/tpc.114.130807
Toruño, T.Y., Stergiopoulos, I., Coaker, G., 2016. Plant-Pathogen Effectors: Cellular Probes Interfering with Plant Defenses in Spatial and Temporal Manners. Annu. Rev. Phytopathol. 54, 419–441. https://doi.org/10.1146/annurev-phyto-080615-100204
Townsend, B.B., 1954. Morphology and development of fungal Rhizomorphs. Trans. Br. Mycol. Soc. 37, 222–233. https://doi.org/10.1016/S0007-1536(54)80004-0
Treseder, K.K., Lennon, J.T., 2015. Fungal traits that drive ecosystem dynamics on land. Microbiol. Mol. Biol. Rev. MMBR 79, 243–262. https://doi.org/10.1128/MMBR.00001-15
Tyanova, S., Temu, T., Sinitcyn, P., Carlson, A., Hein, M.Y., Geiger, T., Mann, M., Cox, J., 2016. The Perseus computational platform for comprehensive analysis of (prote)omics data. Nat. Methods 13, 731–740. https://doi.org/10.1038/nmeth.3901
Ullrich, R.C., Anderson, J.B., 1978. Sex and diploidy in Armillaria mellea. Exp. Mycol. 2, 119–129. https://doi.org/10.1016/S0147-5975(78)80025-5
Vanden Wymelenberg, A., Gaskell, J., Mozuch, M., Splinter BonDurant, S., Sabat, G., Ralph, J., Skyba, O., Mansfield, S.D., Blanchette, R.A., Grigoriev, I.V., Kersten, P.J., Cullen, D., 2011. Significant Alteration of Gene Expression in Wood Decay Fungi *Postia placenta* and *Phanerochaete chrysosporium* by Plant Species. Appl. Environ. Microbiol. 77, 4499–4507. https://doi.org/10.1128/AEM.00508-11
Virágh, M., Merényi, Z., Csernetics, Á., Földi, C., Sahu, N., Liu, X.-B., Hibbett, D.S., Nagy, L.G., 2022. Evolutionary Morphogenesis of Sexual Fruiting Bodies in Basidiomycota: Toward a New Evo-Devo Synthesis. Microbiol. Mol. Biol. Rev. 86, e00019-21. https://doi.org/10.1128/MMBR.00019-21
Volk, T.J., 2013. Fungi, in: Encyclopedia of Biodiversity. Elsevier, pp. 624–640. https://doi.org/10.1016/B978-0-12-384719-5.00062-9
Vylkova, S., 2017. Environmental pH modulation by pathogenic fungi as a strategy to conquer the host. PLOS Pathog. 13, e1006149. https://doi.org/10.1371/journal.ppat.1006149
Wang, Z., Winestrand, S., Gillgren, T., Jönsson, L.J., 2018. Chemical and structural factors influencing enzymatic saccharification of wood from aspen, birch and spruce. Biomass Bioenergy 109, 125–134. https://doi.org/10.1016/j.biombioe.2017.12.020
Watkinson, S.C., 1971. Phosphorus translocation in the stranded and unstranded mycelium of *Serpula lacrimans*. Trans. Br. Mycol. Soc. 57, 535–539. https://doi.org/10.1016/S0007-1536(71)80070-0
Wells, J.M., Boddy, L., 1990. Wood decay, and phosphorus and fungal biomass allocation, in mycelial cord systems. New Phytol. 116, 285–295. https://doi.org/10.1111/j.1469-8137.1990.tb04716.x
Wingfield, B.D., Ambler, J.M., Coetzee, M.P.A., de Beer, Z.W., Duong, T.A., Joubert, F., Hammerbacher, A., McTaggart, A.R., Naidoo, K., Nguyen, H.D.T., Ponomareva, E., Santana, Q.S., Seifert, K.A., Steenkamp, E.T., Trollip, C., van der Nest, M.A., Visagie, C.M., Wilken, P.M., Wingfield, M.J., Yilmaz, N., 2016. IMA Genome-F 6: Draft genome

sequences of Armillaria fuscipes, Ceratocystiopsis minuta, Ceratocystis adiposa, Endoconidiophora laricicola, E. polonica and Penicillium freii DAOMC 242723. IMA Fungus 7, 217–227. https://doi.org/10.5598/imafungus.2016.07.01.11

Wisecaver, J.H., Alexander, W.G., King, S.B., Todd Hittinger, C., Rokas, A., 2016. Dynamic Evolution of Nitric Oxide Detoxifying Flavohemoglobins, a Family of Single-Protein Metabolic Modules in Bacteria and Eukaryotes. Mol. Biol. Evol. 33, 1979–1987. https://doi.org/10.1093/molbev/msw073

Wong, J.W. - H., Plett, K.L., Natera, S.H.A., Roessner, U., Anderson, I.C., Plett, J.M., 2020. Comparative metabolomics implicates threitol as a fungal signal supporting colonization of *Armillaria luteobubalina* on eucalypt roots. Plant Cell Environ. 43, 374–386. https://doi.org/10.1111/pce.13672

Woods, A.J., 1994. The behaviour and impacts of Armillaria ostoyae in mature stands and plantations in the Shuswap region of British Columbia. https://doi.org/10.14288/1.0103805

Worrall, J.J., Anagnost, S.E., Zabel, R.A., 1997. Comparison of Wood Decay among Diverse Lignicolous Fungi. Mycologia 89, 199. https://doi.org/10.2307/3761073

Xu, D., Xue, M., Shen, Z., Jia, X., Hou, X., Lai, D., Zhou, L., 2021. Phytotoxic Secondary Metabolites from Fungi. Toxins 13, 261. https://doi.org/10.3390/toxins13040261

Yafetto, L., Davis, D.J., Money, N.P., 2009. Biomechanics of invasive growth by *Armillaria* rhizomorphs. Fungal Genet. Biol. 46, 688–694. https://doi.org/10.1016/j.fgb.2009.04.005

Yang, G., Tang, L., Gong, Y., Xie, J., Fu, Y., Jiang, D., Li, G., Collinge, D.B., Chen, W., Cheng, J., 2018. A cerato-platanin protein SsCP1 targets plant PR1 and contributes to virulence of *Sclerotinia sclerotiorum*. New Phytol. 217, 739–755. https://doi.org/10.1111/nph.14842

Young, D., Rice, J., Martin, R., Lindquist, E., Lipzen, A., Grigoriev, I., Hibbett, D., 2015. Degradation of Bunker C Fuel Oil by White-Rot Fungi in Sawdust Cultures Suggests Potential Applications in Bioremediation. PLOS ONE 10, e0130381. https://doi.org/10.1371/journal.pone.0130381

Yuan, Y., Jiang, B., Chen, H., Wu, W., Wu, S., Jin, Y., Xiao, H., 2021. Recent advances in understanding the effects of lignin structural characteristics on enzymatic hydrolysis. Biotechnol. Biofuels 14, 205. https://doi.org/10.1186/s13068-021-02054-1

Zhang, J., Presley, G.N., Hammel, K.E., Ryu, J.-S., Menke, J.R., Figueroa, M., Hu, D., Orr, G., Schilling, J.S., 2016. Localizing gene regulation reveals a staggered wood decay mechanism for the brown rot fungus *Postia placenta*. Proc. Natl. Acad. Sci. 113, 10968–10973. https://doi.org/10.1073/pnas.1608454113

Zhang, Y., Yan, H., Wei, X., Zhang, J., Wang, H., Liu, D., 2017. Expression analysis and functional characterization of a pathogen-induced thaumatin-like gene in wheat conferring enhanced resistance to *Puccinia triticina*. J. Plant Interact. 12, 332–339. https://doi.org/10.1080/17429145.2017.1367042

Zhang, Z., Chen, Y., Li, B., Chen, T., Tian, S., 2020. Reactive oxygen species: A generalist in regulating development and pathogenicity of phytopathogenic fungi. Comput. Struct. Biotechnol. J. 18, 3344–3349. https://doi.org/10.1016/j.csbj.2020.10.024

Zhao, Z., Liu, H., Wang, C., Xu, J.-R., 2013. Comparative analysis of fungal genomes reveals different plant cell wall degrading capacity in fungi. BMC Genomics 14, 274. https://doi.org/10.1186/1471-2164-14-274

Summary

Armillaria species are a group of fungi that can cause devastating root rot diseases in woody ecosystems, including forests, tree plantations, ornamental plants, vineyards, and gardens. These fungi can occur, colonize or infect hosts depending on a variety of factors such as the environmental conditions, host plant, and host health. Some species of *Armillaria* are primary necrotrophs, causing severe damage to trees, while others are saprotrophs, and feed on dead plant biomass. In addition to basidiospores, *Armillaria* can spread through root-like structures called rhizomorphs or through mycelia, which can spread underground from infected roots to the next host or substrate. As *Armillaria* can persist in a site for a long time, it can be difficult to control, however, studies have discussed strategies to control *Armillaria* root disease which include root collar excavation methods, planting less susceptible tree species, reducing stress on potential hosts and implementing management practices that favor biological control agents of *Armillaria*. Further, ongoing research is exploring the mechanism of pathogenicity in *Armillaria* species and their potential impacts on ecosystems and global climate change. Genomic and transcriptomic studies of *Armillaria*, as well as studies of soil microbial communities, may also provide new insights into the biology of *Armillaria* and potential disease control strategies.

The main objective of this dissertation was to investigate the functional mechanisms associated with two important traits in the lifestyle of *Armillaria* species - wood decay and evolution of pathogenicity. To do so, we used a combination of gene expression profiling and high-resolution phylogenomic comparisons.

To understand the mechanisms behind the wood decay abilities of *Armillaria* species, we selected two conifer-colonizing species - *Armillaria ostoyae* (pathogen - necrotroph) and *Armillaria cepistipes* (saprotroph) - and allowed them to colonize sterilized spruce roots. After colonizing the wood, we isolated four types of tissues - the invasive rhizomorphs and invasive mycelium from the colonized root, and the non-invasive rhizomorphs and mycelium from fungi growing in the absence of wood. We

performed proteomics and transcriptomics analyses on the samples and found that the tissue types showed clear separation of the invasive and non-invasive mycelium, whereas the two types of rhizomorphs had lesser differences. This was also reflected in the differentially expressed genes in both the omics analysis, with a higher number of differentially expressed genes (DEGs)/differentially abundant proteins (DAPs) in the mycelium compared to the rhizomorphs. On comparing the wood-decay patterns of two species, we found that while both species showed similar responses to wood, the saprotrophic species showed a stronger transcription- and protein-level response to wood than the pathogen. This suggests that saprotrophs may have a more rapid colonizing and substrate-degrading wood-decay strategy, which may be the result of the intense competition they face with other microbes on dead wood. We observed that pectin-related plant cell wall degrading enzymes (PCWDEs) were dominant among the genes that were differentially expressed in response to wood in both species and lignin-degrading enzymes were mostly down-regulated. This aligns with previous reports of the limited lignin-degrading capacity and gene repertoire in *Armillaria* species. In addition, we observed a significant difference in the expression of transporters between the invasive rhizomorphs and mycelium. Upregulated transporters in rhizomorphs *vs.* mycelium were likely involved in sugar transport, such as major facilitator sugar transport-like, sugar/inositol transporter, and sugar transporters. This suggests that rhizomorphs may not be involved in active wood decay, but rather may be involved in the transfer of decomposition intermediates between different parts of the colony.

Our findings suggest that wood-decay-related gene expression patterns in *Armillaria* species were unusual for white-rot fungi. These included the lack of an early burst of lignin-degrading enzymes, which is typical for white-rot fungi and the upregulation of cellulases, pectinases and other genes involved in iron uptake and oxoglutarate/iron-dependent dioxygenases. Previous research has questioned the white-rot nature of *Armillaria*, as it has been shown to attack cellulose but not lignin in the early stages of decay. In fact, some species of *Armillaria* have been associated with Type I or Type II soft rot, which is characterized by a complete set of enzymes for

degrading cellulose and hemicellulose, but a lack of lignin degradation activity. Several other wood-decaying basidiomycetes have also been reported to exhibit soft-rot behavior, which is typically only seen in Ascomycota. We propose that white-rot evolved in an early Agaricomycetes ancestor, which inherited the soft-rot machinery from their common ancestors with the Ascomycota. Thus resulting combination of white-rot and soft-rot toolkits might enable *Armillaria* and other unusual white-rot fungi to switch between decay types and selectively deploy either of the strategies for wood decay.

To put these findings into an evolutionary perspective and to better understand the diversity and evolution of wood decay fungi, we performed phylogenomic comparisons using new and published *Armillaria* genomes. We analyzed whole genomes of fungi from diverse ecologies along with 15 *Armillaria* species and five outgroups from the Physalacriaceae, which increased the sampling density in this group almost 4-fold compared to previous comparative studies. Using comparative phylogenomics we confirmed the previous findings revealing genome expansions in *Armillaria* species compared to related fungi, with a gain of over 2,913 genes inferred for the most recent common ancestor of *Armillaria*. This expansion has been accompanied by significant enrichment of genes related to plant biomass utilization including those involved in pectin degradation, cellulose binding, and the breakdown of extracellular and aromatic compounds as well as pathogenicity-related genes such as deuterolysins, aspartic peptidases, chitin deacetylases, SCP-like proteins, ceratoplatanins and LysM domains. Additionally, also we identified a number of novel gene families that are unique to the genus *Armillaria* and may be important in explaining their unique characteristics and abilities.

Analysis of carbohydrate active enzymes (CAZymes) revealed that *Armillaria* species possess the complete enzymatic repertoire for degrading woody plant biomass, similar to white rot fungi and necrotrophs. However, phylogenetic principal component analysis (PCA) of PCWDEs showed that *Armillaria* species are distinct from white rot and litter decomposer fungi with respect to their cellulases and

pectinases genes. We also found that *Armillaria* species have more genes for AA3_1, GH1, and GH45 enzymes, but fewer genes for CBM1 and GH5_5 enzymes, compared to white rot and litter decomposer fungi. Additionally, the GH44 gene family, which is specific to Basidiomycota, is missing in *Armillaria*, indicating that gene losses may have contributed to the evolution of their lifestyle. *Armillaria* species and other Physalacriaceae are enriched in certain plant PCWDE families such as those involved in pectin degradation including CBM67, GH78, and PL1. We also found that these fungi have more genes for pectin-acting families such as GH28, GH53, GH88, CE8, and CE12, compared to white rot and litter decomposers. However, *Armillaria* genomes were depleted in certain other pectin-degradation-related families, such as PL1_7, PL26, PL3_2, and PL4_1, which are abundant in white rot and some litter decomposer species. Overall, using a simple gene-copy number-based approach, our findings suggest that *Armillaria* and other Physalacriaceae possess a diverse set of PCWDE genes that allow them to effectively decay wood. However, their PCWDE gene repertoire is distinct from that of white rot fungi and hints towards an approach similar to that of soft rot fungi, which are found only in the Ascomycota. We found several PCWDEs involved in cellulose, hemicellulose and pectin degradation, that were overrepresented in both the Ascomycota and the Physalacriaceae compared to white rot and litter decomposer fungi which could either be a result of co-expansion or horizontal transfer of genes. To test the latter scenario, we followed a systematic approach to identifying horizontal gene transfer (HGT) events.

Using alien-index (AI), we first identified the putative horizontally transferred (HT) candidates in *Armillaria* and the Physalacriaceae, which top hits coming from Ascomycota, Mucoromycota and Zoompagomycota. Followed by scrutinized filtering based on a combination of phylogenetic support and protein similarity-based searches we identified 101 strongly supported HT events in Physalacriaceae, corresponding to 1089 individual genes. These events were predominantly associated with Ascomycota as donors, particularly the Sordariomycetes and Dothideomycetes. Gene expression studies revealed that many of the HT genes were involved in wood decay and pathogenicity, suggesting that HGT may have played a role in the evolution of these

traits in *Armillaria*. Previously, we noticed through gene expression analysis that *Armillaria* species have a wood decay strategy similar to the soft-rot of Ascomycota. Although white rot is the more common method of wood degradation in the Agaricales, our phylogenetic (PCA) surprisingly distinguished *Armillaria* from white rot species. This conflict may be addressed by the CAZymes acquired by HGT from Ascomycota, establishing HGT as a source of innovation in the development of fungal plant biomass-degrading systems in Basidiomycota.

Further, to study the molecular mechanisms underlying the infection process, we analyzed the current (wood-decay), previously published (fungal development) and new RNA-Seq data from our collaborators (stem-invasion and in-planta assays). We found that different genes and gene groups were enriched in different stages of the infection process. For instance, cellulose-, hemicellulose-, pectin- and lignin-related genes, which are involved in the breakdown of plant cell walls, were enriched in stem invasion and wood-decay experiments. Whereas other gene groups related to pathogenicity or stress response were enriched in the in-planta assays. We also observed species- and strain-specific enrichment patterns, suggesting strain-specific differences in wood colonization and virulence.

Overall, this work reveals the genetic basis of the wood-decay lifestyle of this widespread genus and provides insight into the molecular mechanisms of the early and late stages of colonization of host plants. We propose that the *Armillaria* genomes have evolved as a result of a variety of genetic innovations, including HGT, and that genes acquired early in the onset of the genus were incorporated into gene regulatory networks of pathogenicity and the breakdown of plant biomass. These new findings and evolutionary explanations on the unique biology of *Armillaria* species, if combined with system biology approaches and emerging molecular tools could facilitate the research on their molecular mechanisms of virulence.

Összefoglaló

Az *Armillaria* fajok az Agaricomycetes osztályba tartozó gombák, amelyek gyökérrothadásos betegségeket okozhatnak a fás ökoszisztémákban. Az *Armillaria* gyökérszerű struktúrákkal, úgynevezett rizomorfok vagy a micéliumok segítségével terjed, ami megnehezíti a védekezést. Ebben a disszertációban génexpressziós vizsgálatok és filogenomikai összehasonlítások segítségével vizsgáltuk a fa korhadásának mechanizmusait és az *Armillaria* fajok patogenitásának evolúcióját. Eredményeink azt sugallják, hogy az *Armillaria* fajok az Agaricomycetes fajokra nézve szokatlan génexpressziós mintázattal rendelkeznek, mivel hiányzik a fehérkorhasztó gombáknál jellemzően megfigyelhető ligninbontó enzimek korai aktiválódása. Korábbi, az *Armillaria* által okozott fakárosodás mikroszkópos és kémiai elemzésén alapuló kutatások azt sugallták, hogy ezek a fajok a cellulózt támadják, és az I. vagy II. típusú lágyrothadás jellemzőit mutatják. Eredményeink evolúciós perspektívába helyezése érdekében filogenomikai összehasonlításokat végeztünk az *Armillaria* genomjaival és különböző életmódú gombákkal, és azt találtuk, hogy bár az *Armillaria* fajok rendelkeznek a teljes enzimrepertoárral a fás növényi biomassza lebontásához, ez a génkészletük eltér a fehérkorhasztó és az ún. ‘Litter decomposer’ gombákétól, és számos szempontból az Ascomycota-ban található lágykorhasztó gombákéhoz hasonlít. Továbbá azonosítottunk számos olyan növényi sejtfalbontó enzimet (PCWDE-k), amelyek a cellulóz, hemicellulóz és pektin lebontásában vesznek részt, és amelyek mind az Ascomycota, mind a *Armillaria* fajokban felülreprezentáltak a fehérkorhasztó és ‘Litter decomposer’ gombákhoz képest, ami vagy koexpanzió vagy horizontális géntranszfer eredménye lehet. A horizontális géntranszfer (HGT) események elemzése 101 erősen támogatott HGT eseményt mutatott ki az *Armillaria*-ban, ami 775 génnek felel meg, főként az Ascomycota-ba tartozó Sordariomycetes és Dothideomycetes osztályokból mint donorokból. A vizsgálat továbbá különböző géneket és géncsoportokat talált, amelyek a fertőzési folyamat különböző szakaszaiban feldúsultak, a fa kolonizációjában és virulenciájában faj- és törzs-specifikus különbségekkel. Összességében eredményeink azt sugallják, hogy az

Armillaria genomjai különböző genetikai innovációk, köztük HGT révén fejlődtek, és azt gondoljuk, hogy ezen új eredmények rendszerbiológiai megközelítésekkel és új molekuláris eszközökkel való kombinálása megkönnyítheti a virulencia molekuláris mechanizmusainak további kutatását.

List of publications (MTMT ID: 10071410)

Mandatory peer-reviewed publications for the fulfillment of the doctoral process:

1. **Sahu, N.**, Indic, B., Wong-Bajracharya, J., Merényi, Z., Ke, H.-M., Ahrendt, S., Monk, T.-L., Kocsubé, S., Drula, E., Lipzen, A., Bálint, B., Henrissat, B., Andreopoulos, B., Martin, F.M., Harder, C.B., Rigling, D., Ford, K.L., Foster, G.D., Pangilinan, J., Papanicolaou, A., Barry, K., LaButti, K., Virágh, M., Koriabine, M., Yan, M., Riley, R., Champramary, S., Plett, K.L., Grigoriev, I.V., Tsai, I.J., Slot, J., Sipos, G., Plett, J., Nagy, L.G., 2022. Genomic innovation and horizontal gene transfer shaped plant colonization and biomass degradation strategies of a globally prevalent fungal pathogen (preprint). https://doi.org/10.1101/2022.11.10.515791 (IF: NA)

2. **Sahu, N.**, Merényi, Z., Bálint, B., Kiss, B., Sipos, G., Owens, R.A., Nagy, L.G., 2021. Hallmarks of Basidiomycete soft- and white-rot in wood-decay -omics data of two *Armillaria* species. Microorganisms 9, 149. https://doi.org/10.3390/microorganisms9010149 (IF_{2021}: 4.926)

Complete list of publications (Cumulative impact factor: 71.64)

1. Nagy, L.G., Vonk, P.J., Künzler, M., Földi, C., Virágh, M., Ohm, R.A., Hennicke, F., Bálint, B., Csernetics, Á., Hegedüs, B., Hou, Z., Liu, X.B., Nan, S., Pareek, M., **Sahu, N.**, Szathmári, B., Varga, T., Wu, H., Yang, X., Merényi, Z., 2023. Lessons on fruiting body morphogenesis from genomes and transcriptomes of Agaricomycetes. Stud. Mycol. https://doi.org/10.3114/sim.2022.104.01 (IF_{2021}: 25.56)

2. Merenyi, Z., Krizsan, K., **Sahu, N.**, Liu, X.-B., Balint, B., Stajich, J., Spatafora, J.W., Nagy, L.G., 2022. Taxonomic vs genomic fungi: contrasting evolutionary loss of protistan genomic heritage and emergence of fungal novelties (preprint). https://doi.org/10.1101/2022.11.15.516418

3. **Sahu, N.**, Indic, B., Wong-Bajracharya, J., Merényi, Z., Ke, H.-M., Ahrendt, S., Monk, T.-L., Kocsubé, S., Drula, E., Lipzen, A., Bálint, B., Henrissat, B., Andreopoulos,

B., Martin, F.M., Harder, C.B., Rigling, D., Ford, K.L., Foster, G.D., Pangilinan, J., Papanicolaou, A., Barry, K., LaButti, K., Virágh, M., Koriabine, M., Yan, M., Riley, R., Champramary, S., Plett, K.L., Grigoriev, I.V., Tsai, I.J., Slot, J., Sipos, G., Plett, J., Nagy, L.G., 2022. Genomic innovation and horizontal gene transfer shaped plant colonization and biomass degradation strategies of a globally prevalent fungal pathogen (preprint). https://doi.org/10.1101/2022.11.10.515791

4. Chen, L., Champramary, S., **Sahu, N.**, Indic, B., Szűcs, A., Nagy, G., Maróti, G., Pap, B., Languar, O., Vágvölgyi, C., Nagy, L.G., Kredics, L., Sipos, G., 2022. Dual RNA-Seq profiling unveils mycoparasitic activities of *Trichoderma atroviride* against haploid *Armillaria ostoyae* in antagonistic interaction assays (preprint). https://doi.org/10.1101/2022.11.02.514975

5. Pareek, M., Hegedüs, B., Hou, Z., Csernetics, Á., Wu, H., Virágh, M., **Sahu, N.**, Liu, X.-B., Nagy, L., 2022. Preassembled Cas9 ribonucleoprotein-mediated gene deletion odentifies the carbon catabolite repressor and its target genes in *Coprinopsis cinerea*. Appl. Environ. Microbiol. e00940-22. https://doi.org/10.1128/aem.00940-22 (IF_{2021}: 5.005)

6. Virágh, M., Merényi, Z., Csernetics, Á., Földi, C., **Sahu, N.**, Liu, X.-B., Hibbett, D.S., Nagy, L.G., 2022. Evolutionary morphogenesis of sexual fruiting bodies in Basidiomycota: Toward a new evo-devo synthesis. Microbiol. Mol. Biol. Rev. 86, e00019-21. https://doi.org/10.1128/MMBR.00019-21 (IF_{2021}: 13.044)

7. **Sahu, N.**, Merényi, Z., Bálint, B., Kiss, B., Sipos, G., Owens, R.A., Nagy, L.G., 2021. Hallmarks of Basidiomycete soft- and white-rot in wood-decay -omics data of two *Armillaria* species. Microorganisms 9, 149. https://doi.org/10.3390/microorganisms9010149 (IF_{2021}: 4.926)

8. Almási, É*., **Sahu, N*.**, Krizsán, K., Bálint, B., Kovács, G.M., Kiss, B., Cseklye, J., Drula, E., Henrissat, B., Nagy, I., Chovatia, M., Adam, C., LaButti, K., Lipzen, A., Riley, R., Grigoriev, I.V., Nagy, L.G., 2019. Comparative genomics reveals unique wood- decay strategies and fruiting body development in the Schizophyllaceae. New

Phytol. 224, 902–915. https://doi.org/10.1111/nph.16032 (** Shared first author*) (IF_{2021}: 10.323)

9. Krizsán, K., Almási, É., Merényi, Z., **Sahu, N.**, Virágh, M., Kószó, T., Mondo, S., Kiss, B., Bálint, B., Kües, U., Barry, K., Cseklye, J., Hegedüs, B., Henrissat, B., Johnson, J., Lipzen, A., Ohm, R.A., Nagy, I., Pangilinan, J., Yan, J., Xiong, Y., Grigoriev, I.V., Hibbett, D.S., Nagy, L.G., 2019. Transcriptomic atlas of mushroom development reveals conserved genes behind complex multicellularity in fungi. Proc. Natl. Acad. Sci. 116, 7409–7418. https://doi.org/10.1073/pnas.1817822116 (IF_{2021}: 12.779)

10. Mishra, S.R., Panda, A.N., Ray, L., **Sahu, N.**, Mishra, G., Jadhao, S., Suar, M., Adhya, T.K., Rastogi, G., Pattnaik, A.K., Raina, V., 2016a. Draft genome sequence of *Pseudomonas* sp. strain BMS12, a plant Growth-Promoting and Protease-Producing Bacterium, Isolated from the rhizosphere sediment of *Phragmites karka* of Chilika Lake, India. Genome Announc. 4, e00342-16. https://doi.org/10.1128/genomeA.00342-16 (IF: NA)

11. Mishra, S.R., Ray, L., Panda, A.N., **Sahu, N.**, Xess, S.S., Jadhao, S., Suar, M., Adhya, T.K., Rastogi, G., Pattnaik, A.K., Raina, V., 2016b. Draft genome sequence of *Acinetobacter* sp. strain BMW17, a cellulolytic and plant growth-promoting bacterium Isolated from the rhizospheric region of *Phragmites karka* of Chilika Lake, India. Genome Announc. 4, e00395-16. https://doi.org/10.1128/genomeA.00395-16 (IF: NA)

12. Panda, A.N., Mishra, S.R., Ray, L., **Sahu, N.**, Acharya, A., Jadhao, S., Suar, M., Adhya, T.K., Rastogi, G., Pattnaik, A.K., Raina, V., 2016. Draft genome sequence of *Halobacillus* sp. strain KGW1, a moderately halophilic and alkaline protease-producing bacterium isolated from the rhizospheric region of *Phragmites karka* from Chilika Lake, Odisha, India. Genome Announc. 4, e00361-16. https://doi.org/10.1128/genomeA.00361-16 (IF: NA)

Supplementary information

Table S1: List of CAZymes and their putative substrates.

CAZy_families	References	Abbreviation	Substrate	Category
AA1	Nagy et al. 2015	AA1	Lignin	PCWDE
AA1_1	Miyauchi et al. 2020	AA1_1	Lignin	PCWDE
AA1_2	Levasseur et al. 2013, Liu et al. 2019	AA1_2	Lignin	PCWDE
AA1_3	Levasseur et al. 2013	AA1_3	Lignin	PCWDE
Multicopper oxidase	Riley et al. 2014	AA1_dist	Lignin	PCWDE
AA10	Miyauchi et al. 2020	AA10	Cellulose	PCWDE
AA11	Støpamo et al. 2021	AA11	Cellulose/Chitin, LPMO	PCWDE, FCW
Lytic polysaccharide monooxygenase	Støpamo et al. 2021	AA11_dist	Cellulose/Chitin, LPMO	PCWDE, FCW
AA14	Miyauchi et al. 2020	AA14	Hemicellulose	PCWDE, FCW
AA15	Miyauchi et al. 2020	AA15	Chitin, Cellulose	FCW
AA16	Miyauchi et al. 2020	AA16	Cellulose	PCWDE
AA2	Riley et al. 2014, Nagy et al. 2015, Miyauchi et al. 2020	AA2	Lignin	PCWDE
Class II peroxidase	Riley et al. 2014	AA2_dist	Lignin	PCWDE
AA3	Sützl et al. 2018	AA3	Lignin monomers	PCWDE
AA3_1	Rytioja et al. 2014 , Miyauchi et al. 2018	AA3_1	Cellulose	PCWDE
AA3_2	Sützl et al. 2018	AA3_2	Lignin monomers	PCWDE
AA3_3	Sützl et al. 2018	AA3_3	Lignin monomers	PCWDE
AA3_4	Sützl et al. 2018	AA3_4	Lignin monomers	PCWDE

GMC oxidoreductase	Shah et al. 2015	AA3_dist	Lignin monomers	PCWDE
AA5	Strasser et al. 2015	AA5	Lignin	PCWDE
AA5_1	Levasseur et al. 2013, Daou et al. 2021	AA5_1	Lignin monomers	PCWDE
AA5_2	Levasseur et al. 2013, Koschorreck et al. 2022	AA5_2	Lignin monomers	PCWDE
Copper radical oxidase	Levasseur et al. 2013, Koschorreck et al. 2022	AA5_dist	Lignin monomers	PCWDE
AA8	Rytioja et al. 2014 , Miyauchi et al. 2018	AA8	Cellulose	PCWDE
AA9	Miyauchi et al. 2020	AA9	Cellulose	PCWDE
CBM1	Miyauchi et al. 2020	CBM1	Cellulose	PCWDE
CBM12	Miyauchi et al. 2020	CBM12	Chitin	FCW
CBM14	Miyauchi et al. 2020	CBM14	Chitn	FCW
CBM18	Miyauchi et al. 2020	CBM18	Chitin	FCW
CBM43	Miyauchi et al. 2020	CBM43	Glucan	FCW
CBM5	Miyauchi et al. 2020	CBM5	Chitin	FCW
CBM50	Krizsan et al. 2019	CBM50	Chitin	FCW
CBM63	Miyauchi et al. 2020	CBM63	Cellulose	PCWDE
CBM67	Miyauchi et al. 2020	CBM67	Pectin	PCWDE
CE12	Miyauchi et al. 2020	CE12	Pectin	PCWDE
CE15	Miyauchi et al. 2020	CE15	Hemicellulose	PCWDE
CE16	Floudas et al. 2012, Floudas et al. 2015, Nagy et al. 2016	CE16	Hemicellulose	PCWDE
CE4	Krizsan et al. 2019	CE4	Chitin	FCW
CE5	Miyauchi et al. 2020	CE5	Hemicellulose, Cutin, Suberin	PCWDE
CE8	Miyauchi et al. 2020	CE8	Pectin	PCWDE
EXPN	Ding et al. 2022	EXPN	Cellulose	PCWDE
GH1	Rytioja et al. 2014 , Miyauchi et al. 2018	GH1	Cellulose	PCWDE

GH10	Miyauchi et al. 2020	GH10	Hemicellulose	PCWDE
GH105	Miyauchi et al. 2020	GH105	Pectin	PCWDE
GH106	Miyauchi et al. 2020	GH106	Pectin	PCWDE
GH11	Miyauchi et al. 2020	GH11	Hemicellulose	PCWDE
GH113	Miyauchi et al. 2020	GH113	Hemicellulose	PCWDE
GH115	Miyauchi et al. 2020	GH115	Hemicellulose	PCWDE
GH12	Rytioja et al. 2014, Miyauchi et al. 2020	GH12	Cellulose, Hemicellulose	PCWDE
GH125	Miyauchi et al. 2020	GH125	Mannan	FCW
GH128	Miyauchi et al. 2020	GH128	Glucan	FCW
GH131	Miyauchi et al. 2020	GH131	Cellulose	PCWDE
GH132	Miyauchi et al. 2020	GH132	Glucan	FCW
GH134	Miyauchi et al. 2020	GH134	Hemicellulose	PCWDE
GH135	Miyauchi et al. 2020	GH135	Galactan	FCW
GH152	Krizsan et al. 2019	GH152	Glucan	FCW
GH16	Miyauchi et al. 2020	GH16	Glucan	FCW
GH16_2	Krizsan et al. 2019	GH16_2	Glucan	FCW
GH17	Miyauchi et al. 2020	GH17	Glucan	FCW
GH18	Miyauchi et al. 2020	GH18	Chitin	FCW
GH19	Miyauchi et al. 2020	GH19	Chitin	FCW
GH2	Rytioja et al. 2014	GH2	Hemicellulose	PCWDE
GH20	Miyauchi et al. 2020	GH20	Chitin	FCW
GH23	Miyauchi et al. 2020	GH23	Peptidoglycan	FCW
GH24	Miyauchi et al. 2020	GH24	Peptidoglycan	FCW
GH25	Miyauchi et al. 2020	GH25	Peptidoglycan	FCW
GH26	Rytioja et al. 2014, Miyauchi et al. 2020	GH26	Hemicellulose, Mannan	PCWDE, FCW
GH27	Rytioja et al. 2014	GH27	Hemicellulose	PCWDE
GH28	Miyauchi et al. 2020	GH28	Pectin	PCWDE

GH29	Floudas et al. 2015	GH29	Hemicellulose	PCWDE
GH3	Rytioja et al. 2014, Miyauchi et al. 2020	GH3	Cellulose, Hemicellulose	PCWDE, FCW
GH30	Miyauchi et al. 2018	GH30	Hemicellulose	PCWDE
GH30_3	Miyauchi et al. 2020	GH30_3	Glucan	FCW
GH30_5	Miyauchi et al. 2020	GH30_5	Galactan	FCW
GH30_7	Miyauchi et al. 2020	GH30_7	Hemicellulose	PCWDE
GH31	Rytioja et al. 2014	GH31	Hemicellulose	PCWDE
GH35	Rytioja et al. 2014	GH35	Hemicellulose	PCWDE
GH36	Rytioja et al. 2014	GH36	Hemicellulose	PCWDE
GH43	Rytioja et al. 2014, Miyauchi et al. 2020	GH43	Hemicellulose	PCWDE
GH44	Miyauchi et al. 2020	GH44	Cellulose	PCWDE
GH45	Miyauchi et al. 2020	GH45	Cellulose	PCWDE
GH46	Miyauchi et al. 2020	GH46	Chitin	FCW
GH48	Miyauchi et al. 2020	GH48	Cellulose	PCWDE
GH5	Rytioja et al. 2014, Miyauchi et al. 2020	GH5	Cellulose, Hemicellulose	PCWDE
GH5_1	Miyauchi et al. 2020	GH5_1	Cellulose	PCWDE
GH5_15	Miyauchi et al. 2020	GH5_15	Glucan	FCW
GH5_22	Miyauchi et al. 2020	GH5_22	Cellulose, Hemicellulose	PCWDE
GH5_31	Miyauchi et al. 2020	GH5_31	Mannan	FCW
GH5_4	Miyauchi et al. 2020	GH5_4	Cellulose	PCWDE
GH5_49	Krizsan et al. 2019	GH5_49	Glucan	FCW
GH5_5	Miyauchi et al. 2020	GH5_5	Cellulose	PCWDE
GH5_7	Miyauchi et al. 2020	GH5_7	Hemicellulose	PCWDE
GH5_9	Miyauchi et al. 2020	GH5_9	Glucan	FCW
GH51	Rytioja et al. 2014, Miyauchi et al. 2020	GH51	Hemicellulose, Pectin	PCWDE
GH52	Miyauchi et al. 2020	GH52	Hemicellulose	PCWDE

GH53	Miyauchi et al. 2020	GH53	Pectin	PCWDE
GH54	Rytioja et al. 2014, Miyauchi et al. 2020	GH54	Hemicellulose, Pectin	PCWDE
GH55	Miyauchi et al. 2020	GH55	Glucan	FCW
GH6	Miyauchi et al. 2020	GH6	Cellulose	PCWDE
GH62	Rytioja et al. 2014, Miyauchi et al. 2020	GH62	Hemicellulose, Pectin	PCWDE
GH64	Miyauchi et al. 2020	GH64	Glucan	FCW
GH67	Miyauchi et al. 2020	GH67	Hemicellulose	PCWDE
GH7	Miyauchi et al. 2020	GH7	Cellulose	PCWDE
GH71	Miyauchi et al. 2020	GH71	Glucan	FCW
GH72	Miyauchi et al. 2020	GH72	Glucan	FCW
GH74	Miyauchi et al. 2020	GH74	Hemicellulose	PCWDE
GH75	Miyauchi et al. 2020	GH75	Chitin	FCW
GH76	Miyauchi et al. 2020	GH76	Mannan	FCW
GH78	Miyauchi et al. 2020	GH78	Pectin	PCWDE
GH8	Miyauchi et al. 2020	GH8	Hemicellulose	PCWDE
GH81	Miyauchi et al. 2020	GH81	Glucan	FCW
GH88	Miyauchi et al. 2020	GH88	Pectin	PCWDE
GH9	Rytioja et al. 2014, Miyauchi et al. 2020	GH9	Cellulose	PCWDE
GH92	Miyauchi et al. 2020	GH92	Mannan	FCW
GH93	Miyauchi et al. 2020	GH93	Hemicellulose	PCWDE
GH95	Rytioja et al. 2014, Floudas et al. 2015	GH95	Hemicellulose	PCWDE
GT18	Nagy et al. 2022	GT18	FCW	FCW
GT2	Nagy et al. 2022	GT2	FCW	FCW
GT24	Nagy et al. 2022	GT24	FCW	FCW
GT48	Nagy et al. 2022	GT48	FCW	FCW
GT8	Nagy et al. 2022	GT8	FCW	FCW

PL1	Miyauchi et al. 2020	PL1	Pectin	PCWDE
PL1_10	Atanasova et al. 2018	PL1_10	Pectin	PCWDE
PL1_4	Atanasova et al. 2018	PL1_4	Pectin	PCWDE
PL1_7	Atanasova et al. 2018	PL1_7	Pectin	PCWDE
PL1_9	Atanasova et al. 2018	PL1_9	Pectin	PCWDE
PL11	Miyauchi et al. 2020	PL11	Pectin	PCWDE
PL14_4	Miyauchi et al. 2020	PL14_4	Pectin	PCWDE
PL26	Miyauchi et al. 2020	PL26	Pectin	PCWDE
PL3	Miyauchi et al. 2020	PL3	Pectin	PCWDE
PL3_2	Atanasova et al. 2018	PL3_2	Pectin	PCWDE
PL4	Miyauchi et al. 2020	PL4	Pectin	PCWDE
PL4_1	Atanasova et al. 2018	PL4_1	Pectin	PCWDE
PL4_3	Atanasova et al. 2018	PL4_3	Pectin	PCWDE
PL8_4	Miyauchi et al. 2020	PL8_4	Pectin	PCWDE
PL9	Miyauchi et al. 2020	PL9	Pectin	PCWDE
PL9_3	Atanasova et al. 2018	PL9_3	Pectin	PCWDE

(AA: auxiliary activity, CBM: carbohydrate binding module, CE: carbohydrate esterase, GH: glycoside hysrolase, GT: glycosyl transferase, PL: polysaccharide lyase, PCWDE: plant cell wall degrading enzyme, FCW: fungal-cell wall)

Table S2: Dataset used for comparative genomic analyses. Species belonging to the order Agaricales along with 2 species from Boletales (Paxin1 and Suibr2) as outgroup were used for COMPARE analyses. (Dataset 1) All species from the list were used for gene copy number-based analyses (Dataset 2).

Species	Abbreviation	Lifestyle	Order	Category	PMID/DOI
Acidomyces richmondensis BFW	Aciri1_iso	ASCO	Capnodiales	Ascomycota	26973616
Agaricus bisporus var bisporus (H97) v2.0	Agabi_varbis H97_2	LD	Agaricales	Basidiomycota	23045686
Agrocybe pediades AH 40210 v1.0	Agrped1	LD	Agaricales	Basidiomycota	33211093
Alternaria alternata SRC1lrK2f v1.0	Altal1	ASCO	Pleosporales	Ascomycota	27434633
Alternaria brassicicola	Altbr1	ASCO	Pleosporales	Ascomycota	23236275
Amanita muscaria Koide v1.0	Amamu1	ECM	Agaricales	Basidiomycota	25706625
Amanita thiersii Skay4041 v1.0	Amath1	LD	Agaricales	Basidiomycota	24923322
Amniculicola lignicola CBS 123094 v1.0	Amnli1	ASCO	Pleosporales	Ascomycota	32206138
Aplosporella prunicola CBS 121.167 v1.0	Aplpr1	ASCO	Botryosphaeriales	Ascomycota	32206138

Armillaria borealis FPL87.14 v1.0	Armbor1	Physac	Agaricales	Basidiomycota	This study
Armillaria cepistipes B5	Armcep1	Physac	Agaricales	Basidiomycota	29085064
Armillaria ectypa FPL83.16 v1.0	Armect1	Physac	Agaricales	Basidiomycota	This study
Armillaria fumosa CBS 122221 v1.0	Armfum1	Physac	Agaricales	Basidiomycota	This study
Armillaria fuscipes strain CMW2740	Armfus	Physac	Agaricales	Basidiomycota	27433447
Armillaria gallica 21-2 v1.0	Armga1	Physac	Agaricales	Basidiomycota	29085064
Armillaria luteobubalina HWK02 v1.0	Armlut1	Physac	Agaricales	Basidiomycota	This study
Armillaria mellea DSM 3731	Armme1_1	Physac	Agaricales	Basidiomycota	23656496
Armillaria mellea ELDO17 v1.0	Armmel1	Physac	Agaricales	Basidiomycota	This study
Armillaria nabsnona CMW6904 v1.0	Armnab1	Physac	Agaricales	Basidiomycota	This study
Armillaria novae-zelandiae 2840 v1.0	Armnov1	Physac	Agaricales	Basidiomycota	This study
Armillaria ostoyae C18/9	Armosto1	Physac	Agaricales	Basidiomycota	29085064

Armillaria solidipes 28-4 v1.0	Armost1	Physac	Agaricales	Basidiomycota	29085064
Armillaria tabescens CCBAS 213 v1.0	Armtab1	Physac	Agaricales	Basidiomycota	This study
Ascochyta rabiei ArDII	Ascra1	ASCO	Pleosporales	Ascomycota	27091329
Ascocoryne sarcoides NRRL50072	Ascsa1	ASCO	Helotiales	Ascomycota	22396667
Aureobasidium pullulans var. pullulans EXF-150	Aurpu_var_pul1	ASCO	Dothideales	Ascomycota	24984952
Aureobasidium pullulans var. subglaciale EXF-2481	Aurpu_var_sub1	ASCO	Dothideales	Ascomycota	24984952
Auricularia subglabra v2.0	Aurde3_1	WR	Auriculariales	Basidiomycota	22745431
Auriculariopsis ampla NL-1724 v1.0	Auramp1	UR	Agaricales	Basidiomycota	31257601
Bjerkandera adusta v1.0	Bjead1_1	WR	Polyporales	Basidiomycota	23935031
Botryobasidium botryosum v1.0	Botbo1	UR	Cantharellales	Basidiomycota	24958869
Calocera cornea v1.0	Calco1	BR	Dacrymycetales	Basidiomycota	26659563

Calocera viscosa v1.0	Calvi1	BR	Dacrymycetales	Basidiomycota	26659563
Chaetomium globosum v1.0	Chagl_1	ASCO	Sordariales	Ascomycota	25720678
Chondrostereum purpureum	Chopu	PATH	Agaricales	Basidiomycota	30822315
Cladosporium fulvum v1.0	Clafu1	ASCO	Capnodiales	Ascomycota	23209441
Clitocybe gibba IJFM A808 v1.0	Cligib1	LD	Agaricales	Basidiomycota	33211093
Colletotrichum tofieldiae 0861	Colto1	ASCO	Glomerellales	Ascomycota	27150427
Coniochaeta sp. 2T2.1 v1.0	Conioc1	ASCO	Coniochaetales	Ascomycota	31572496
Coniophora olivacea MUCL 20566 v1.0	Conol1	BR	Boletales	Basidiomycota	29145801
Coniophora puteana v1.0	Conpu1	BR	Boletales	Basidiomycota	22745431
Coprinellus micaceus FP101781 v2.0	Copmic2	LD	Agaricales	Basidiomycota	30886374
Coprinopsis cinerea AmutBmut pab1-1 v1.0	Copci_AmutBmut1	LD	Agaricales	Basidiomycota	26510163
Coprinopsis marcescibilis CBS121175 v1.0	Copmar1	LD	Agaricales	Basidiomycota	30886374

Crepidotus variabilis CBS 506.95 v1.0	Crevar1	UR	Agaricales	Basidiomycota	33211093
Crucibulum laeve CBS 166.37 v1.0	Crula1	LD	Agaricales	Basidiomycota	30886374
Cryphonectria parasitica EP155 v2.0	Crypa2	ASCO	Diaporthales	Ascomycota	32207662
Cyathus striatus AH 40144 v1.0	Cyastr2	LD	Agaricales	Basidiomycota	33211093
Cylindrobasidium torrendii FP15055 v1.0	Cylto1	Physac	Agaricales	Basidiomycota	25683379
Daedalea quercina v1.0	Daequ1	BR	Polyporales	Basidiomycota	26659563
Dendrothele bispora CBS 962.96 v1.0	Denbi1	UR	Agaricales	Basidiomycota	30886374
Dichomitus squalens CBS464.89 v1.0	Dicsqu464_1	WR	Polyporales	Basidiomycota	31048399
Exidia glandulosa v1.0	Exigl1	WR	Auriculariales	Basidiomycota	26659563
Fibroporia radiculosa TFFH 294	Fibra1	BR	Polyporales	Basidiomycota	22247176
Fibulorhizoctonia sp. CBS 109695 v1.0	Fibsp1	WR	Atheliales	Basidiomycota	26659563

Fistulina hepatica v1.0	Fishe1	BR	Agaricales	Basidiomycota	25683379
Flagelloscypha sp. PMI_526 v1.0	FlaPMI526_1	ECM	Agaricales	Basidiomycota	With permission from Gregory Bonito
Flammulina rossica	Flaro	Physac	Agaricales	Basidiomycota	31597238
Flammulina velutipes KACC42780	Flave	Physac	Agaricales	Basidiomycota	24714189
Fomitopsis pinicola FP-58527 SS1 v3.0	Fompi3	BR	Polyporales	Basidiomycota	22745431
Galerina marginata v1.0	Galma1	WR	Agaricales	Basidiomycota	24958869
Gloeophyllum trabeum v1.0	Glotr1_1	BR	Gloeophyllales	Basidiomycota	22745431
Guyanagaster necrorhizus MCA 3950 v1.0	Guyne1	Physac	Agaricales	Basidiomycota	34245690
Gymnopilus junonius AH 44721 v1.0	Gymjun1	WR	Agaricales	Basidiomycota	33211093
Gymnopus androsaceus JB14 v1.0	Gyman1	LD	Agaricales	Basidiomycota	31760680
Gymnopus luxurians v1.0	Gymlu1	LD	Agaricales	Basidiomycota	25706625

Hebeloma cylindrosporum h7 v2.0	Hebcy2	ECM	Agaricales	Basidiomycota	25706625
Heliocybe sulcata OMC1185 v1.0	Helsul1	BR	Gloeophyllales	Basidiomycota	30886374
Heterobasidion annosum v2.0	Hetan2	PATH	Russulales	Basidiomycota	22463738
Hydnomerulius pinastri v2.0	Hydpi2	BR	Boletales	Basidiomycota	25706625
Hymenopellis radicata IJFM A160 v1.0	Hymrad1	Physac	Agaricales	Basidiomycota	33211093
Hypholoma sublateritium v1.0	Hypsu1	WR	Agaricales	Basidiomycota	25706625
Hypoxylon rubiginosum ER1909 v1.0	HyprubER1909_1	ASCO	Xylariales	Ascomycota	34797921
Hypsizygus marmoreus 51987-8	Hypma	WR	Agaricales	Basidiomycota	30382831
Jaapia argillacea v1.0	Jaaar1	UR	Jaapiales	Basidiomycota	24958869
Laccaria amethystina LaAM-08-1 v2.0	Lacam2	ECM	Agaricales	Basidiomycota	25706625
Laccaria bicolor v2.0	Lacbi2	ECM	Agaricales	Basidiomycota	18322534

Laetiporus sulphureus var. sulphureus v1.0	Laesu1	BR	Polyporales	Basidiomycota	26659563
Lentinula edodes B17 v1.1	Lened_B_1_1	WR	Agaricales	Basidiomycota	29845094
Lentinus tigrinus ALCF2SS1-7 v1.0	Lenti7_1	WR	Polyporales	Basidiomycota	30398645
Lepista nuda CBS 247.69 v1.0	Lepnud1	LD	Agaricales	Basidiomycota	33211093
Macrolepiota fuliginosa MF-IS2 v1.0	Macfu1	LD	Agaricales	Basidiomycota	33211093
Marasmius fiardii PR-910 v1.0	Marfi1	LD	Agaricales	Basidiomycota	33046698
Moniliophthora perniciosa FA553	Monpe1_1	PATH	Agaricales	Basidiomycota	19019209
Mycena crocata CBHHK184 v1.0	Myccro1	LD	Agaricales	Basidiomycota	With permission from Francis Martin
Mycena epipterygia CBHHK145m v1.0	Mycepi1	LD	Agaricales	Basidiomycota	With permission from Francis Martin
Mycena floridula CBHHK072 v1.0	Mycflo1	LD	Agaricales	Basidiomycota	With permission from Francis Martin

Neolentinus lepideus v1.0	Neole1	BR	Gloeophyllales	Basidiomycota	26659563
Oudemansiella mucida CBS 558.79 v1.0	Oudmuc1	Physac	Agaricales	Basidiomycota	33211093
Paecilomyces niveus CO7 v1.0	Bysni1	ASCO	Eurotiales	Ascomycota	29930063
Paecilomyces variotii CBS144490 HYG1 v1.0	Paevar_HGY_1	ASCO	Eurotiales	Ascomycota	30619145
Panaeolus papilionaceus CIRM-BRFM 715 v1.0	Panpap1	LD	Agaricales	Basidiomycota	33211093
Paxillus adelphus Ve08.2h10 v2.0	Paxru2	ECM	Boletales	Basidiomycota	25706625
Paxillus involutus ATCC 200175 v1.0	Paxin1	ECM	Boletales	Basidiomycota	25706625
Peniophora sp. CONTA v1.0	Lopni1	WR	Russulales	Basidiomycota	30886374
Phanerochaete chrysosporium RP-78 v2.2	Phchr2	WR	Polyporales	Basidiomycota	24853079
Phlebia radiata Fr. (isolate 79 FBCC0043)	Phlrad1	WR	Polyporales	Basidiomycota	27602055
Pholiota alnicola AH 47727 v1.0	Phoaln1	WR	Agaricales	Basidiomycota	33211093

Pholiota conissans CIRM-BRFM 674 v1.0	Phocon1	WR	Agaricales	Basidiomycota	33211093
Phoma tracheiphila IPT5 v1.0	Photr1	ASCO	Pleosporales	Ascomycota	32206138
Phyllosticta citriasiana CBS 120486 v1.0	Phycit1	ASCO	Botryosphaeriales	Ascomycota	31512371
Piloderma olivaceum F 1598 v1.0	Pilcr1	ECM	Atheliales	Basidiomycota	25706625
Pisolithus microcarpus 441 v1.0	Pismi1	ECM	Boletales	Basidiomycota	25706625
Pisolithus tinctorius Marx 270 v1.0	Pisti1	ECM	Boletales	Basidiomycota	25706625
Pleurotus eryngii ATCC 90797 v1.0	Pleery1	WR	Agaricales	Basidiomycota	33211093
Pleurotus ostreatus PC15 v2.0	PleosPC15_2	WR	Agaricales	Basidiomycota	24958869
Pluteus cervinus NL-1719 v1.0	Plucer1	UR	Agaricales	Basidiomycota	30886374
Polyporus arcularius v1.0	Polar1	WR	Polyporales	Basidiomycota	30886374
Postia placenta MAD-698-R-SB12 v1.0	PosplRSB12_1	BR	Polyporales	Basidiomycota	28831381

Psilocybe cubensis v1.0	Psicub1_1	LD	Agaricales	Basidiomycota	28763571
Psilocybe serbica v1.0	Psiser1	LD	Agaricales	Basidiomycota	28763571
Pterula gracilis CBS309.79 v1.0	Ptegra1	LD	Agaricales	Basidiomycota	30886374
Pycnoporus sanguineus BRFM 1264 v1.0	Pycsa1	WR	Polyporales	Basidiomycota	32531032
Pyrenochaeta sp. DS3sAY3a v1.0	Pyrsp1	ASCO	Pleosporales	Ascomycota	27434633
Rhizoctonia solani AG-1 IB	Rhiso1	PATH	Cantharellales	Basidiomycota	23280342
Rhizopogon vesiculosus Smith	Rhives1	ECM	Boletales	Basidiomycota	28450370
Rhizopogon vinicolor AM-OR11-026 v1.0	Rhivi1	ECM	Boletales	Basidiomycota	28450370
Rhodocollybia butyracea AH 40177 v1.0	Rhobut1_1	LD	Agaricales	Basidiomycota	33211093
Rickenella mellea v1.0 (SZMC22713)	Ricmel1	LD	Hymenochaetales	Basidiomycota	30902897
Schizophyllum commune H4-8 v3.0	Schco3	UR	Agaricales	Basidiomycota	35604096

Schizopora paradoxa KUC8140 v1.0	Schpa1	WR	Hymenochaetales	Basidiomycota	26188242
Scleroderma citrinum Foug A v1.0	Sclci1	ECM	Boletales	Basidiomycota	25706625
Serpula lacrymans S7.3 v2.0	SerlaS7_3_2	BR	Boletales	Basidiomycota	21764756
Stereum hirsutum FP-91666 SS1 v1.0	Stehi1	WR	Russulales	Basidiomycota	22745431
Suillus brevipes Sb2 v2.0	Suibr2	ECM	Boletales	Basidiomycota	25728665
Suillus luteus UH-Slu-Lm8-n1 v3.0	Suilu4	ECM	Boletales	Basidiomycota	25706625
Thielavia terrestris v2.0	Thite2	ASCO	Sordariales	Ascomycota	21964414
Trametes versicolor v1.0	Trave1	WR	Polyporales	Basidiomycota	22745431
Tulasnella calospora AL13/4D v1.0	Tulca1	ECM	Cantharellales	Basidiomycota	25706625
Volvariella volvacea V23	Volvo1	LD	Agaricales	Basidiomycota	23526973
Wolfiporia cocos MD-104 SS10 v1.0	Wolco1	BR	Polyporales	Basidiomycota	22745431

(ASCO: Ascomycota, BR: brown-rot, ECM: ectomycorrhizal, LD: litter decomposer, Physac: Physalacriaceae, UR: uncertain, WR: white-rot)